Neural Network qua an Information Processing System through the Medium of Rhythmic Oscillation

Tsutsumi, Kazuyoshi

(Degree)
博士（学術）

(Date of Degree)
1985-03-31

(Date of Publication)
2014-03-10

(Resource Type)
doctoral thesis

(Report Number)
甲0521

(URL)
https://hdl.handle.net/20.500.14094/D1000521

DOCTORAL DISSERTATION

NEURAL NETWORK QUA AN INFORMATION PROCESSING SYSTEM THROUGH THE MEDIUM OF RHYTHMIC OSCILLATION

KAZUYOSHI TSUTSUMI

THE GRADUATE SCHOOL OF SCIENCE AND TECHNOLOGY

KOBE UNIVERSITY

DECEMBER 1984

Doctoral Dissertation

Neural Network
qua an Information Processing System
through the Medium of Rhythmic Oscillation

(Rhythmic Oscillationを媒体とする情報処理システムとしての神経回路網)

Kazuyoshi Tsutsumi

The Graduate School of Science and Technology

Kobe University

December 1984

Acknowledgements

The author wishes to express his deepest thanks to Prof. Haruya Matsumoto who has given excellent advice and constant encouragement throughout the entire course of this work.

He wishes to express his sincere gratitude to Prof. Kazumasa Hirai, Associate Prof. Shinzo Kitamura, and Associate Prof. Hatsukazu Tanaka for their kind direction of the research leading to the completion of this thesis.

He also wishes to express his thanks to Prof. Chizuko Adachi, for her useful suggestions about the neurophysiological findings, to Joan and Grant Turri-Petrie for their help with the English, and to Masachika Fujita (presently with Kobe Steel Ltd.), Mr. Hiroyuki Yamaguchi (presently with Matsushita Electric Industrial Co. Ltd.), and Mr. Kazutomo Naganawa (presently with Omron Tateisi Electronics Co.) for their valuable cooperation.

It is also a pleasure to thank the students in the laboratory of Information and Instrumentation, particularly Mr. Mohammad Ali Sanamrad and Mr. Hirohisa Hirukawa.

Finally, it is with the greatest pleasure that he thanks his parents for their help, encouragement, and understanding at all times, but especially, of course, while this work was in progress.

Abstract

The neural network qua an information processing system through the medium of rhythmic oscillation is examined in this thesis.

In Chap.2, a synaptic modification algorithm in consideration of the generation of rhythmic oscillation is newly proposed. Our preliminary investigation into the rhythmic oscillation in the regular ring network led to the selection of the parameters (that is, the average membrane potential (AMP) and the average impulse density (AID)) in the synaptic modification algorithm, in which the decrease of synaptic strength is supposed to be essential. This synaptic modification algorithm using AMP and AID enables both the rhythmic oscillation and the non-oscillatory state to be dealt with in the algorithm without distinction. Simulation demonstrates cases in which the algorithm catches and holds the rhythmic oscillation in disturbed ring networks where rhythmic oscillation was previously extinguished.

In Chap.3, the relationship between the mechanism of memory and bursts of nerve impulses is discussed and a new memory model based on the algorithm described in Chap.2 is proposed. When the constants in the algorithm are fixed, two modes, namely the storing mode and the recalling mode, can be selected according to the excitatory input level to excitatory cells alone. This indicates that the ring neural network to which the synaptic modification algorithm is applied may function as a memory which stores and recalls information in the form of bursts of nerve impulses. Also considered is the possibility that multiple pieces

of information can be selectively stored in the overlapped ring network.

For the ring neural network to function as a generator of rhythmic oscillation, mechanisms are required by which rhythmic oscillation is generated and maintained and then its period controlled. In Chap.4, it is demonstrated by simulation that those mechanisms can be actualized by employing the synaptic modification algorithm proposed in Chap.2 and by applying inputs from the outside to excitatory and inhibitory cells. The two-mode selection mechanism described in Chap.3 solves the problem of the re-modification caused by the dispersion of AIDs with the application of the excitatory synchronous input to inhibitory cells.

In Chap.5, a new learning model of the cerebellum is proposed based on the theories described in Chaps.2, 3, and 4. The synaptic modification algorithm proposed in Chap.2 is applied to all the modifiable synapses in the model, through which process the granule-Golgi network works as a generator of rhythmic oscillation and the basket-stellate-Purkinje network acts as a wave synthesizer. The final output of this model after learning has the inverse phase of the signals from the climbing fibers.

Contents

Chapter 1

Introduction

First appearing on the scientific scene as a prototype of the present Neumann-type computer, EDVAC employed for the first time the logical operational unit, the so called E-element, which was adopted on the analogy of a neuron model by McCulloch and Pitts (Neumann, 1945). Since then, computer technology has developed rapidly and its capacity and speed have increased tremendously. The human brain performs pattern recognition and associative processing naturally and with ease, but even though the development of electronics has made a great impact on the various scientific fields, it is now clear that the mechanism of human information processing includes essential problems insoluble with only the capacity and speed of a computer.

In the most progressive field of computer science at present, the aim of the research is turning toward improving on the kind of computer architecture employed by the Neumann-type computer. However the structure of human brain is not necessarily being taken into account in this research. The fact that information processing systems constructed in consideration of neural cells have come to require a different structure from that of the human brain may be significant. Looking back on the 1940's, this divergence in approach is considered to result from the fact that the mechanism of self-organization by modifiable synapses was not clarified at that time. It would be of great

significance to know the methodology of the human information processing system which has developed over the long period of evolution, not only for scientific interest in itself, but also as a technology for creating a new type of processing system.

In the nervous system, information is transmitted by nerve impulses created by membranes with non-linear permeability. Various mathematical models of the membrane have made it clear that the nerve impulses are kinds of solitary waves with the same shapes and that they are very stable in the absence of interference or attenuation (Scott, 1975; Toda, 1975; Maginu, 1978). The transmission speed is on the order of milliseconds, which is much slower than that of the latest electronic devices. In spite of this, the speed at which information is processed as a whole is very high. This indicates that the nervous system has a large degree of parallel processing.

These days, brain research is exciting a lot of interest in various fields of scientific investigation. In the information science, there have been many studies concerning the mechanism of and the ability for information processing in the neural network (Block, 1962a,b; Minsky, 1969; Kuijpers et al., 1973). Some synaptic modification algorithms directing the performance of these networks have been put forward, and they play an important role in explaining the mechanisms of association and memory (Nakano, 1972; Fukushima, 1973; Wigström, 1973, 1974, 1975; Ellias et al., 1975). Neural network models in which feature extraction cells are located hierarchically, based on neurophysiological findings, have been proposed, and they contribute to the solution of the essential mechanisms of pattern

recognition, i.e., shift, extension, contraction, distortion, etc. (Fukushima, 1975, 1980; Deutsch, 1981). A neural network model for the development of direction selectivity has been proposed (Nagano, 1979), and research has also been done to try to explain the anatomical structure of the nervous system (Malsburg, 1973, 1978; Nagano, 1977, 1980, 1981). Recently, the goal-seeking problem has been investigated by the construction of associative search networks (Barto et al., 1981a,b, 1982). These networks have the potential to control the manipulator with many degrees of freedom, if they can be enhanced by the introduction of a storage mechanism for temporal pattern sequences (Willwacher, 1982).

However, it has often been observed that the density of the impulses from a cell varies from time to time in the real nervous system and it is a well-known fact that the input signals from the sensory organs and the output signals to the actuators consist of bursts of nerve impulses (Pearson, 1979). Since neurons are threshold elements, bursts of nerve impulses are created in a simple neuron under the injection of slow varying current. Injecting sinusoidally modulated current into the soma of an identified pond snail's neuron, entrained responses and phase-locked responses have been analyzed (Holden et al., 1981a,b, 1982). In the identified neural networks, for example those of leeches, cockroaches, lobsters, etc., the mechanisms of locomotory rhythm have been investigated and the central part of such frameworks has been found to be bursts of nerve impulses (Friesen et al., 1977; Clarac et al., 1982; Heetderks et al., 1982; Thompson, 1982). A model of the spinal rhythm generator in

which alternating bursts of nerve impulses are drawn as the final output has been proposed (Kawahara et al., 1982).

It should be remembered that signals varying their impulse densities rhythmically are obtained not only from fixed synapses from the genetic information, but also from the synaptic modification resulting from the application of some algorithm, this latter mechanism assuring stability against structural disturbances in the neural network. In the models for learning, information itself is thought to be a time-invariant analog or digital value (in impulse density). Consequently, the algorithms already proposed are mostly applicable to those networks which can only deal with the time-invariant signals mentioned above, and the relationship between the synaptic modification algorithm and the bursts of nerve impulses (that is, rhythmic oscillation in impulse density) has never been studied.

Cases have actually been researched in which rhythmic oscillation occurs in the neural network with feedback inhibition composed of analog neuron models with time delay (Morishita et al., 1972; Stein et al., 1974a,b; Tokura et al., 1977; Mitchell et al., 1981). The problem is where rhythmic oscillation should be placed in the information processing of the neural network: whether its existence is limited to part of the real nervous system or whether it is concerned with all of the neuronal signals in forms of life ranging from the lower animals to human beings. If the latter is the case, new theoretical approaches are required including a synaptic modification algorithm (Tsutsumi et al., 1984). As a first step toward the solution of this problem, a synaptic modification algorithm is proposed in Chap.2 and its

action on bursts of nerve impulses is studied.

It is generally accepted that synaptic plasticity is involved in the mechanism of memory and that information is distributively stored. Even if the neural network sustains local structural damage, loss of information does not necessarily occur. This phenomenon is assumed to be directly related to the processing of ambiguous information and to the problem of association. In Chap.3, a new memory model based on the synaptic modification algorithm described in Chap.2 is proposed, and the relationship between the mechanism of memory and bursts of nerve impulses is examined (Tsutsumi et al., to appear).

The periods of the oscillation generated by the algorithm differ with the network constants etc. If certain mechanisms to control the period of rhythmic oscillation can be found in the ring neural network, these mechanisms may explain various rhythmical phenomena. In Chap.4, it is analyzed how the generation and control of rhythmic oscillation can be actualized in the ring neural network (Tsutsumi et al., to appear).

It would be of great significance to know which kind of signal is utilized by the central nervous system located between the sensory organs and the actuators. The structure of the cerebellum is unique among the parts of the central nervous system, and the anatomy and physiology of its cortical elements are fairly well known, which make it an ideal subject for study. Employing the synaptic modification algorithm and the related theories for rhythmic oscillation described in Chaps.2, 3, and 4, a new learning model of the cerebellum is put forward in Chap.5 (Tsutsumi et al., in review).

In Chap.6, the proposals and the results detailed in this thesis are summarized and the course of future research is discussed.

Chapter 2

Synaptic Modification Algorithm

In consideration of the generation of bursts of nerve impulses (that is, rhythmic oscillation in impulse density) in the ring neural network, a synaptic modification algorithm is newly proposed. Our preliminary investigation into the rhythmic oscillation in the regular ring network led to the selection of the parameters, that is, the average membrane potential (AMP) and the average impulse density (AID) in the synaptic modification algorithm, where the decrease of synaptic strength is supposed to be essential. This synaptic modification algorithm using AMP and AID enables both the rhythmic oscillation and the non-oscillatory state to be dealt with in the algorithm without distinction. Simulation demonstrates cases in which the algorithm catches and holds the rhythmic oscillation in disturbed ring networks where the rhythmic oscillation was previously extinguished.

2.1 Introduction

Rhythmic oscillation generally occurs in the regular ring network with feedback inhibition and in fact such signals can be observed in the real nervous system. Since, however, various additional connections can cause a disturbance which easily extinguishes the rhythmic oscillation in the network, some

function for maintaining the rhythmic oscillation is to be expected to exist in the synapses if such signals play an important part in the nervous system. As a first step toward the solution of this problem, this chapter proposes a synaptic modification algorithm and studies how it acts on bursts of nerve impulses.

Firstly, in Sect. 2.2, the neural network with feedback inhibition composed of analog neuron models with time delay is formulated. In Sect.2.3, various parameters are defined for the rhythmic oscillation occurring in the regular ring network, which is a special form of the neural network with feedback inhibition, and the characteristics of each parameter in relation to the network constants are investigated. It is ascertained that only the average impulse density (AID) is particularly unaffected. In Sect. 2.4, the influence on rhythmic oscillation of various disturbing connections added to the regular ring network is also studied, and it is shown that these connections can easily extinguish the rhythmic oscillation. In this case the AID from each cell changes greatly with the disappearance of rhythmic oscillation.

Accordingly, we assume that the value of the AID which is particularly unaffected in the regular ring network will be equal to the AID of the uniform rhythmic oscillation generated in a generally-connected neural network with feedback inhibition. Under this assumption, a new synaptic modification algorithm is proposed in Sect.2.5. In this algorithm, levels of the outputs of the neural cells which exceed the ordinary value of the AID in the regular ring network are interpreted as being of high

density, and the strength of a synapse decreases when high density impulses pass through it for a certain length of time. By then introducing the average membrane potential (AMP) into the algorithm, both the rhythmic oscillation and the non-oscillatory state can be dealt with without distinction. Simulation shows in Sect.2.6 that the rhythmic oscillation can be brought back and then held (in the sense that the modification speed drops to an extremely low level), by applying the synaptic modification algorithm to some disturbed ring networks where the rhythmic oscillation was previously extinguished. The bursts of nerve impulses created by this algorithm are probably related to the mechanism of memory and association, since the characteristics of all modifiable synapses are fundamentally the same. In Sect. 2.7, the problems remaining to be solved and a proposed course for future research are discussed.

2.2 Neural Network with Feedback Inhibition

The neural network with feedback inhibition considered here is shown in Fig.2.1. It consists of two types of neural cells, namely excitatory and inhibitory cells, and the outputs of the former are fed back to themselves via the latter. Here, the additional inputs from the outsides are added only to the excitatory cells, and our interest is focused on the effects of feedback. These cells are connected by synapses and the strength of each of them is independent. The analog neuron models with time delay are employed according to the objective mentioned in

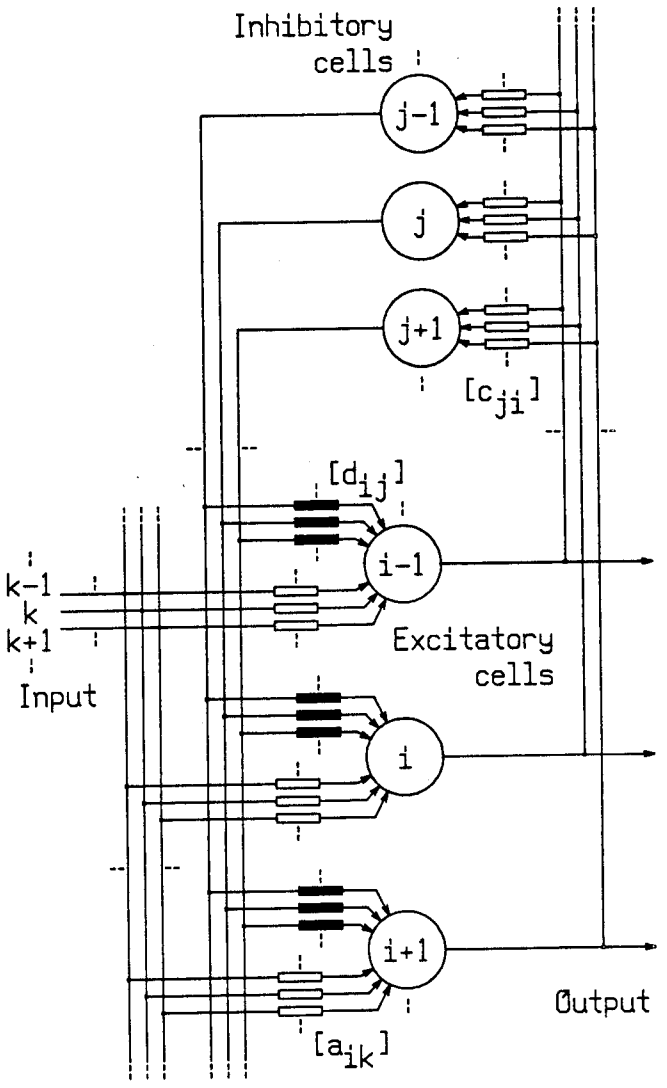

Fig.2.1. A schematic diagram of the neural network with feedback inhibition. The additional inputs from the outside are added only to the excitatory cells in order to concentrate on the effects of feedback.

the introduction of this chapter. Therefore, the network equations can be presented as follows:

$$\tau_1 \frac{d}{dt} x_i^{(1)}(t) + x_i^{(1)}(t) = u_i^{(1)}(t) - \sum_{j=1}^{N_2} d_{ij} \lceil x_j^{(2)}(t) \rceil^+$$

$$u_i^{(1)}(t) = \sum_{k=1}^{M} a_{ik} v_k(t) \qquad (i=1,2,---,N_1)$$

$$\tau_2 \frac{d}{dt} x_j^{(2)}(t) + x_j^{(2)}(t) = \sum_{i=1}^{N_1} c_{ji} \lceil x_i^{(1)}(t) \rceil^+ \qquad (2.1)$$

$$(j=1,2,---,N_2)$$

where

$$\lceil \xi \rceil^+ = \begin{cases} \xi & \xi > 0 \\ 0 & \xi \leq 0 \end{cases} . \qquad (2.2)$$

Here $x_i^{(1)}(t)$ and $x_j^{(2)}(t)$ are the membrane potentials of the excitatory cells and the inhibitory cells respectively and they are converted into impulse densities by Eq.(2.2). τ_1 and τ_2 are the integral time constants of each layer, that is, the speeds of the responses, and a_{ik}, c_{ji}, and d_{ij} are the synaptic strengths which correspond to Fig.2.1.

2.3 Ring Neural Network

2.3.1 Rhythmic Oscillation

The neural network described by Eq.(2.1) comes to be ring-structured by choosing synaptic strengths adequately. Among them, the network with the following synaptic strengths is called the regular ring network, in which a state of rhythmically

$$c_{ji} = \begin{cases} \alpha & \text{if } i=j \\ 0 & \text{otherwise} \end{cases}$$

$$d_{ij} = \begin{cases} \beta_1 & \text{if } j=i+1 \\ \beta_2 & \text{if } j=i-1 \\ 0 & \text{otherwise} \end{cases} \qquad (2.3)$$

$$(i=1,2,---,N_1,\ j=1,2,---,N_2,\ N_1=N_2=N)$$

varying impulse density can exist. Figure 2.2a illustrates the structure of the regular ring network and Fig.2.2b shows the membrane potentials of excitatory cells $x_i^{(1)}(t)$, $(i=1,2,---,5)$ when $N=5$, $\tau_1=2.0$, $\tau_2=10.0$, $u_i^{(1)}(t)=u$, $(i=1,2,---,5)$, $\alpha=1.0$, $\beta_1=3.0$ and $\beta_2=0.5$, where a set of oscillations with different phases occurs steadily.

Here we define the periods p and p^+ as shown in Fig.2.2b, and the average membrane potential (AMP) and the average impulse density (AID) as follows:

$$\text{AMP} : \text{av}\,[\,\zeta(t)\,] = (1/p)\int_{t-p}^{t} \zeta(t')\,dt' \qquad (2.4)$$

$$\text{AID} : \text{av}\,[\,\lceil\,\zeta(t)\,\rceil^{+}\,] = (1/p)\int_{t-p}^{t} \lceil\,\zeta(t')\,\rceil^{+}\,dt' \qquad (2.5)$$

The parameters p, p^{+}, AMP, and AID change with the values of the network constants τ_1, τ_2, β_1, β_2, and N. In what follows,

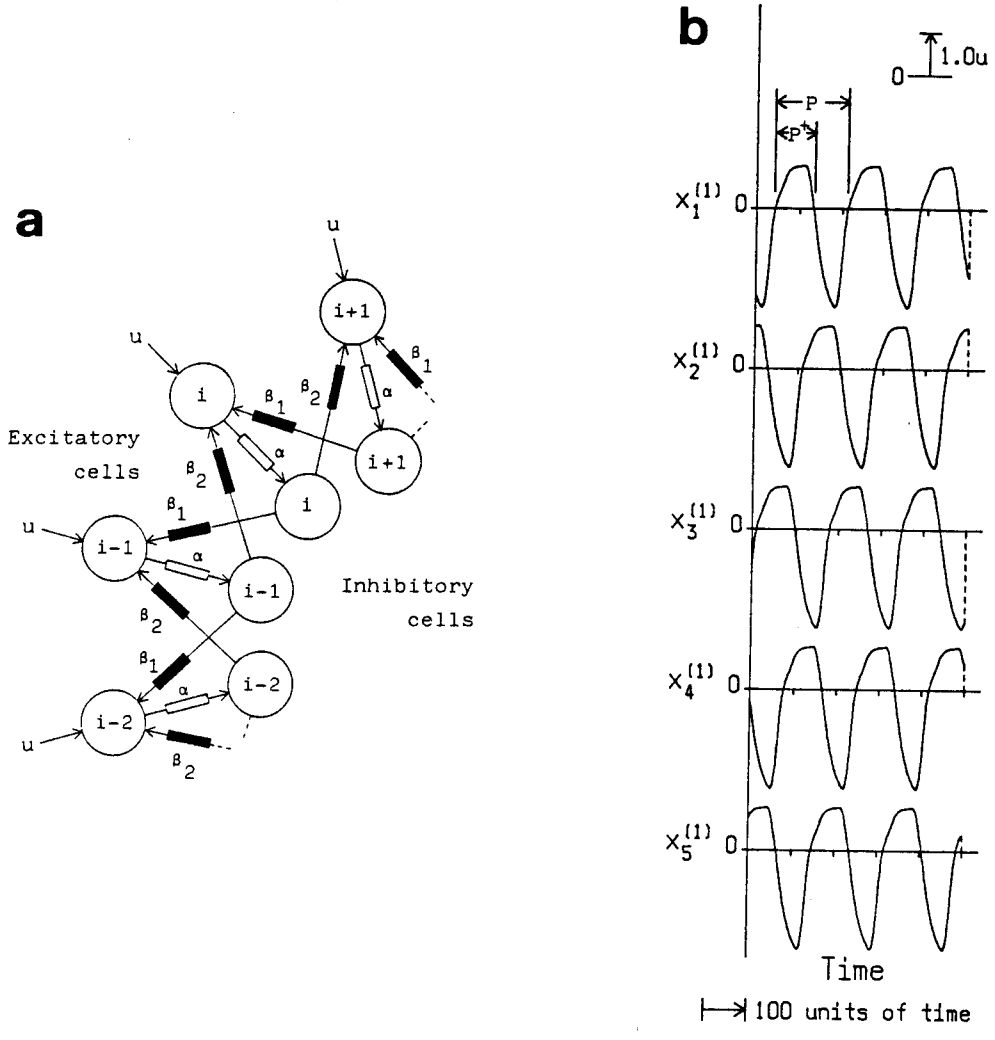

Fig.2.2. **a** The structure of the ring neural network. **b** The membrane potentials of excitatory cells, $x_i^{(1)}(t)$, (i=1,2,---,5), in the regular ring network, when N=5, τ_1=2.0, τ_2=10.0, $u_i^{(1)}(t)$=u, (i=1,2,---,5), α=1.0, β_1=3.0, and β_2=0.5.

the influence of each network constant on the parameters is discussed. In the following figures, the regions around the boundaries which are especially difficult to calculate are omitted, because it seems more important to understand fully the overall characteristics of the change.

2.3.2 Integral Time Constants

The relationships between the integral time constants τ_1 and τ_2 and the parameters for the outputs of excitatory cells, that is, p, p^+, p^+/p, AMP, AID, and AID/(AID-AMP) are shown in Figs.2.3a-c and 2.4a-c, respectively, when N=5, β_1=3.0, and β_2=0.5. The influence of τ_1 and τ_2 on the parameters is equal because $\lceil x_j^{(2)}(t) \rceil^+ = x_j^{(2)}(t)$ in Eq.(2.1), and therefore the figures are symmetrical about the straight line $\tau_1 = \tau_2$ (see Appendix A-1).

As illustrated in Figs.2.3a-c and 2.4a-c, the periods p and p^+ linearly increase with the increase in τ_1 and τ_2, although p^+/p is constant and AMP, AID, and AID/(AID-AMP) (which means the ratio of the excitation to the inhibition) are not affected by τ_1 and τ_2. This implies that the rhythmic oscillation under discussion in this subsection only expands and contracts along the time axis with regard to the changes in τ_1 and τ_2.

2.3.3 Synaptic Strengths

Figures 2.5a-c and 2.6a-c show the relationships between synaptic strengths β_1 and β_2 and the parameters when N=5,

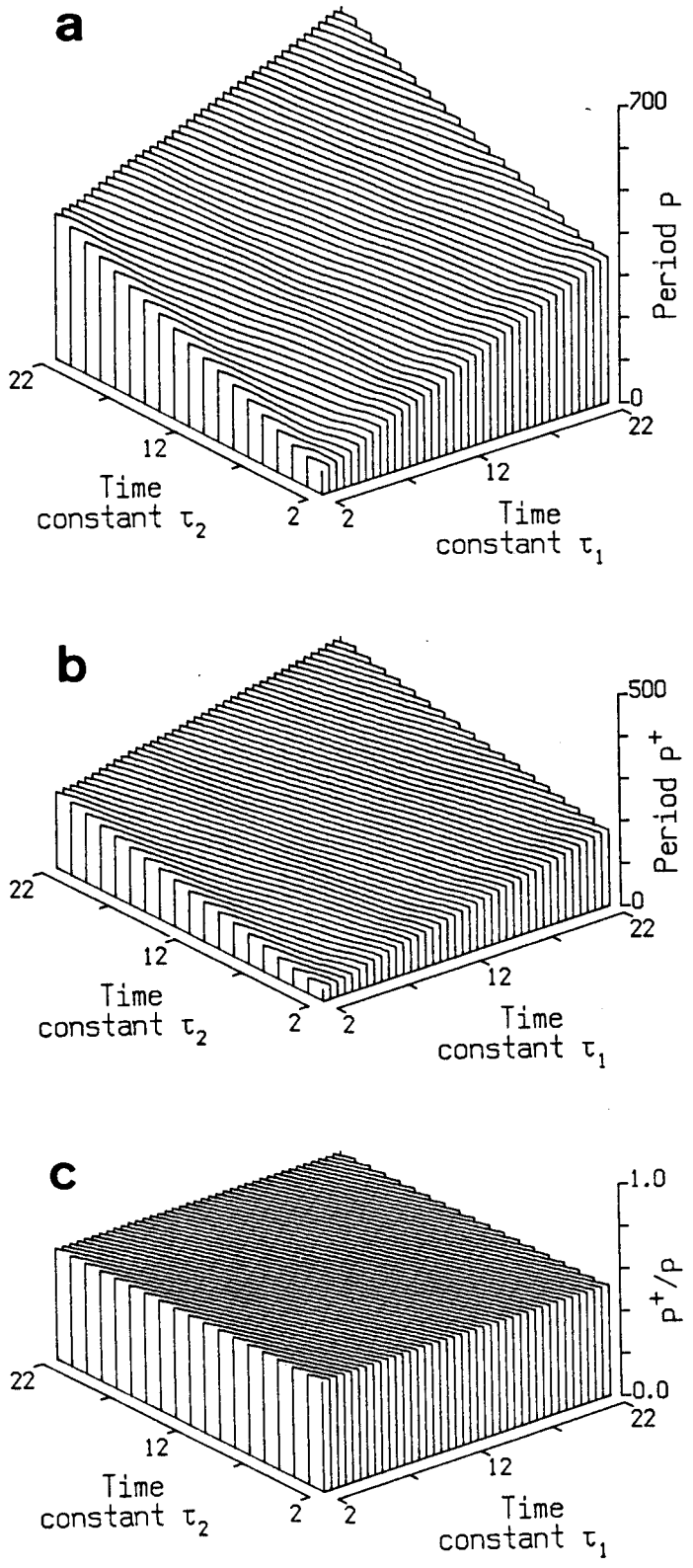

Fig.2.3a-c. The relationships between the time constants τ_1 and τ_2 and the parameters p, p^+, or p^+/p.

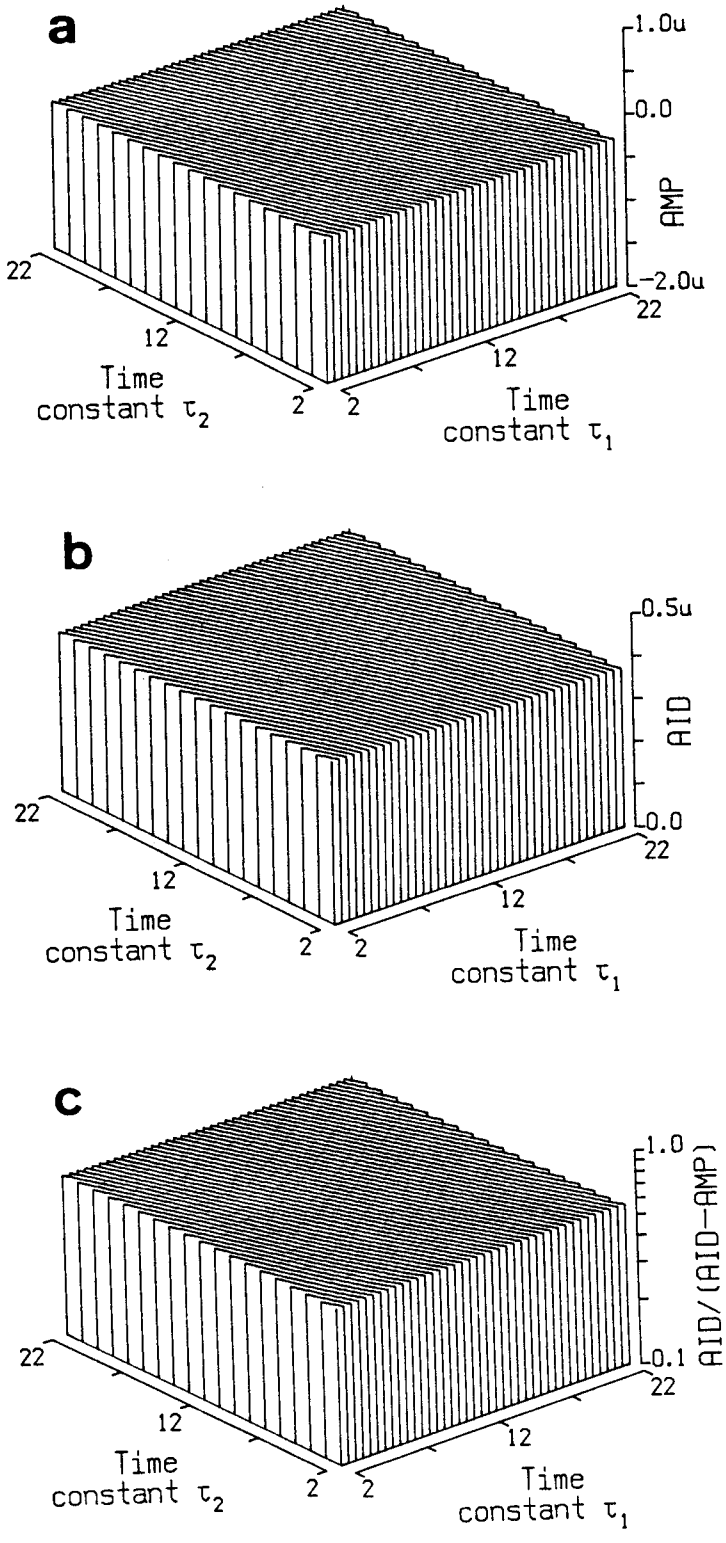

Fig.2.4a-c. The relationships between the time constants τ_1 and τ_2 and AMP, AID, or AID/(AID-AMP), which means the ratio of the excitation to the inhibition.

τ_1=2.0, and τ_2=10.0, where a maximum of 144 couples of β_1 and β_2 are chosen to calculate by using spline interpolation.

In Fig.2.5a and b, when β_1 is small or β_2 is large, p and p^+ change abruptly with β_1 and β_2 and the rhythmic oscillation disappears. On the other hand, p and p^+ are hardly affected by β_1 and β_2 when β_1 is large and β_2 is small. This indicates that β_1 and β_2 have little influence on p and p^+ when the synaptic strength in one direction of the ring structure is much greater than that in the other, that is, when the direction of the ring is definite. However, since rhythmic oscillation cannot exist when the synaptic strength β_2 is extremely small, it is necessary for stability of the rhythmic oscillation against minute changes of τ_1 and τ_2 that the synaptic strengths in both the clockwise and the anticlockwise directions be adequately balanced. This holds not for the relative synaptic strengths but for the absolute strengths at a certain level and above, as is evident from Fig.2.5c when both β_1 and β_2 are small, where p^+/p increases abruptly because the direction is definite, but the total inhibition is very small.

In Fig.2.6a-c, although β_2 has no influence on the AMP in contrast to its influence on the periods p and p^+, β_1, which determines the direction of the ring, produces a proportional change on the AMP. On the other hand, the AID is not affected by β_1 or β_2 and remains constant. Therefore it can be concluded that β_1 and β_2 have influence only on the negative part of $x_i^{(1)}(t)$.

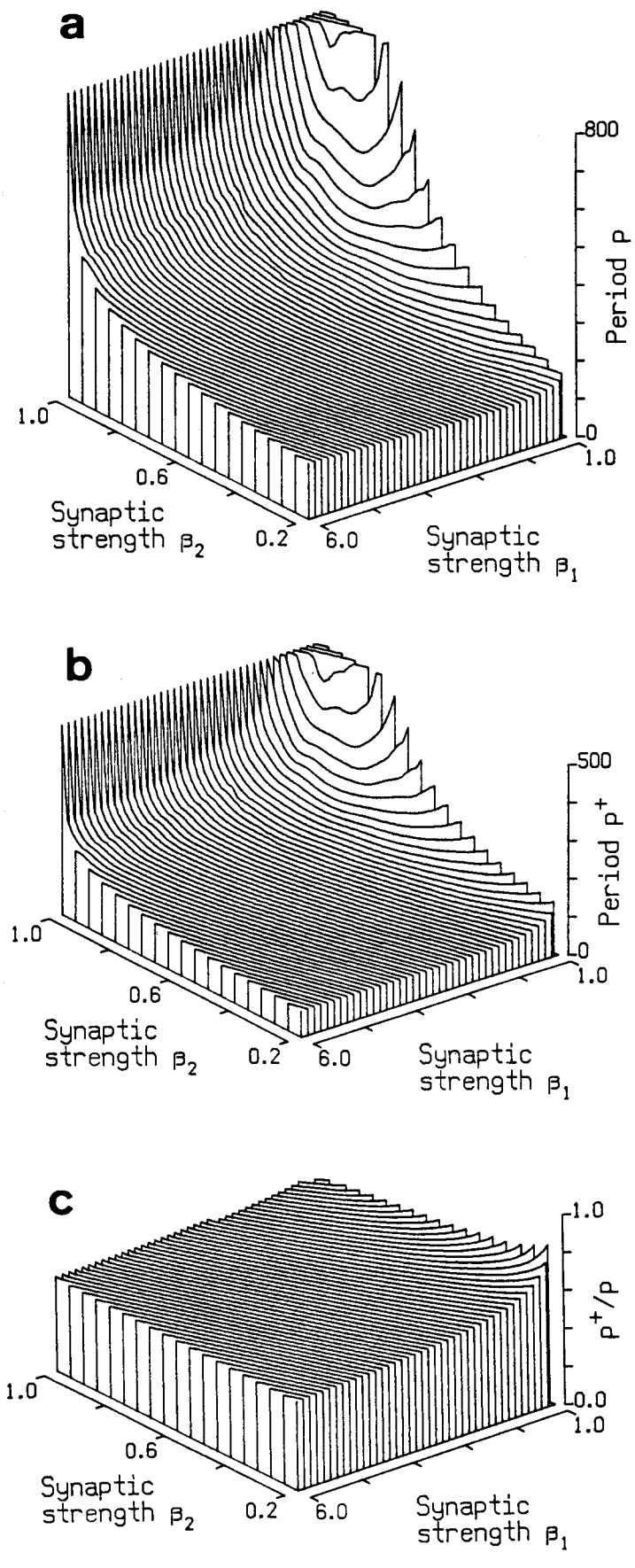

Fig.2.5a-c. The relationships between the synaptic strengths β_1 and β_2 and p, p^+, or p^+/p.

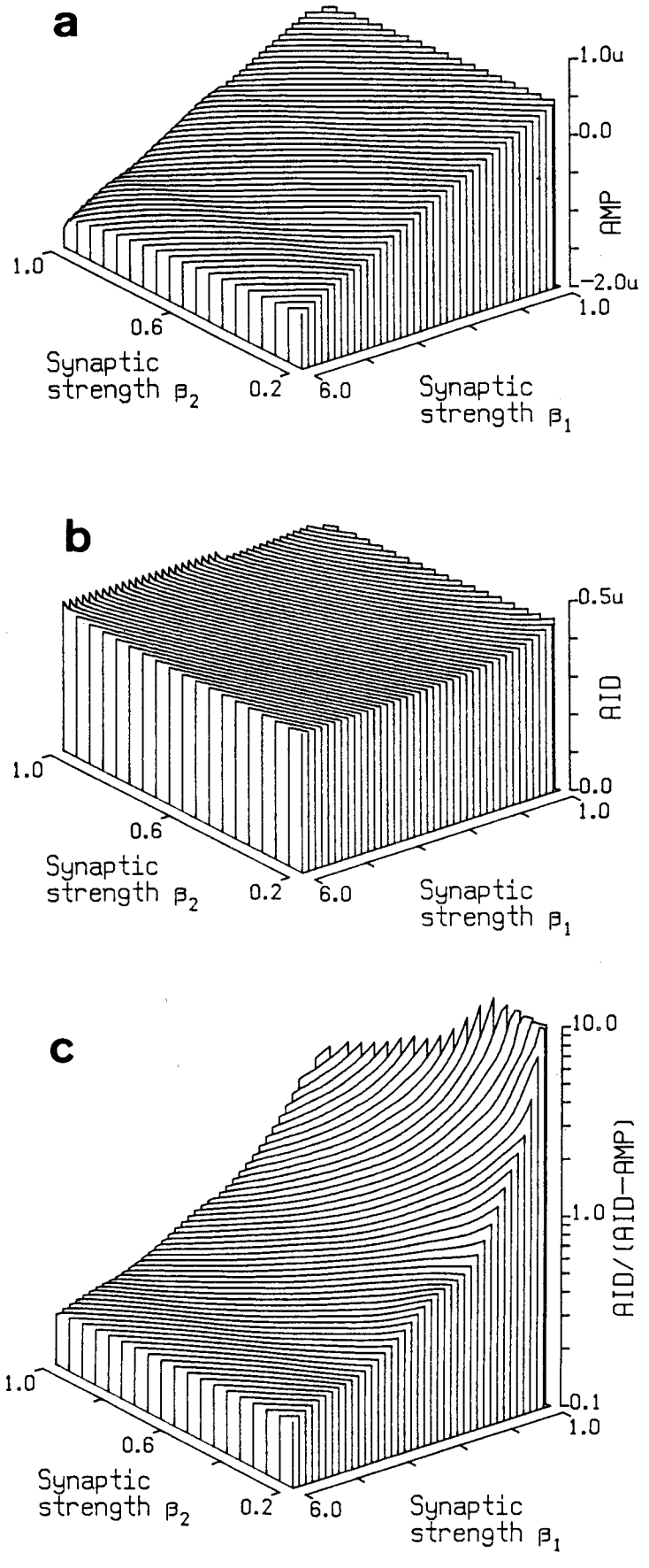

Fig.2.6a-c. The relationships between the synaptic strengths β_1 and β_2 and AMP, AID, or AID/(AID-AMP).

2.3.4 The Number of Cells

The characteristics of rhythmic oscillation are also affected by the number of cells. Figures 2.7a-c and 2.8a-c illustrate the relationships between the number of cells N (N:odd number) and the parameters on 4 pairs of τ_1, τ_2, β_1, and β_2. As shown in Fig.2.7a-c, p and p^+ increase linearly in proportion to the number of cells except in the case of N=3, (so that the extended lines may pass through the point of origin), and therefore p^+/p is almost constant. When N≥5, the influence of the number of cells on the periodical property is very similar to that of the time constants: the periods p and p^+ may be linearly controlled by the number of cells and/or the time constants.

In Fig.2.8a-c, the AMP decreases and tends to converge on certain values depending on β_1 and β_2 as the number of cells is increased. The reason for this may be that the total inhibition of one round to each cell is different if the number of cells is different, even if every local arc of the ring network is the same. Also, the graph may become saturated since the influence from the more distant cells is smaller. On the other hand, the AID remains almost constant independent of τ_1, τ_2, β_1, and β_2 when N≥5, although it also increases gradually with an increasing number of cells.

2.4 Disturbed Ring Network

In this section, cases are considered in which the regular

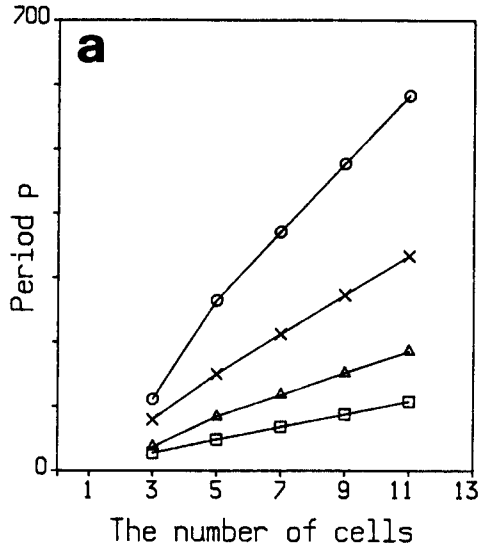

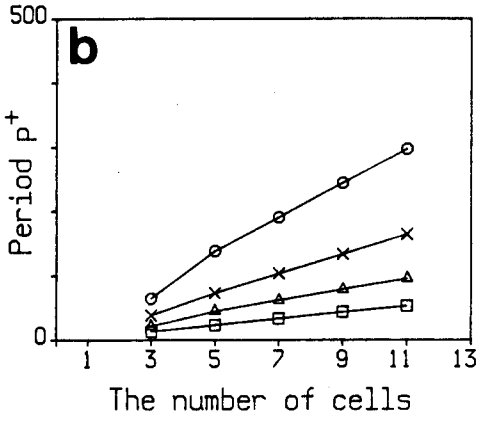

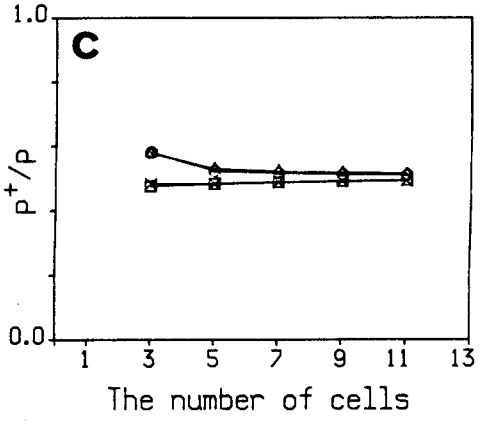

Fig.2.7a-c. The relationships between the number of cells N and p, p^+, or p^+/p. Here,

- ○ - ○ : τ_1=2.0, τ_2=10.0, β_1=3.0, and β_2=0.8.
- × - × : τ_1=2.0, τ_2=10.0, β_1=5.0, and β_2=0.3.
- △ - △ : τ_1=2.0, τ_2=2.0, β_1=3.0, and β_2=0.8.
- □ - □ : τ_1=2.0, τ_2=2.0, β_1=5.0, and β_2=0.3.

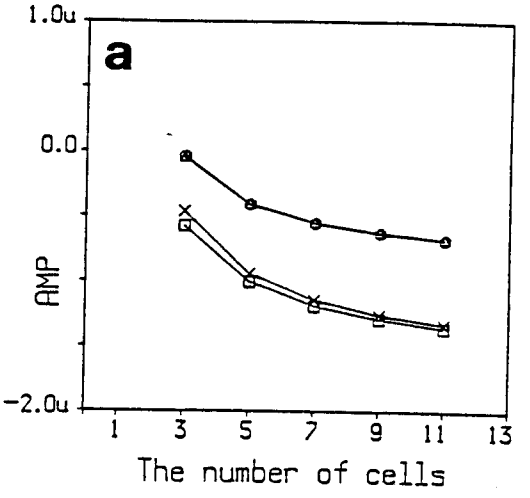

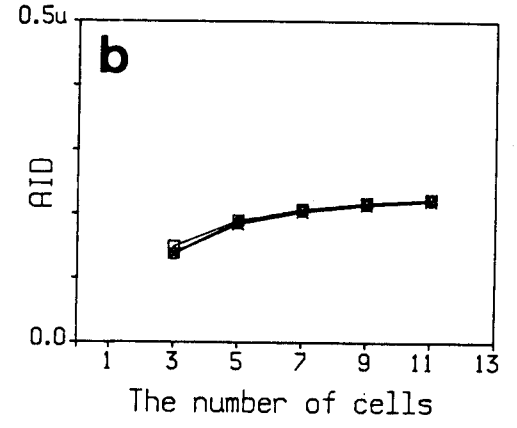

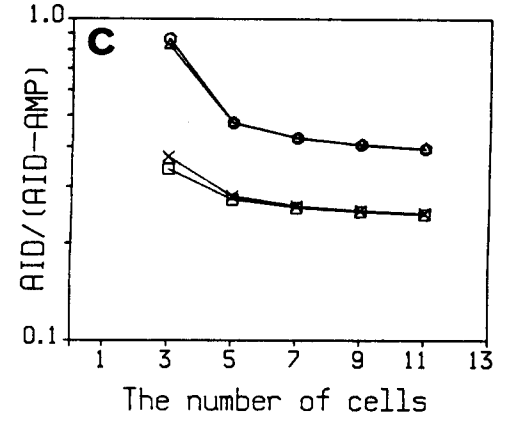

Fig.2.8a-c. The relationships between the number of cells N and AMP, AID, or AID/(AID-AMP). The values in these four cases are the same as the ones in Fig.2.7.

ring network described in Sect.2.3 is disturbed by various connections.

Figure 2.9 illustrates $\lceil x_i^{(1)}(t) \rceil^+$ in the disturbed ring network with one disturbance $d_{13} = \beta_{dist}$, in which β_{dist}=0.0, 0.45, and 0.75 in turn from left to right. In the case of β_{dist}=0.45, the period is longer and the output waveform of each cell loses its uniformity, compared with the case of β_{dist}=0.0. The trends are clearly upward with the increasing strength of the disturbance and the rhythmic oscillation disappears when β_{dist}=0.75: cell No.3 and cell No.5 emit only non-oscillatory signals and the others have no output.

This figure further shows that the AID of each of the cells which was unaffected in the regular ring network comes to differ from cell to cell as a result of the disturbance and the maximum difference is reached when the rhythmic oscillation disappears. Of course, there are cases where the outputs are unchanged by a disturbance of comparable strength, since the effect depends on the position and the number of cells. However, it is a fact that the rhythmic oscillation in the regular ring network can be extinguished by various additional connections.

Although it is difficult to fully understand the influence of the disturbance on the output in every case, such an effort will not always be necessary when the synaptic modification algorithm is pursued according to the objective of this chapter. The first step in explaining the adequacy of the algorithm is to check whether the disappeared oscillation can be brought back or not. In this sense, only the cases where the disturbance changes the outputs are important. Figure 2.9 is one of the simplest and

most typical examples of the disturbance which changes the outputs.

2.5 Synaptic Modification Algorithm

Various synaptic modification algorithms for examining the ability for learning of the neural network have been proposed since Hebb offered his in 1949. However, where the above-mentioned oscillation should be positioned in the study of learning has never been discussed and hence there exists no synaptic modification algorithm related to this problem.

In this section, a new synaptic modification algorithm is proposed. Firstly, we concentrate on the AID which was particularly unaffected among the parameters for rhythmic oscillation in the regular ring network described in Sect.2.3. We assume that this AID value will be equal to the AID of uniform rhythmic oscillation occurring in a generally-connected neural network with feedback inhibition, in the sense that it is so well-defined that it can represent the existence of or the state of rhythmic oscillation. Then we attach great importance to neurophysiological knowledge that the strength of a synapse decreases when high density impulses pass through it for a certain length of time, and we interpret levels of the outputs of the neural cells which exceed the AID of the rhythmic oscillation in the regular ring network as being high density impulses.

In general, a synaptic modification algorithm should be defined by the relationship between two kinds of information,

that is, the signal reaching a synapse and the post-synaptic state. Not the membrane potential itself but its average over a certain period of time, namely AMP, is adopted here as post-synaptic information. Hence the introduction of the AID and AMP enables the synaptic modification algorithm to treat both the rhythmic oscillation and the non-oscillatory state in the same way.

As a result of this consideration, the synaptic modification algorithm is constructed as shown below: synaptic strength $w_{ji}(t)$ from cell No.i in layer No.q to cell No.j in layer No.r at time t will be modified after a unit of time Δt by Eqs.(2.6) and (2.7).

$$w_{ji}(t+\Delta t) = w_{ji}(t) + \Delta w_{ji}(t) \tag{2.6}$$

where

$$\Delta w_{ji}(t) = -\delta^{(q)} \left\lceil av\left[\left\lceil x_i^{(q)}(t)\right\rceil^+\right] - \theta^{(q)}\right\rceil^+ \times \left\lceil av\left[x_j^{(r)}(t)\right] - \eta^{(r)}\right\rceil^+ . \tag{2.7}$$

The synaptic strength is decreased as the difference between the AID and θ is increased when the AID exceeds θ, and as the AMP of the post-synaptic cell exceeds η.

Here the window function $\psi(t, \sigma)$ is introduced and av[$\cdot$] which was defined by Eqs.(2.4) and (2.5), is practically redefined as follows:

$$\text{AMP} : av\left[\zeta(t)\right] = \int_{-\infty}^{t} \psi(t', \sigma)\, \zeta(t')\, dt' \tag{2.8}$$

$$\text{AID} : \text{av}\,[\,\lceil\,\zeta(t)\,\rceil^{+}\,] = \int_{-\infty}^{t} \psi(t', \sigma)\,\lceil\,\zeta(t')\,\rceil^{+}\,dt' \,. \quad (2.9)$$

The window function $\psi(t', \sigma)$ is used to count nerve impulses in the period from $t-\sigma$ to the present t, regardless the existence of rhythmic oscillation. The following rectangular window function $\psi(t', \sigma)$ is the simplest one.

$$\psi(t', \sigma) = \begin{cases} 1/\sigma & t - \sigma \leq t' \leq t \\ 0 & \text{otherwise} \end{cases} \quad (2.10)$$

Equations (2.8) and (2.9) are equivalent to Eqs.(2.4) and (2.5) if $\sigma = p$. This formation enables the reduction of the influence of the calculating position on the AMP and the AID.

2.6 Synaptic Modification

The synaptic modification algorithm proposed in Sect.2.5 is applied to the disturbed ring networks where the rhythmic oscillation has been previously extinguished.

Figure 2.10 shows the result of the application of the modification algorithm whose constants are $\delta^{(1)}=0.0004/u^2$, $\theta^{(1)}=0.4u$, $\eta^{(1)}=-2.0u$, $\delta^{(2)}=0.0012/u^2$, $\theta^{(2)}=0.4u$, and $\eta^{(2)}=0.0u$ to the network on the right in Fig.2.9, where the rectangular window function defined by Eq.(2.10), (σ =500 units of time) is applied to calculate the AMP and the AID. Each figure from the left corresponds to the output impulse densities of

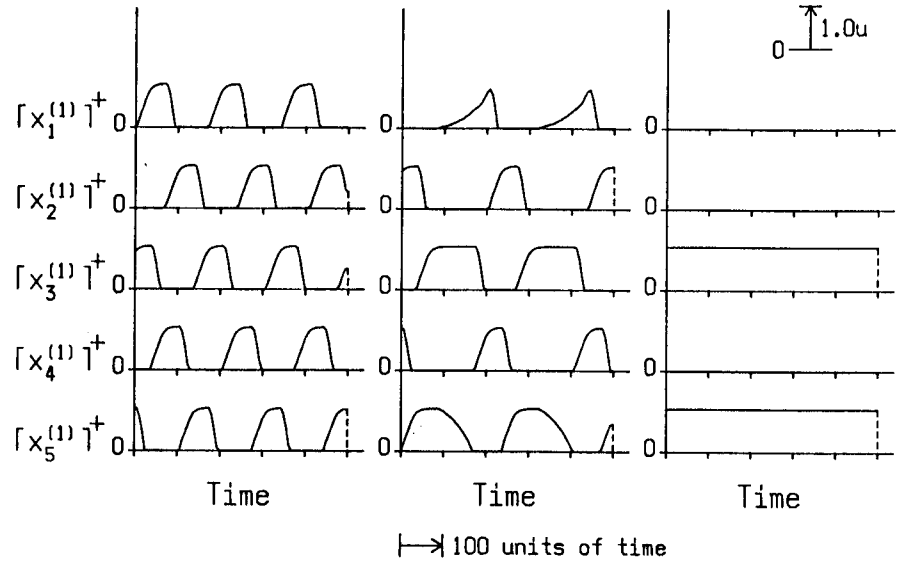

Fig.2.9. The outputs of excitatory cells in impulse density, $\lceil x_i^{(1)}(t) \rceil^+$, (i=1,2,---,5), in the disturbed ring network with one disturbance $d_{13} = \beta_{dist}$. β_{dist}=0.0, 0.45, and 0.75 in turn from left to right.

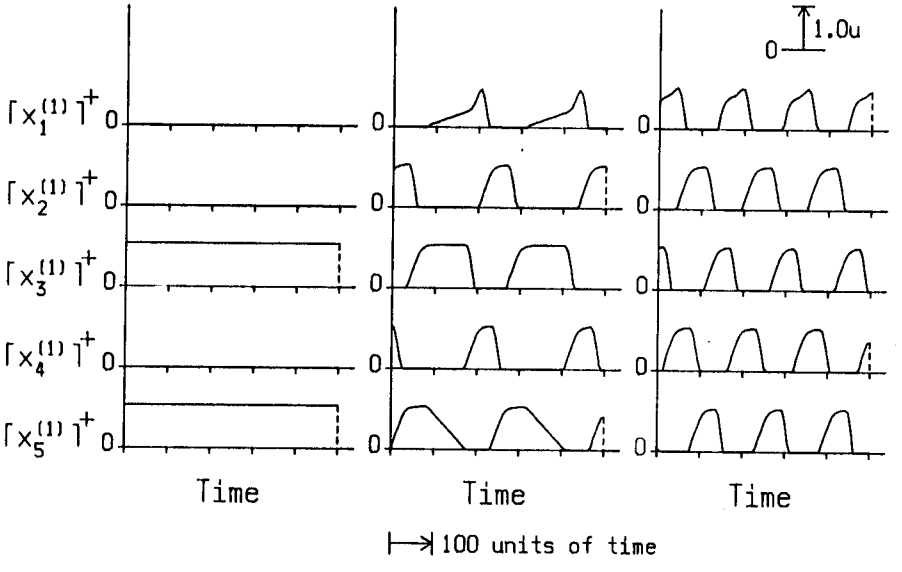

Fig.2.10. The result for the synaptic modification of applying the algorithm proposed in Sect.2.5 to the network on the right in Fig.2.9. The constants in the algorithm are $\delta^{(1)}=0.0004/u^2$, $\theta^{(1)}=0.4u$, $\eta^{(1)}=-2.0u$, $\delta^{(2)}=0.0012/u^2$, $\theta^{(2)}=0.4u$, and $\eta^{(2)}=0.0u$. Each figure from the left corresponds to the outputs of excitatory cells at a set of synaptic strengths (see Appendix A-2) after 0, 180, or 3000 modification steps.

excitatory cells at a set of synaptic strengths (see Appendix A-2) after 0, 180, or 3000 modification steps (equal to units of time), respectively.

Although $\lceil x_i^{(1)}(t) \rceil^+$ is not varying some time after the application of the algorithm [of course $x_i^{(1)}(t)$ varies at each step], the rhythmic oscillation is suddenly brought back after about 180 modification steps. At this point, the output waveforms are not uniform because of the imbalance of the inhibition. Further modification induces the period of the oscillation to become shorter and the output waveforms to become more uniform.

How the AID of each excitatory cell changes with the progress of the synaptic modification is shown in Fig.2.11a. The AID of each cell abruptly gathers around the threshold $\theta^{(1)}$ at the same time as the reappearance of rhythmic oscillation. After that it tends to converge gradually on $\theta^{(1)}$. Figure 2.11b illustrates the changes in the AMPs of excitatory cells, and after the reappearance of rhythmic oscillation the AMP of each cell converges around a certain value which depends on the amount of the inhibition. Figure 2.11c further shows the transitions in the AIDs (equal to the AMPs) of inhibitory cells, where each AID also gathers around the threshold $\theta^{(2)}$ after 700 modification steps. The differences between the threshold $\theta^{(1)}$ or $\theta^{(2)}$ and the pre-synaptic AIDs of excitatory cells or inhibitory cells whose AIDs exceed it decrease at a stage of sufficient modification, while the post-synaptic AMPs of those cells still differ from the value of $\eta^{(1)}$ or $\eta^{(2)}$. Therefore, as is evident from Eq.(2.7), the modification speed after the reappearance of rhythmic oscillation becomes extremely slow compared with that of

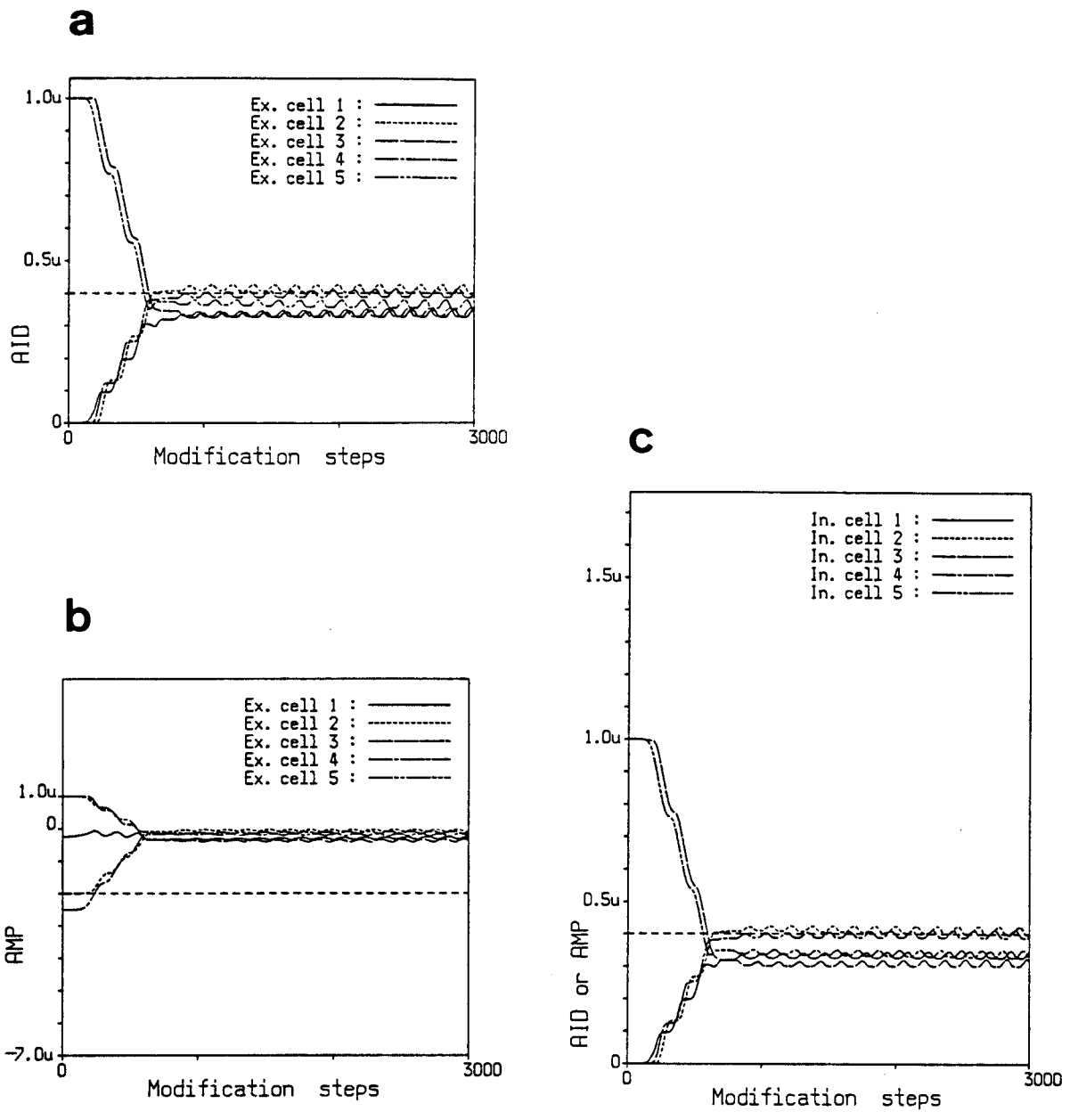

Fig.2.11a-c. The transitions in the parameters, namely the AID and the AMP, with the progress of the synaptic modification shown in Fig.2.10. **a** The changes in the AIDs of excitatory cells. The AID of each cell gathers around the threshold $\theta^{(1)}$ (equal to 0.4u) when rhythmic oscillation reappears in the network. **b** The changes in the AMPs of excitatory cells. The difference between the value of $\eta^{(1)}$ (equal to -2.0u) and each AMP provides post-synaptic information in the synaptic modification algorithm. **c** The changes in the AIDs (equivalent to the AMPs in this case) of inhibitory cells. Here $\theta^{(2)}$=0.4u and $\eta^{(2)}$=0.0u.

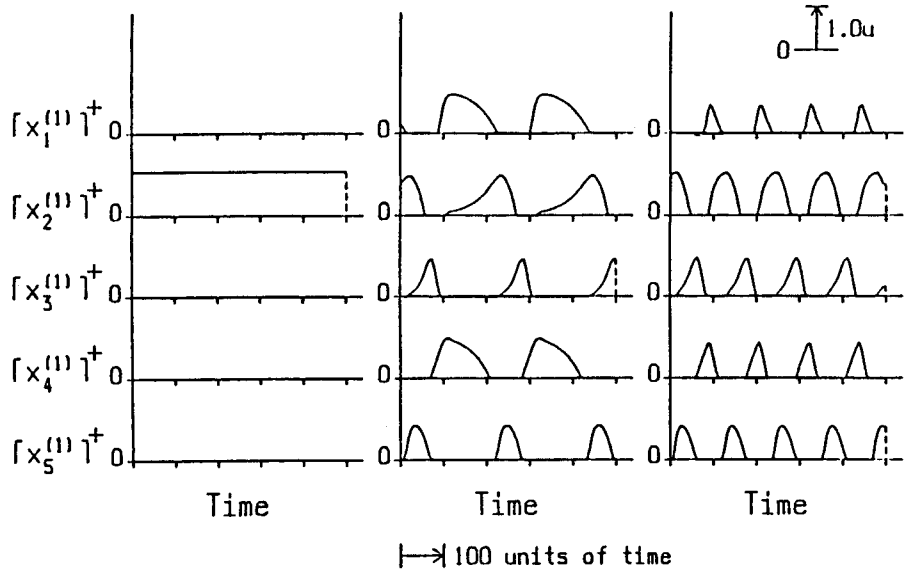

Fig.2.12. The result for the synaptic modification of applying the algorithm to the disturbed ring network with more complicated disturbances. Each figure from the left corresponds to the outputs of excitatory cells at a set of synaptic strengths (see Appendix A-3) after 0, 3000, or 6000 modification steps. The constants in the algorithm are the same as the ones used in Fig.2.10.

the non-oscillatory stage. This means that the synaptic modification algorithm can catch and hold the rhythmic oscillation. The ripples of the AIDs or the AMPs which appear after 800 modification steps in Fig.2.11a-c are caused by the window whose width is short in comparison to the period of the oscillation.

It should be noted that the rhythmic oscillation can be brought back and that the connection from cell No.3 to cell No.1 is not significantly attenuated, while the other connections are modified little by little. This suggests that it will be possible to store and recall information in the form of rhythmic oscillation in a network where the inputs are impressed, since it is not anticipated that the connections will be seriously damaged

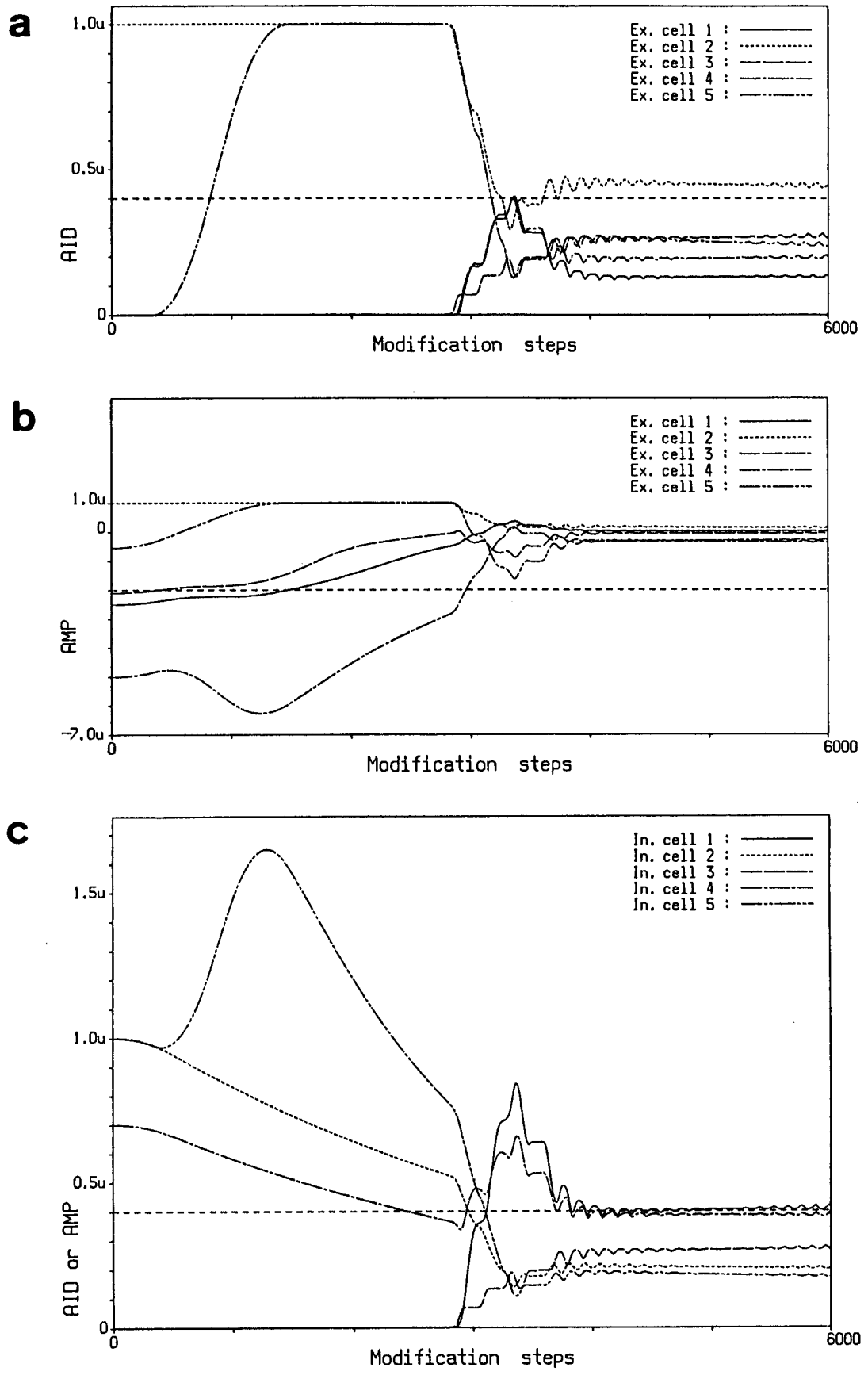

Fig.2.13a-c. The transitions in the AID and the AMP with the progress of the synaptic modification shown in Fig.2.12. a The changes in the AIDs of excitatory cells. b The changes in the AMPs of excitatory cells. c The changes in the AIDs of inhibitory cells.

when multi-rings are overlapped.

Figure 2.12 shows the result of the application of the synaptic modification algorithm to the disturbed ring network with more complicated disturbances. Each figure from the left corresponds to the outputs of excitatory cells at a set of synaptic strengths (see Appendix A-3) after 0, 3000, or 6000 modification steps respectively. Here the constants in the algorithm are the same as the ones in the previous example. The changes in the AIDs and the AMPs of excitatory cells and the AIDs of inhibitory cells are illustrated in Fig.2.13a-c. The figure indicates that the algorithm can catch and hold rhythmic oscillation in the same way, although the process toward the reappearance of rhythmic oscillation is more complicated and the greater number of modification steps is necessary.

2.7 Discussion

We have proposed a synaptic modification algorithm which makes allowance for the appearance of rhythmic oscillation in the ring neural network with feedback inhibition. It forms the foundation of the algorithm to decrease a synaptic strength in proportion to the result of $\lceil \text{AID}-\theta \rceil^{+}$ of the pre-synaptic cell and according to the level of the post-synaptic AMP.

AID, which is a very stable parameter among others in the regular ring network, was adopted, supposing that if uniform rhythmic oscillation were to occur in a generally-connected neural network with feedback inhibition, its AIDs would be of

approximately equal value. This formulation has an adequate effect in minimizing the differences between the AIDs in cases of the disappearance and reappearance of rhythmic oscillation. In fact, it has been demonstrated that by applying the algorithm to some networks the rhythmic oscillation can be brought back and then held, (in the sense that the modification speed becomes extremely slow). Inferring from this process, it seems that the operation to minimize the difference between the AIDs of cells might play an important role in looking for the region of rhythmic oscillation in the high dimensional space whose elements are synaptic strengths.

It would be impossible to examine all the combinations of synaptic strengths by which rhythmic oscillation can be generated, and even if it were possible, the problems lying between the learning process and rhythmic oscillation would not be able to be directly resolved. Therefore, it is considered that the best course of action is to propose a synaptic modification algorithm and investigate how it acts on rhythmic oscillation. It will be necessary in that case to pay special attention to minor pieces of neurophysiological findings and to the ratiocination concerning the AID and the AMP.

The experiments for this proposed synaptic modification algorithm were performed in networks with comparatively regular connections from the outset. It will be necessary to apply it to a network with more complicated connections and to discuss in detail how to quantitatively determine the constants in the algorithm. Although only the decreases of synaptic strengths were discussed in this chapter, it will be necessary to consider the

cases where synaptic strengths increase and to correlate the decreases with adaptation or accommodation of the neuronal cell itself. It will further be important to investigate cases where the constants in the algorithm differ, depending on the synapses.

Chapter 3

Memory Model

In this chapter, the synaptic modification algorithm proposed in Chap.2 is applied to some disturbed ring networks and some typical cases are demonstrated in which rhythmic oscillation is caught and then held. When the constants in the algorithm are fixed, two modes, namely the storing mode and the recalling mode, can be selected according to the excitatory input level to excitatory cells alone. This indicates that the ring neural network to which the synaptic modification algorithm is applied may function as a memory which stores and recalls information in the form of bursts of nerve impulses. Also discussed is the possibility that multiple pieces of information can be selectively stored in the overlapped ring network. Hereafter the expression "the synaptic modification algorithm proposed in Chap.2" is replaced by "the algorithm" for the sake of simplicity.

3.1 Introduction

In the study of the neural network, it is generally accepted that synaptic plasticity is involved in the mechanism of memory and that information is distributively stored. Even if the neural network sustains local structural damage, loss of information

does not necessarily occur. This phenomenon is assumed to be directly related to the processing of ambiguous information and to the problem of association.

On the other hand, bursts of nerve impulses are observed in various parts of nervous system and this type of signal is likely to be related to the problems of learning and memory. However, in the models for learning, information itself is thought to be a time-invariant analog or digital value (in impulse density), and the relationship between bursts of nerve impulses and learning has never been studied.

In this chapter, a memory model is newly proposed from our preliminary investigation into the algorithm which is effective in bringing back bursts of nerve impulses, and the relationship between the mechanism of memory and bursts of nerve impulses is discussed.

In Sect.3.2, the algorithm is applied to some disturbed ring networks and some typical cases are demonstrated in which rhythmic oscillation is caught and then held. When the constants in the algorithm are fixed, two modes, namely the storing mode and the recalling mode, can be selected according to the excitatory input level to excitatory cells alone. In Sect.3.3, evidence is given to support this two-mode selection mechanism. This property indicates that the ring neural network to which the algorithm is applied may function as a memory which stores and recalls information in the form of bursts of nerve impulses. In Sect.3.4, the possibility is also discussed that multiple pieces of information can be selectively stored in the overlapped ring network. In Sect.3.5, the results are summarized and the problems

remaining to be solved are suggested.

3.2 Memory and Bursts of Nerve Impulses

We consider the neural network with feedback inhibition composed of excitatory and inhibitory cells which can be represented by Eqs.(2.1) and (2.2). The block diagram of the network is illustrated in Fig.3.1. The output of the excitatory cells is fed back to themselves via the inhibitory cells and one input channel is provided from the outside to the excitatory cells. In this chapter, an input

$$u_i^{(1)}(t) = u > 0 \quad (u:\text{constant}) \tag{3.1}$$

is applied uniformly to the excitatory cells, and the integral time constants and the number of cells are set so $\tau_1=2.0$, $\tau_2=10.0$, and $N_1=N_2=N$.

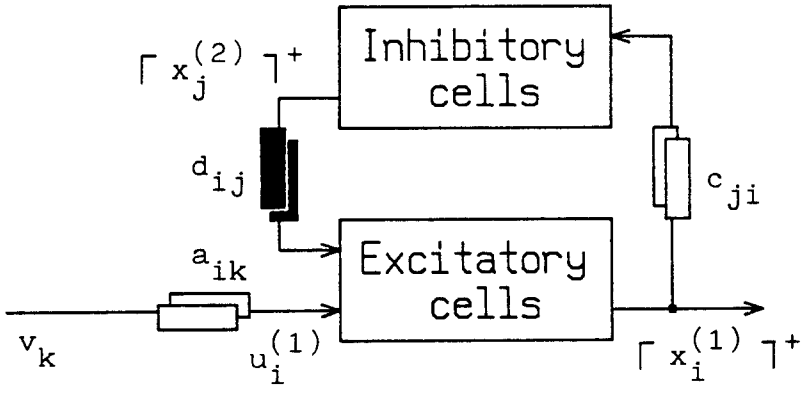

Fig.3.1. The block diagram of the neural network with feedback inhibition. The network has one input channel only to the excitatory cells.

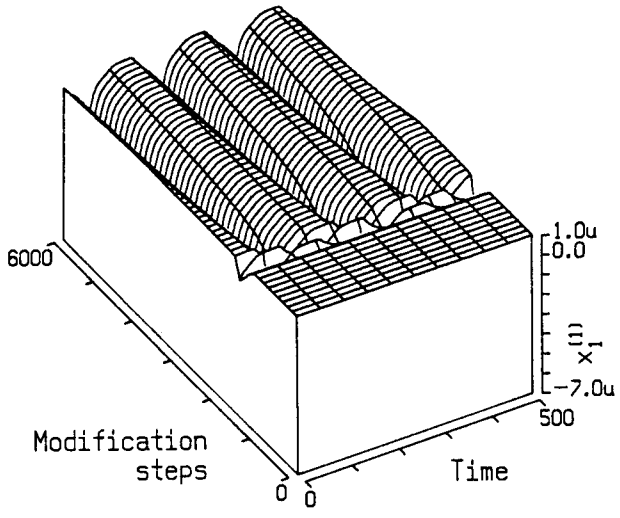

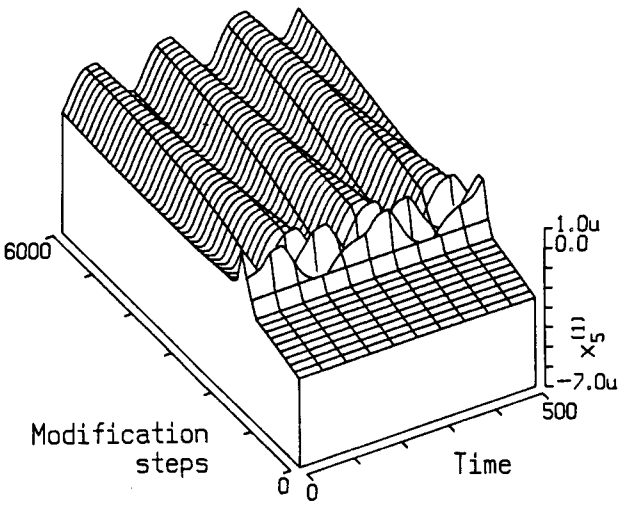

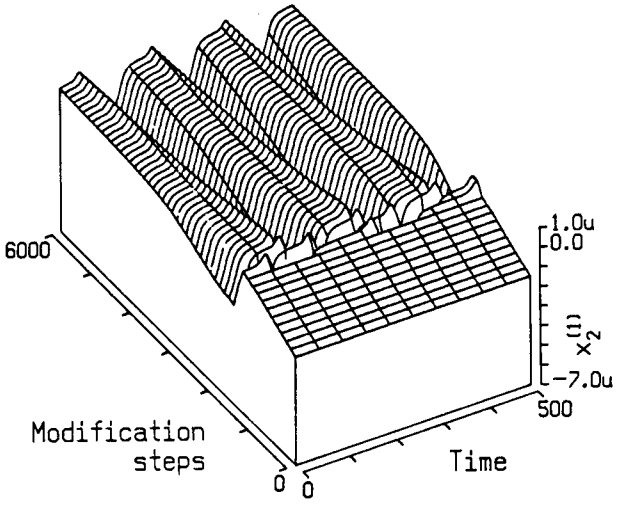

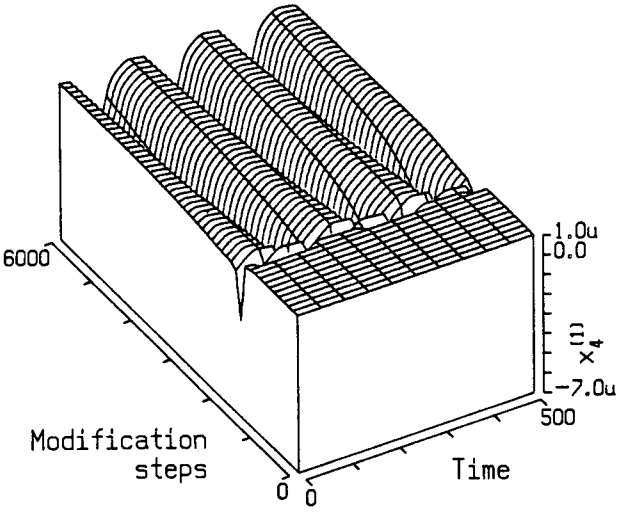

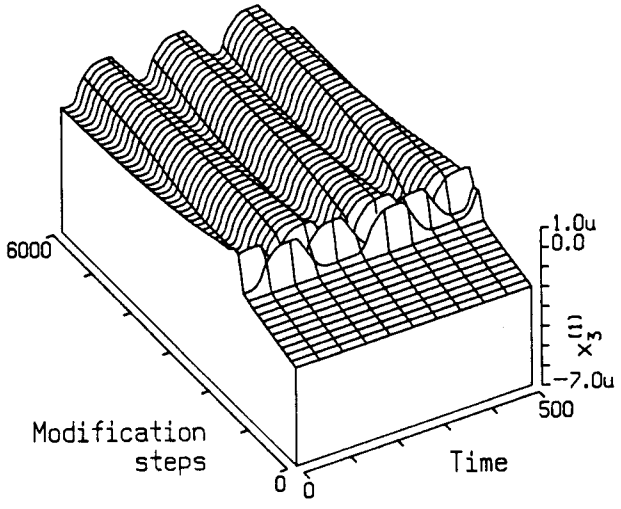

Fig.3.2. The transition of the membrane potentials $x_i^{(1)}(t)$ of excitatory cells when the algorithm is applied to a disturbed ring network (Network 1). Rhythmic oscillation appears at around 1200 modification steps, and after that it is maintained. The constants in the algorithm are $\delta^{(1)}=0.0004/u^2$, $\theta^{(1)}=0.4u$, $\eta^{(1)}=-2.0u$, $\delta^{(2)}=0.0012/u^2$, $\theta^{(2)}=0.4u$, and $\eta^{(2)}=0.0u$. σ in the window function is set up at 500 units of time.

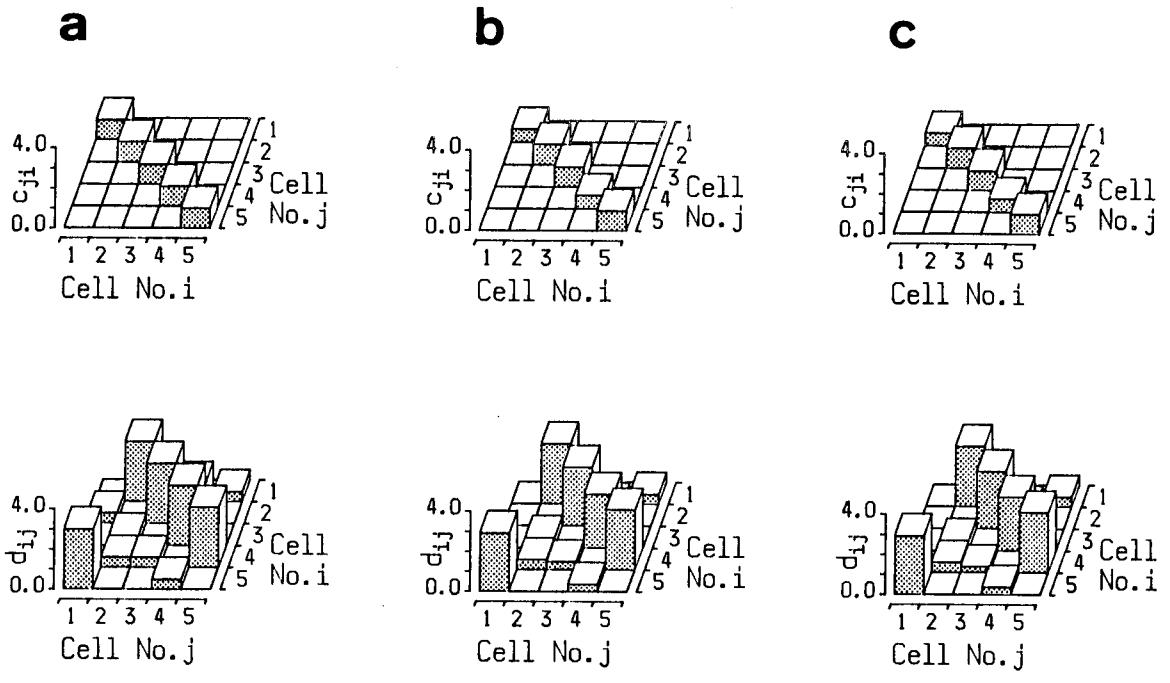

Fig.3.3a-c. The changes of synaptic strengths c_{ji} and d_{ij} with the progress of the synaptic modification in Network 1. **a** Before modification. **b** After 3600 modification steps. **c** After 6000 modification steps.

Figure 3.2 shows the transition of the membrane potentials $x_i^{(1)}(t)$ of excitatory cells when the algorithm is applied to a disturbed ring network with two disturbing connections (Network 1). The number of cells N is equal to 5, and the constants in the algorithm are set so $\delta^{(1)}=0.0004/u^2$, $\theta^{(1)}=0.4u$, $\eta^{(1)}=-2.0u$, $\delta^{(2)}=0.0012/u^2$, $\theta^{(2)}=0.4u$, and $\eta^{(2)}=0.0u$. in the window function is set up at 500 units of time. This three-dimensional figure is drawn by shifting $x_i^{(1)}(t)$ according to the synaptic strengths at each modification step. Figure 3.2 may help in the visual and intuitive understanding of their overall transition. The sets of synaptic strengths after 0, 3600, and 6000 modification steps (equal to units of

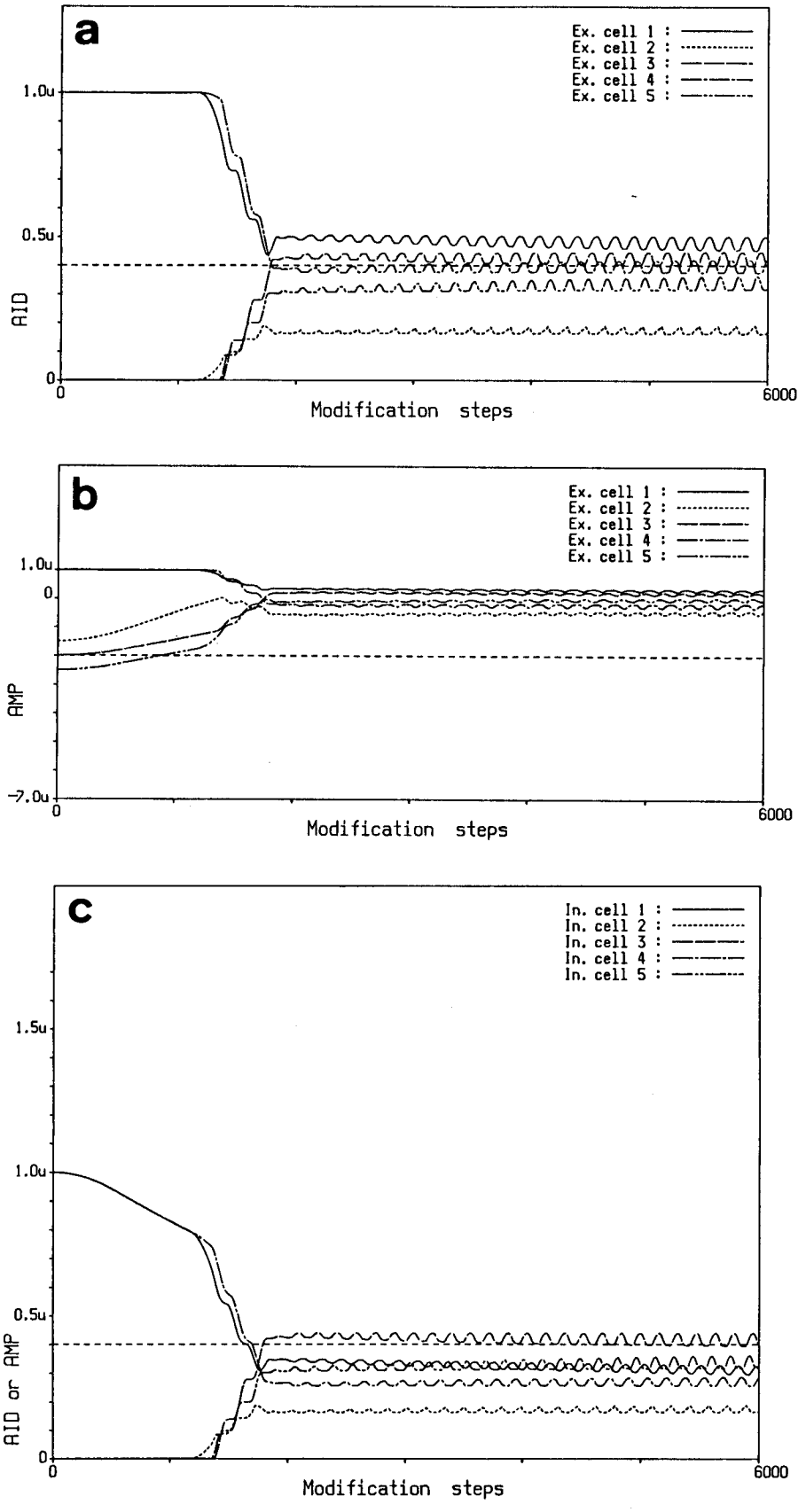

Fig.3.4a-c. The changes in the AIDs and the AMPs during the synaptic modification in Network 1. After the generation of rhythmic oscillation at around 1200 modification steps, the AIDs of both excitatory cells and inhibitory cells decrease nearly below the threshold $\theta^{(1)}$ or $\theta^{(2)}$. **a** AID of excitatory cells. **b** AMP of excitatory cells. **c** AID of inhibitory cells.

time) are shown in Fig.3.3a-c.

Before modification, each excitatory cell outputs a non-oscillatory signal under the imbalance of inhibition caused by the disturbing connections. With the progress of the synaptic modification, the state of balance of the inhibition is changed step by step. In this case, the tendency continues up to around 1200 modification steps and immediately after that rhythmic oscillation is generated. It may also be seen in the figure that the period of the rhythmic oscillation rapidly converges on a certain value and then it remains constant.

Figure 3.4a-c further shows the changes in, respectively, the AIDs of excitatory cells, the AMPs of excitatory cells and the AIDs of inhibitory cells during the synaptic modification in Network 1. Each parameter continues to vary gradually until the oscillation appears at around 1200 modification steps and then the AIDs of both excitatory and inhibitory cells decrease nearly below the threshold $\theta^{(1)}$ or $\theta^{(2)}$ in the algorithm. Since the progress of the synaptic modification depends on the difference of AID and θ as shown by Eqs.(2.6) and (2.7), the modification speed drops to an extremely low level once the rhythmic oscillation is brought back. This result indicates that the algorithm can catch the rhythmic oscillation and then hold it in the disturbed ring network; thus, information can be stored in the form of bursts of nerve impulses.

Figure 3.5 shows the transition of the membrane potentials $x_i^{(1)}(t)$ of excitatory cells when the algorithm is applied to another disturbed ring network with more complicated synaptic connections (Network 2). The constants in the algorithm etc. are

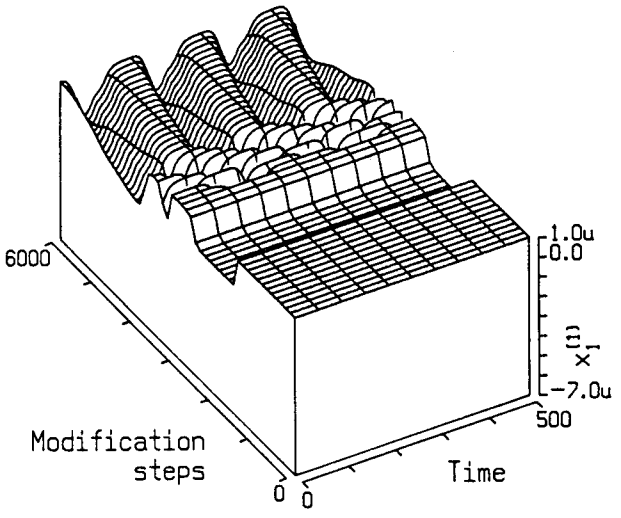

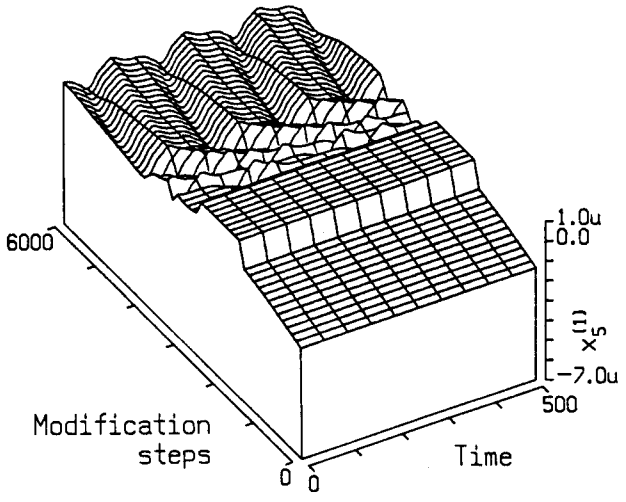

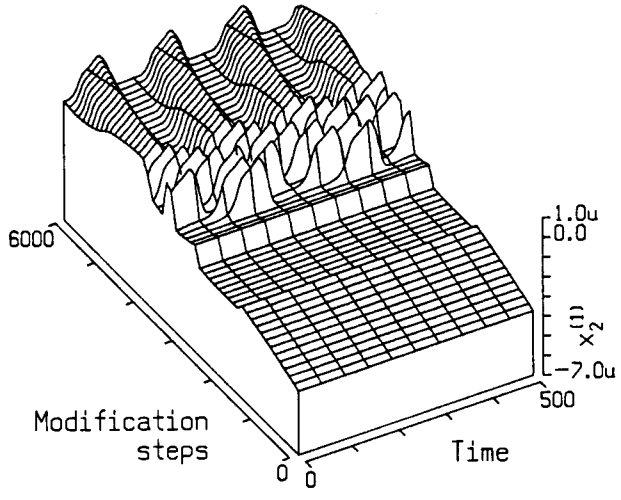

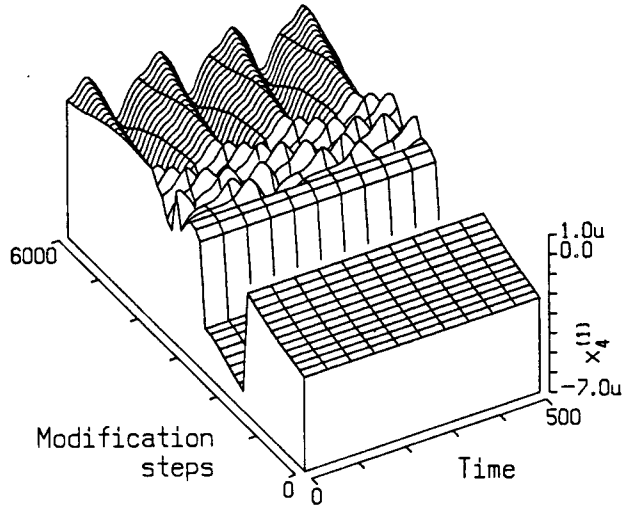

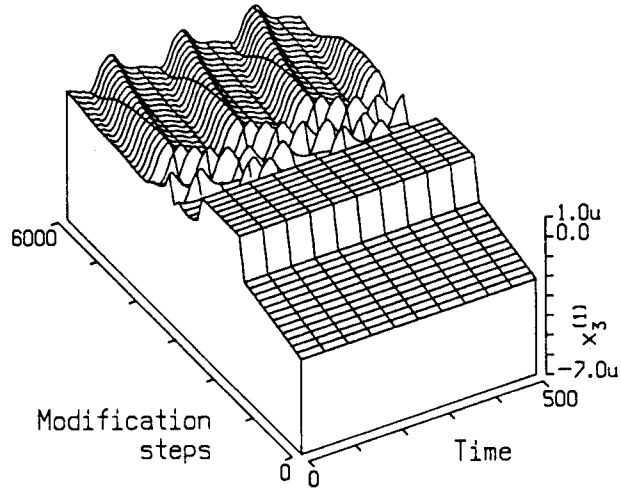

Fig.3.5. The transition of the membrane potentials $x_i^{(1)}(t)$ of excitatory cells when the algorithm is applied to another disturbed ring network with more complicated synaptic connections (Network 2). Rhythmic oscillation appears at around 3000 modification steps, although the process is more complicated. The constants in the algorithm etc. are the same as those of the previous example.

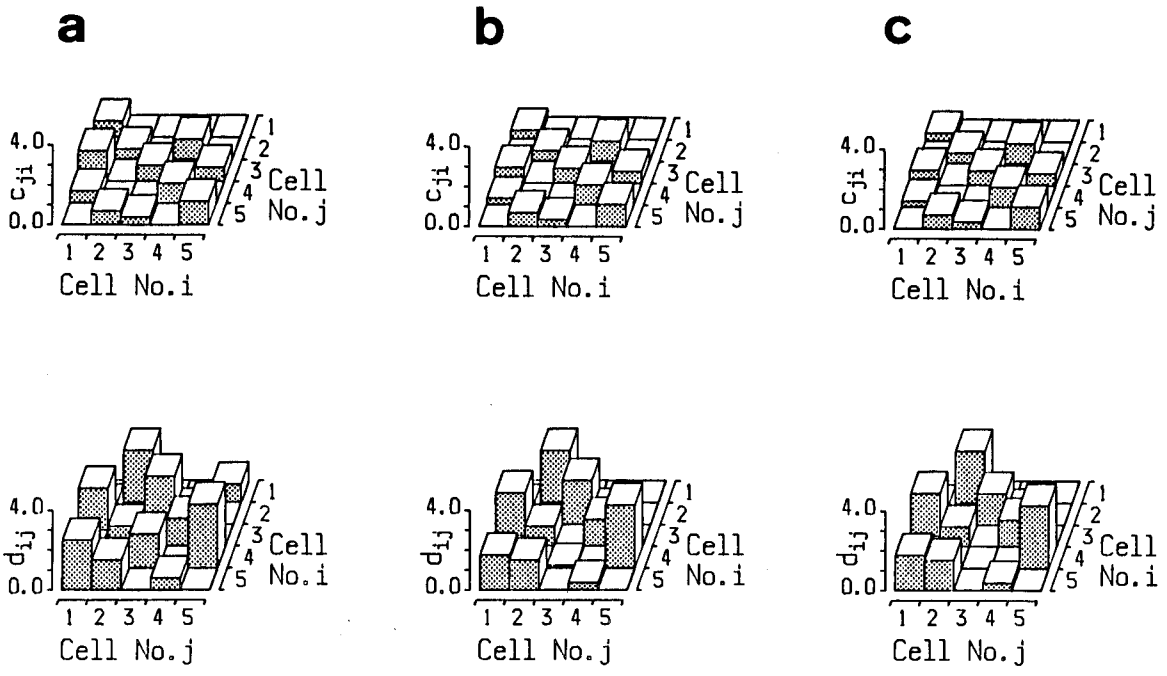

Fig.3.6a-c. The changes of synaptic strengths c_{ji} and d_{ij} with the progress of the synaptic modification in Network 2. **a** Before modification. **b** After 3600 modification steps. **c** After 6000 modification steps.

the same as those of the previous example. The sets of synaptic strengths after 0, 3600, and 6000 modification steps are shown in Fig.3.6a-c. With the progress of the synaptic modification, the balance of inhibition is changed, step by step at some modification steps or abruptly at others. After 3000 modification steps, the oscillation appears and after that its period converges abruptly on a certain value.

Figure 3.7a-c illustrates the changes in, respectively, the AIDs of excitatory cells, the AMPs of excitatory cells, and the AIDs of inhibitory cells during the synaptic modification in Network 2. The AIDs of excitatory cells and inhibitory cells gather around $\theta^{(1)}$ or $\theta^{(2)}$ after 3000 modification steps, the

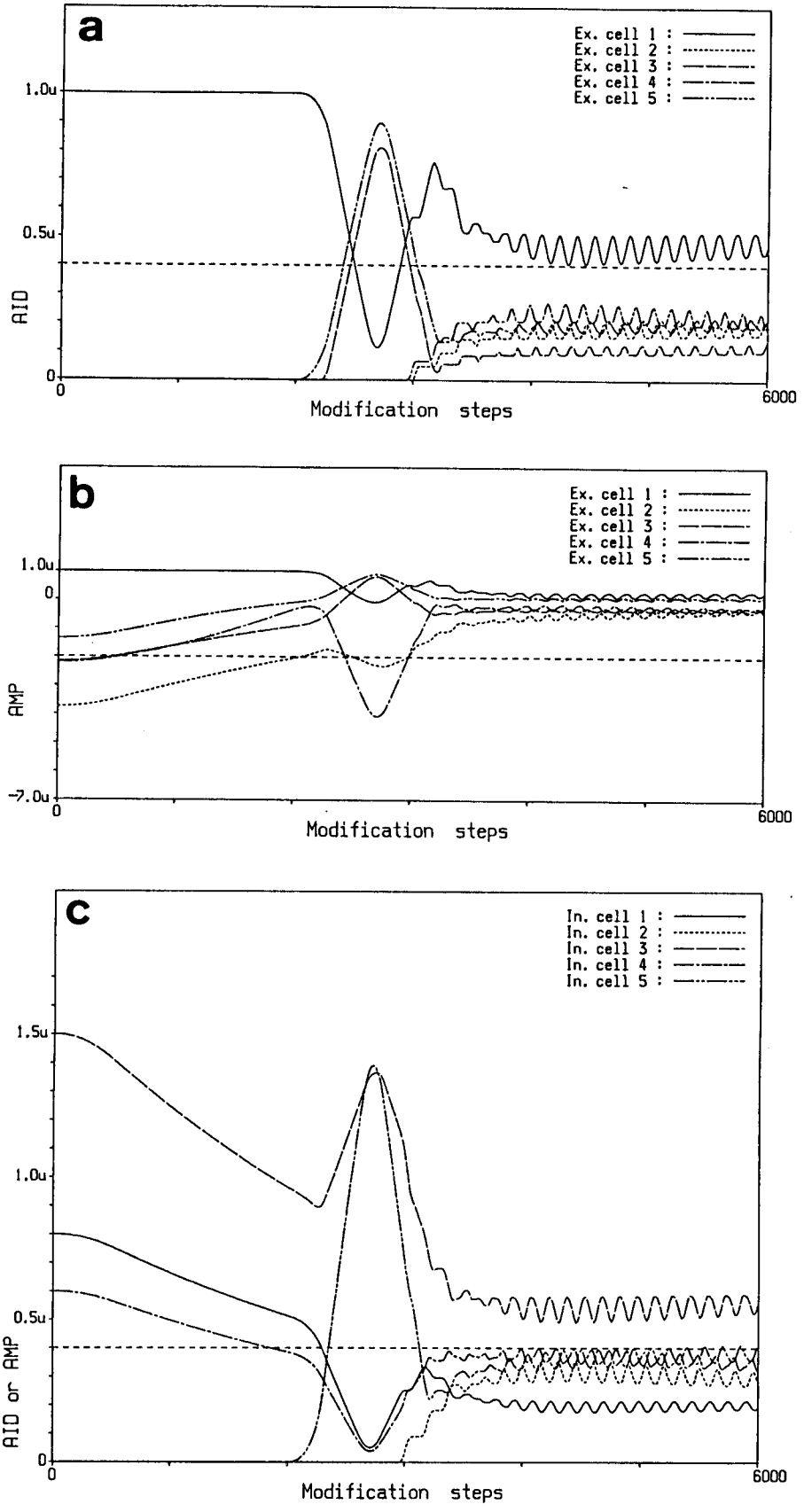

Fig.3.7a-c. The changes in the AIDs and the AMPs during the synaptic modification in Network 2. The AIDs of excitatory cells and inhibitory cells gather around $\theta^{(1)}$ or $\theta^{(2)}$ after 3000 modification steps. **a** AID of excitatory cells. **b** AMP of excitatory cells. **c** AID of inhibitory cells.

process toward the appearance of rhythmic oscillation being more complicated in this case. Here, the AIDs of excitatory cell No.1 and inhibitory cell No.3 still exceed $\theta^{(1)}$ or $\theta^{(2)}$ slightly after the appearance of the oscillation, so therefore the synaptic modification continues gradually. As a result of this modification, the period of the oscillation tends to lengthen after 4000 modification steps as shown in Fig.3.5. However it should be concluded that, from a temporal point of view, the rhythmic oscillation may be caught and then held, since this change of the period is slow.

3.3 Selection of Storing and Recalling

In the network described by Eqs.(2.1) and (2.2) in which the input is applied uniformly to excitatory cells, $x_j^{(2)}(t)$ is positive definite and the following equality holds:

$$\lceil x_j^{(2)}(t) \rceil^+ = x_j^{(2)}(t) \ . \tag{3.2}$$

Therefore Eq.(2.1) becomes

$$\tau_1 \tau_2 \frac{d^2}{dt^2} x_i^{(1)}(t) + (\tau_1 + \tau_2) \frac{d}{dt} x_i^{(1)}(t) + x_i^{(1)}(t)$$

$$= u - \sum_{i'=1}^{N_1} (\sum_{j=1}^{N_2} d_{ij} c_{ji'}) \lceil x_{i'}^{(1)}(t) \rceil^+ \ . \tag{3.3}$$

Equation (3.3) suggests that the input level u causes no time-functional changes but only a variation in the output level $\lceil x_i^{(1)}(t) \rceil^+$. This characteristic produces a significant effect, assuming plausibly that the constants δ, θ, and η in the algorithm are fixed, although they were defined as a function of the input level u in the previous section. That is, either the storing mode in which the synaptic modification occurs, or the recalling mode in which no synaptic modification is carried out, can be selected according to the input level u to the excitatory cells alone. If the input level u is set up high enough so that some of the AIDs of $\lceil x_i^{(1)}(t) \rceil^+$ or $\lceil x_j^{(2)}(t) \rceil^+$ exceed the threshold $\theta^{(1)}$ or $\theta^{(2)}$, the synaptic modification proceeds toward the generation of rhythmic oscillation. On the other hand, if the input is set up low enough so that none of the AIDs of the outputs exceeds the thresholds, the output according to a set of synaptic strengths at the moment is recalled without any synaptic modification.

This further shows that the ring neural network acts as a memory which stores and recalls information in the form of rhythmic oscillation by applying the input u to the network. Even if rhythmic oscillation cannot be generated in the recalling mode, information can be stored by the subsequent application of the high input in the storing mode.

In the storing mode, $\lceil x_i^{(1)}(t) \rceil^+ - \theta^{(1)}$ or $\lceil x_j^{(2)}(t) \rceil^+ - \theta^{(2)}$ increases with the increasing input u. Therefore the higher the input level u, the faster the modification speed, as is evident from Eq.(2.7). It is a generally accepted experience that one may easily remember things by applying deep concentration. If

this concentration corresponds to the increased input, this high speed modification process is assumed to be the micro-scopic mechanism which explains man's experience.

Further, a case may be assumed to exist in which there are more than two input passways to the excitatory cells and some of these input passways are crucial for the storing mode. This is thought to correspond to our experience that it is more efficient to try to remember some related matters at the same time.

3.4 Overlapped Ring Network

In Sect.3.2, the algorithm was applied to the single ring-structured networks where N=5. As is evident from the result (see Figs.3.3a-c and 3.6a-c), the synaptic modification works toward the generation of rhythmic oscillation not by reducing only disturbing connections but by modifying the synaptic strengths of the whole network little by little. This suggests the possibility that information can be stored and recalled selectively in the form of bursts of nerve impulses in the overlapped ring network where more than two ring neural networks are overlapped with common synaptic connections.

Figure 3.8a-c shows the result of the application of the algorithm to an overlapped ring network (N=8), in which the excitatory inputs are applied to two groups of excitatory cells alternately at every 1500 modification steps. The figure shows the membrane potentials $x_i^{(1)}(t)$ of excitatory cells at the sets of synaptic strengths after 0, 15000, and 24000 modification

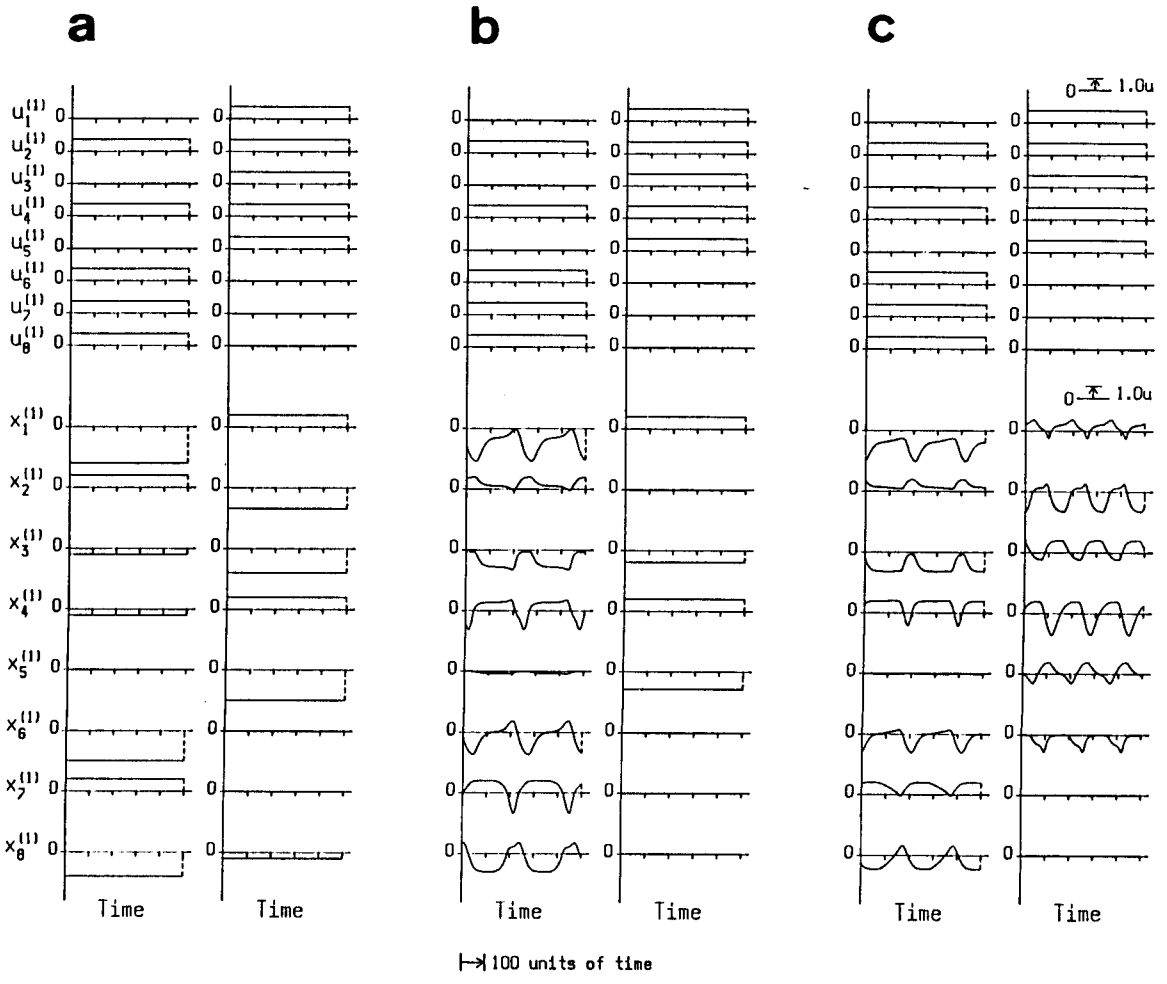

Fig.3.8a-c. The result for the synaptic modification of applying the algorithm to an overlapped ring network. The constants in the algorithm are set so $\delta^{(1)}=0.0001/u^2$, $\theta^{(1)}=0.4u$, $\eta^{(1)}=-2.0u$, $\delta^{(2)}=0.0003/u^2$, $\theta^{(2)}=0.4u$, and $\eta^{(2)}=0.0u$. The inputs are applied to two groups of excitatory cells alternately at every 1500 modification steps. **a** Before modification. **b** After 15000 modification steps. **c** After 24000 modification steps.

steps (see Fig.3.9a-c) in turn from the left. The constants in the algorithm etc. are the same as those in Sect.3.2 except that $\delta^{(1)}=0.0001/u^2$ and $\delta^{(2)}=0.0003/u^2$.

Before modification, some excitatory cells output non-oscillatory signals no matter which input is applied (see Fig.3.8a). With the progress of the synaptic modification, the balance of inhibition is changed in the same way as the networks

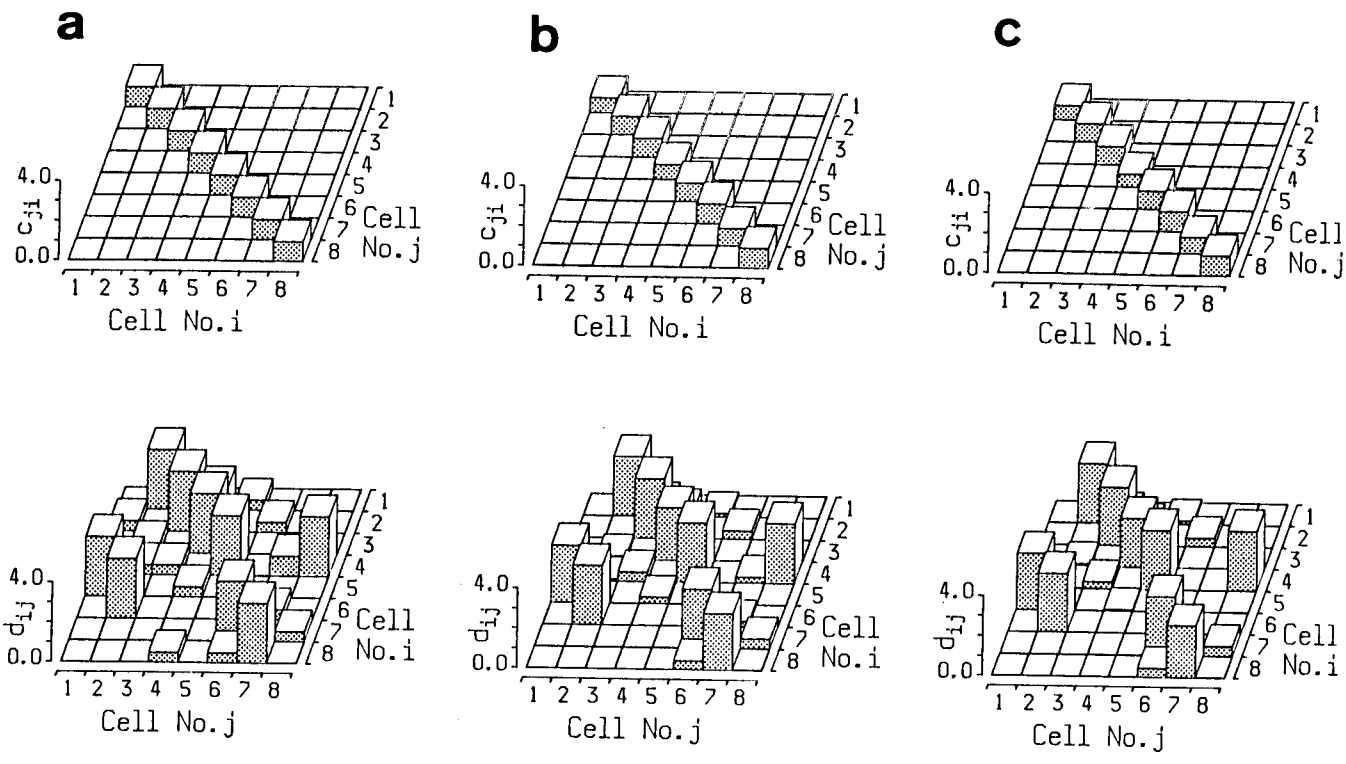

Fig.3.9a-c. The changes of synaptic strengths c_{ji} and d_{ij} with the progress of the synaptic modification in the overlapped ring network. **a** Before modification. **b** After 15000 modification steps. **c** After 24000 modification steps.

discussed previously, and rhythmic oscillation is generated after 15000 modification steps when only one input is applied (see Fig.3.8b). The subsequent modification gives rise to rhythmic oscillation in whichever group of excitatory cells the input is applied to (see Fig.3.8c).

Since the network output corresponds to the positive part of $x_i^{(1)}(t)$, output in the form of rhythmic oscillation appears only in the excitatory cells to which the input is applied. Furthermore, the outputs can be selected according to the inputs to two groups of excitatory cells.

3.5 Discussion

It has been demonstrated that rhythmic oscillation can be generated and then held when the algorithm is applied to various disturbed ring networks. Moreover, by virtue of the two-mode selection mechanism, the storing mode in which the synaptic modification occurs and the recalling mode in which no synaptic modification is carried out, can be selected according to the input level u to excitatory cells alone. This theory can be extended to the overlapped ring network, and it has been demonstrated that multiple pieces of information can be stored and recalled selectively in an overlapped ring network. This means that the ring neural network to which the algorithm is applied may function as a memory which stores and recalls information in the form of bursts of nerve impulses.

Although cases have been mentioned above in which rhythmic oscillation is generated, the process of synaptic modification differs according to the constants in the algorithm, the initial synaptic strengths, etc. In some cases, rhythmic oscillation cannot be generated in the network in spite of the application of the algorithm. The process for generating rhythmic oscillation corresponds to the search for the region of rhythmic oscillation in high-dimensional space whose elements are synaptic strengths. And its path depends on the network constants etc. The behavior of this search is very complicated, and the supposition that the impossibility of the generation of rhythmic oscillation is essential in itself further complicates the problem. The periods of rhythmic oscillation caused by the synaptic modification

differ in each case, as described in Sect.3.2. The periods of oscillation selectively generated in the overlapped ring network also differ from each other, as shown in Sect.3.4. Some mechanisms are necessary for controlling the period if the neural network functions as a generator of rhythmic oscillation which operates as a precise clock in the nervous system.

Although there remain some problems, this memory model introduces a new idea about the status of bursts of nerve impulses, as well as the solution of the mechanism of memory.

Chapter 4

Generator of Rhythmic Oscillation with Period Control Mechanism

For the ring neural network to function as a generator of rhythmic oscillation, mechanisms are required by which rhythmic oscillation is generated and maintained and then its period controlled. In this chapter, it is demonstrated by simulation that those mechanisms can be actualized by employing the algorithm and by applying inputs from the outside to excitatory and inhibitory cells. The two-mode selection mechanism described in Chap.3 solves the problem of the re-modification caused by the dispersion of AIDs with the application of the excitatory synchronous input to inhibitory cells.

4.1 Introduction

It has been confirmed in Chap.2 and 3 that, in networks with certain ring-structured sets of synaptic connections, rhythmic oscillation is generated by the algorithm. However, the periods of the oscillation generated by the algorithm differ with the network constants etc. If certain mechanisms to control the period of rhythmic oscillation can be found in the ring neural network, these mechanisms may explain various rhythmical phenomena.

Here, we discuss how the generation and the control of rhythmic oscillation can be actualized in the ring neural network. Firstly, in Sect.4.2, the ring neural network with two input channels from the outside is described. In Sect.4.3, the mechanism for the generation of rhythmic oscillation is discussed: the algorithm is applied to a disturbed ring network with rather complicated synaptic connections. Simulation illustrates that the algorithm can catch and hold the rhythmic oscillation in the network.

The additive input channel to inhibitory cells is taken into account in the analysis of the network behavior in Sects.4.4 and 4.5, and the way in which the input to inhibitory cells changes the characteristics of the rhythmic oscillation is discussed. It is shown that the oscillatory and excitatory input applied to an inhibitory cell is effective for controlling the period of rhythmic oscillation.

On applying the input to an inhibitory cell, the value of each cell's AID (average impulse density) disperses somewhat. This dispersion frequently restarts the synaptic modification. In Sect.4.5, it is also shown that the two-mode selection mechanism described in Chap.3 solves the problem of the re-modification.

In Sect.4.6, the procedure for using the network as a generator is summarized. The network discussed here is very similar to the granule-Golgi network in the cerebellum. This similarity is illustrated in Sect.4.6 and a new interpretation of the function of the granule-Golgi network is suggested.

4.2 Network Equations

Figure 4.1 shows the block diagram of the neural network with feedback inhibition composed of excitatory and inhibitory cells. In the network, the output of the excitatory cells is fed back to themselves via the inhibitory cells and one input channel each is provided from the outside to the excitatory and the inhibitory cells. The equations for the network employing analog neuron models with integral time constants can be generally represented as follows:

$$\tau_1 \frac{d}{dt} x_i^{(1)}(t) + x_i^{(1)}(t) = u_i^{(1)}(t) - \sum_{j=1}^{N_2} d_{ij} \lceil x_j^{(2)}(t) \rceil^+$$

$$u_i^{(1)}(t) = \sum_{k=1}^{M} a_{ik} v_k(t) \qquad (i=1,2,---,N_1)$$

$$\tau_2 \frac{d}{dt} x_j^{(2)}(t) + x_j^{(2)}(t) = u_j^{(2)}(t) + \sum_{i=1}^{N_1} c_{ji} \lceil x_i^{(1)}(t) \rceil^+ .$$

(4.1)

$$(j=1,2,---,N_2)$$

As stated in Chap.2, when an input

$$u_i^{(1)}(t) = u > 0 \ (u:\text{constant}) \tag{4.2}$$

is applied uniformly to excitatory cells and the input channel to inhibitory cells is neglected, rhythmic oscillation may appear in the regular ring network, as with the membrane potentials $x_i^{(1)}(t)$

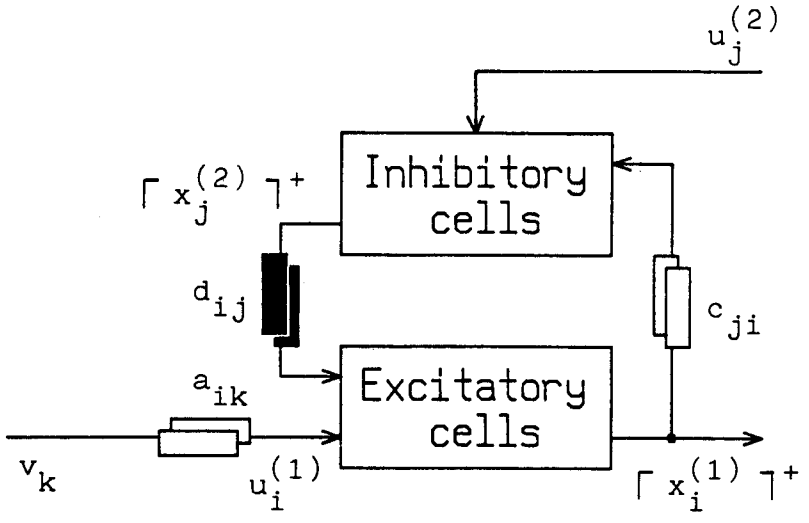

Fig.4.1. The block diagram of the neural network with feedback inhibition. The network has two input channels to the excitatory cells and the inhibitory cells.

on the left-hand side of Fig.4.7a (the set of synaptic strengths etc. are shown in Appendix B-1). In this chapter, the input represented by Eq.(4.2) is applied to excitatory cells in the network and the integral time constants and the number of cells are set so $\tau_1=2.0$, $\tau_2=10.0$, and $N_1=N_2=N=5$.

4.3 Generation of Rhythmic Oscillation

Figure 4.2 shows the transition of the membrane potentials $x_i^{(1)}(t)$ of excitatory cells when the algorithm is applied to a disturbed ring network with rather complicated synaptic connections. The network here has the input channel to excitatory

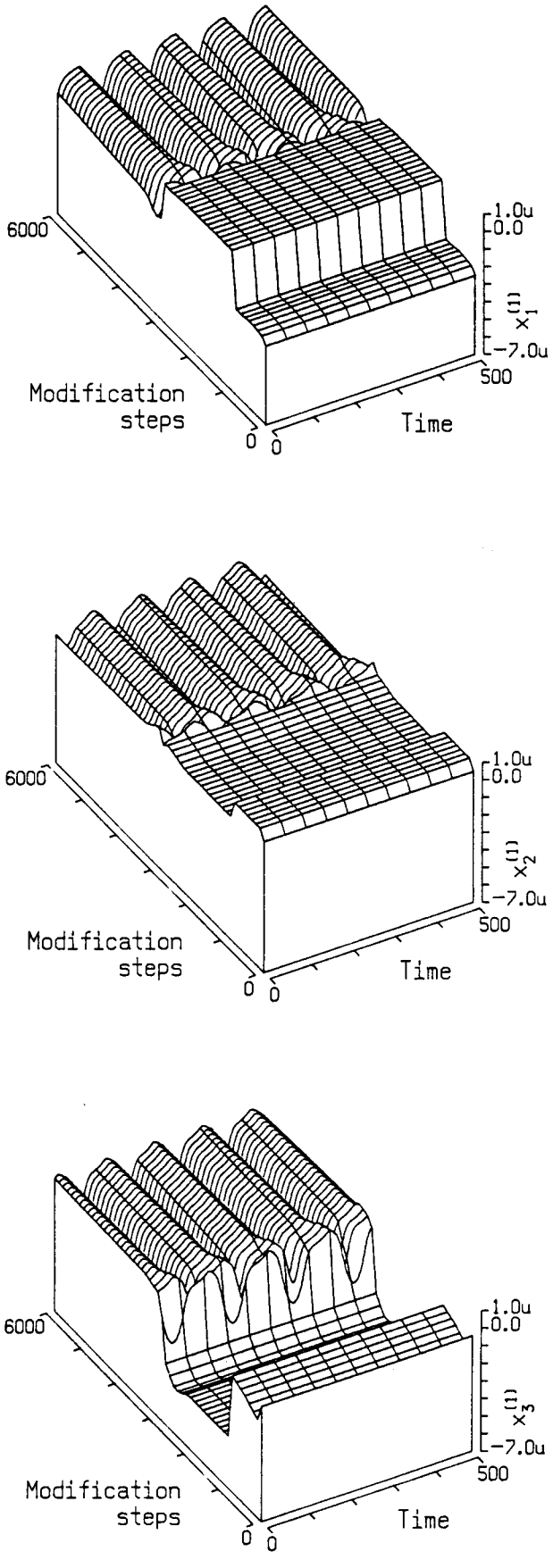

Fig.4.2. The transition of the membrane potentials $x_i^{(1)}(t)$ of excitatory cells when the algorithm is applied to a disturbed ring network (the constants in the algorithm, the sets of synaptic strengths after 0, 3000, and 6000 modification steps, etc. are shown in Appendices B-2 and B-3).

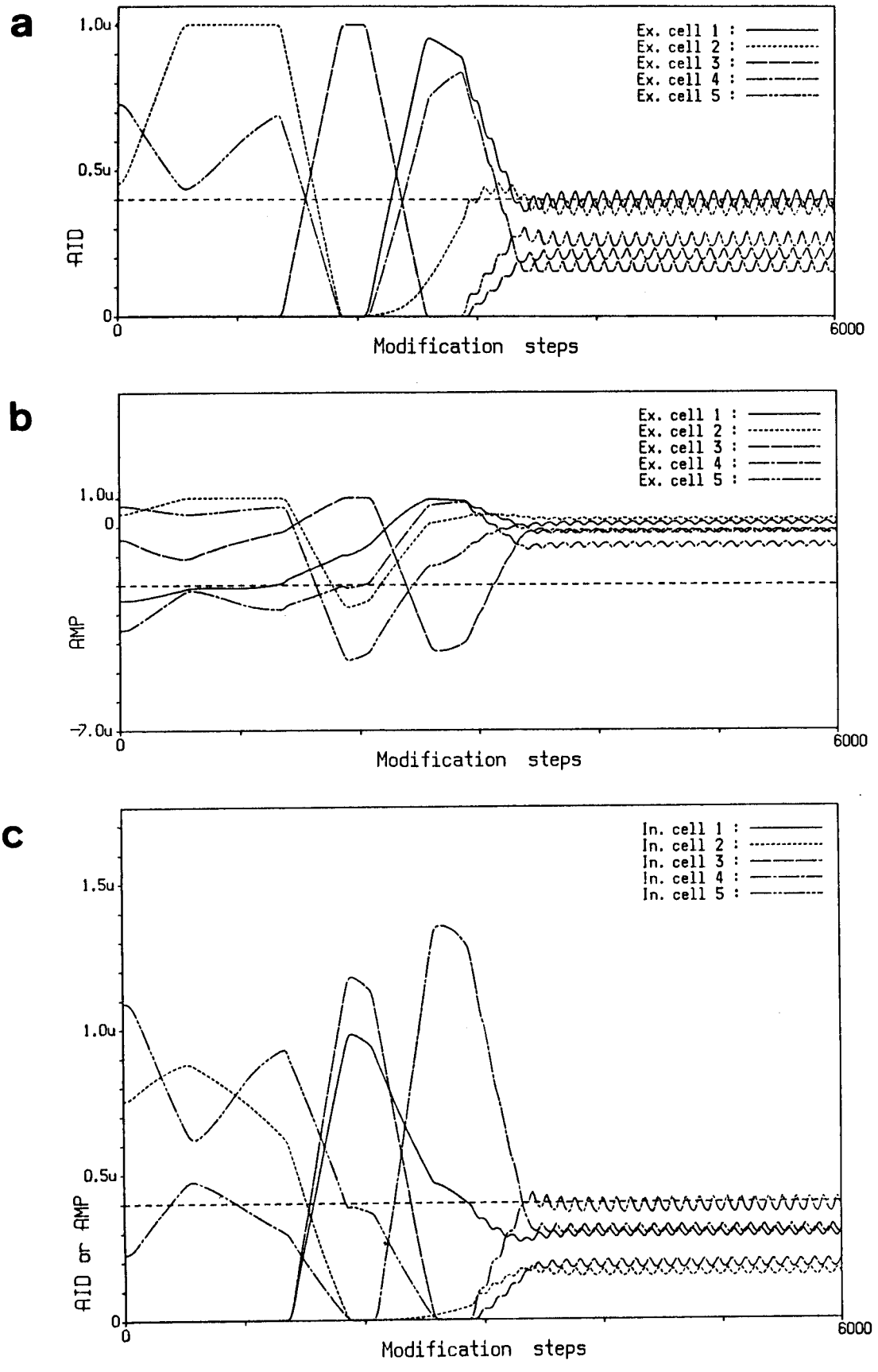

Fig.4.3a-c. The changes in the AIDs and the AMPs during the synaptic modification. **a** AID of excitatory cells. **b** AMP of excitatory cells. **c** AID of inhibitory cells.

cells only. The constants in the algorithm and the window function for calculating the AID and the AMP are shown in Appendix B-2, and the sets of synaptic strengths after 0, 3000, and 6000 modification steps are listed in Appendix B-3.

Before modification, each excitatory cell outputs a non-oscillatory signal under the imbalance of inhibition caused by the disturbing connections. With the progress of the synaptic modification, the state of balance of the inhibition is changed, sometimes gradually, sometimes abruptly. This tendency continues up to around 3000 modification steps and immediately after that rhythmic oscillation appears. It may also be seen in the figure that the period of the rhythmic oscillation rapidly converges on a certain value and then remains constant.

Figure 4.3a-c further shows the changes in, respectively, the AIDs of excitatory cells, the AMPs of excitatory cells and the AIDs of inhibitory cells during the synaptic modification. The parameters continue to fluctuate signally until the oscillation appears at around 3000 modification steps and then the AIDs of both excitatory and inhibitory cells decrease nearly below the threshold $\theta^{(1)}$ or $\theta^{(2)}$. Since the progress of the synaptic modification depends on the difference of the AID and θ as shown by Eqs.(2.6) and (2.7), the modification speed drops to an extremely low level once the rhythmic oscillation is brought back. This indicates that the algorithm can catch the rhythmic oscillation and then hold it even in a disturbed ring network with extremely complicated synaptic connections.

4.4 Control of Period of Rhythmic Oscillation I

From this section onwards, the input channel to inhibitory cells is taken into account. In this section, the effect of a non-oscillatory input $u_j^{(2)}(t)$ applied uniformly to inhibitory cells on the period of rhythmic oscillation is examined.

If the non-oscillatory input applied uniformly to inhibitory cells is excitatory, namely,

$$u_j^{(2)}(t) = u' > 0 \quad (u': \text{constant}) \tag{4.3}$$

then $x_j^{(2)}(t)$ is positive definite and Eq.(3.2) holds. Here we define the equivalent input ${}^*u_i$ as follows:

$${}^*u_i = u - \sum_{j=1}^{N_2} d_{ij}\, u' \,. \tag{4.4}$$

The output impulse densities $\lceil x_i^{(1)}(t) \rceil^+$ of excitatory cells are given by

$$\tau_1 \tau_2 \frac{d^2}{dt^2} x_i^{(1)}(t) + (\tau_1 + \tau_2) \frac{d}{dt} x_i^{(1)}(t) + x_i^{(1)}(t)$$

$$= {}^*u_i - \sum_{i'=1}^{N_1} \Big(\sum_{j=1}^{N_2} d_{ij}\, c_{ji'} \Big) \lceil x_{i'}^{(1)}(t) \rceil^+ \,. \tag{4.5}$$

When the network is regular ring-structured, the periodical characteristic of $\lceil x_i^{(1)}(t) \rceil^+$ cannot be changed by u', in the way described in Chap.3, since the increased u' corresponds to the decreased ${}^*u_i$. When the network is not regular ring-

structured, u' affects the periodical characteristic of $\lceil x_i^{(1)}(t) \rceil^+$ because the ${}^*u_i$ levels differ even if Eq.(5.1) holds. If the non-oscillatory input applied uniformly to inhibitory cells is inhibitory, namely,

$$u_j^{(2)}(t) = u' < 0 \quad (u':\text{constant}) \tag{4.6}$$

then the influence on the periodical characteristic of the network output must be estimated because Eq.(3.2) does not hold.

Figure 4.4 shows the change of the period p of the rhythmic oscillation with the uniform application of the non-oscillatory input to inhibitory cells. In the figure and here after, Network 3 indicates the regular ring network as shown in Sect.4.2, and Network 4 indicates the disturbed ring network with a set of synaptic strengths after 6000 modification steps as shown in Sect.4.3.

In Network 3, the period p remains constant with the application of the excitatory input, but with the application of the inhibitory input, p decreases to its minimal value and then increases. In Network 4, a decrease of p can also be seen, but the curve is different from that of Network 3. This results from the differences in the influences on cells of the uniform non-oscillatory input because of the irregularity of their synaptic strengths. The boundary between the inhibitory and excitatory inputs is not clear, as it is in Network 3, and each different set of synaptic strengths has a corresponding input vs. period curve.

The non-oscillatory input applied uniformly to inhibitory

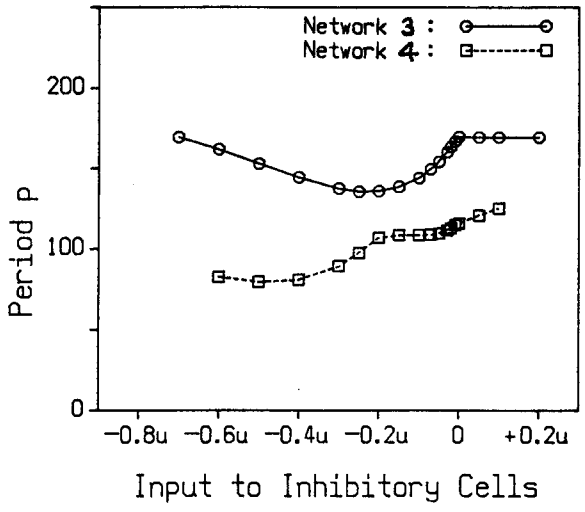

Fig.4.4. The change of the period p of rhythmic oscillation with the uniform application of the non-oscillatory input to inhibitory cells. Network 3 indicates the regular ring network as shown in Sect.4.2, and Network 4 indicates the disturbed ring network which has a set of synaptic strengths after 6000 modification steps as shown in Sect.4.3.

cells affects not only p but also the AID and the AMP of the rhythmic oscillation. In Network 3, the AIDs of excitatory cells decrease with a decrease in the inhibitory input and they decrease more rapidly with an increase in the excitatory input, as shown in Fig.4.5a. Their AMPs similarly decrease with the decreased inhibitory input, but they increase with the increased excitatory input, as shown in Fig.4.6a. This means that the influences of the excitatory input and the inhibitory input on rhythmic oscillation act in opposite directions: the excitatory input to inhibitory cells reduces the absolute values of the membrane potentials of excitatory cells, while the inhibitory input moves them in the positive direction. Since, however, the change in the AID is much smaller than that in the AMP under the influence of the inhibitory input, it should be mentioned that

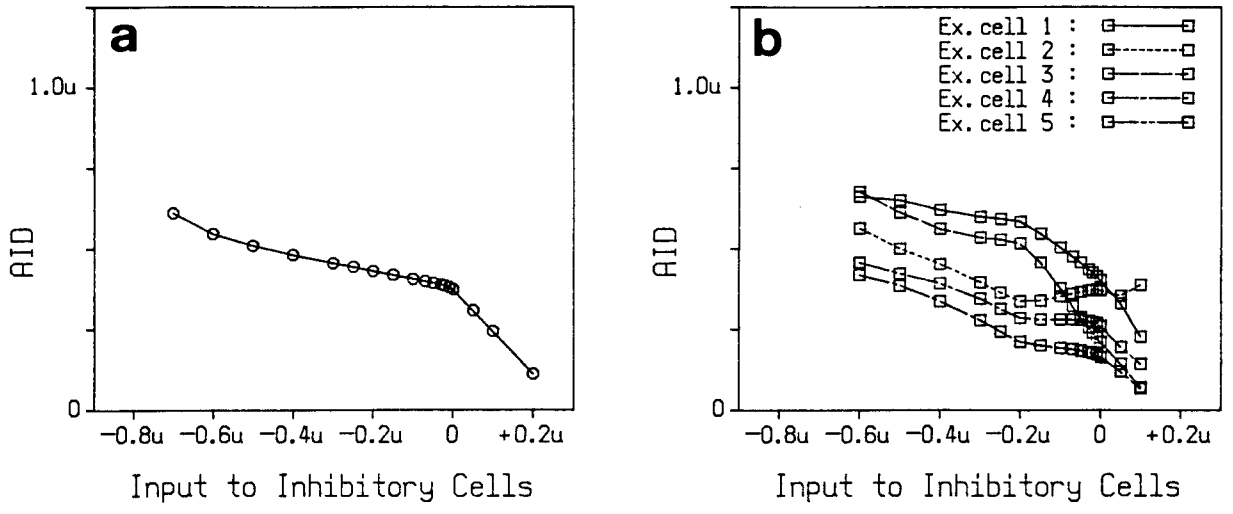

Fig.4.5a and b. The changes in the AIDs of excitatory cells with the uniform application of the non-oscillatory input to inhibitory cells. **a** Network 3. **b** Network 4.

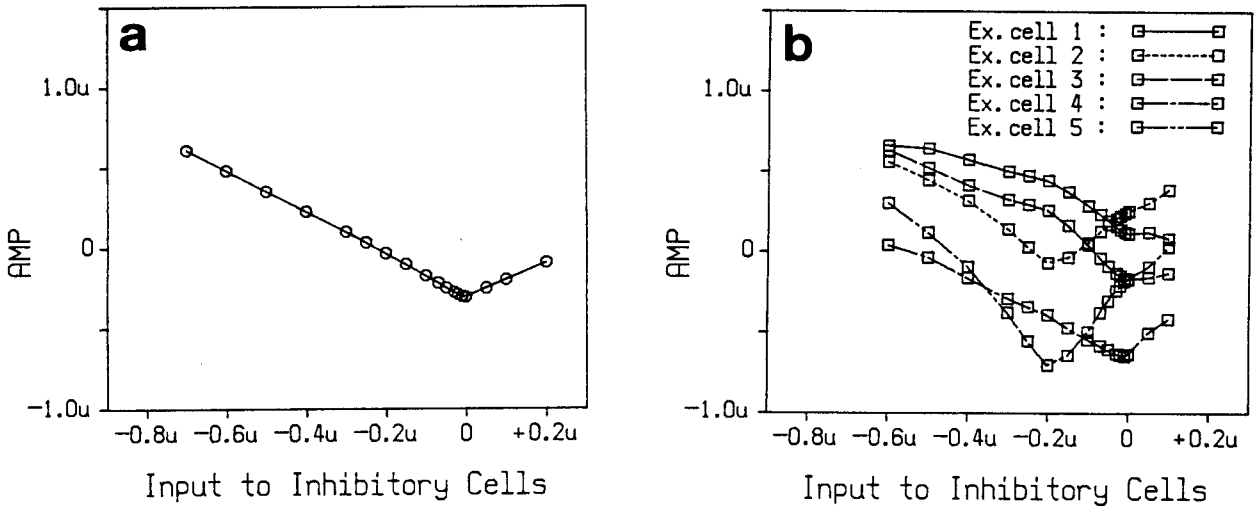

Fig.4.6a and b. The changes in the AMPs of excitatory cells with the uniform application of the non-oscillatory input to inhibitory cells. **a** Network 3. **b** Network 4.

the inhibitory input affects only the negative part of the membrane potential rather than the output impulse density. In Network 3, as shown in Figs.4.4, 4.5a and 4.6a, the 20% range below the peak of the period p can be controlled by u' ranging from 0 to -0.2u without changing the AID.

In Network 4, the changes in the AIDs and the AMPs are similar to those in Network 3, with the 25% range below the peak of the period p able to be controlled by u' ranging from -0.2u to -0.5u, as shown in Figs.4.4, 4.5b and 4.6b. However the changes in the AID and the AMP differ with each excitatory cell because of the irregularity of synaptic strengths and there is no one particular input range to control the period p in disturbed ring networks with different sets of synaptic strengths.

In this section, it has been shown that a non-oscillatory input applied uniformly to inhibitory cells may vary the period p of already generated rhythmic oscillation, without necessarily changing the AIDs. However the changes in input vs. period curves depend on the set of synaptic strengths in the ring neural network (even in the regular ring network). Therefore it must be concluded that it is difficult to control the period p using a non-oscillatory input applied uniformly to inhibitory cells, even though it is possible to change it.

4.5 Control of Period of Rhythmic Oscillation II

In this section, the same kind of input signal as the already generated rhythmic oscillation in the ring neural network

is applied to inhibitory cells.

Figure 4.7a and b shows the results when the oscillatory and excitatory input is applied to inhibitory cells No.1 in Network 3 and Network 4 in Sect.4.4. In the figure, the peak values of the square input $u_1^{(2)}(t)$ are 0, 0.1u, and 0.2u in turn from the left, and its periods p and p^+ are 200 and 90 units of time respectively. The positive part of $u_1^{(2)}(t)$ modifies the waveform of the output $\lceil x_i^{(1)}(t) \rceil^+$, and the period p of the output eventually coincides with that of $u_1^{(2)}(t)$ when the level of $u_1^{(2)}(t)$ is high enough. Figure 4.8a and b shows which pair of the periods p and p^+ of the synchronous signal $u_1^{(2)}(t)$ can lock the period p of the network output, where the peak values of $u_1^{(2)}(t)$ are 0.2u in Fig.4.8a and c and 0.3u in Fig.4.8b and d. In both Network 3 and Network 4, lockable regions exist, having lower boundaries but no upper ones. If the condition $30 \lesssim p-p^+ \lesssim 170$ in Network 3 or $30 \lesssim p-p^+ \lesssim 110$ in Network 4 is satisfied, any large synchronous signal with a long period p may lock the period of the rhythmic oscillation of the network output.

The application of the synchronous signal $u_1^{(2)}(t)$ causes a dispersion of the value of each cell's AID: the AIDs of some cells increase and they often exceed the threshold $\theta^{(1)}$ or $\theta^{(2)}$. These increases restart the algorithm, even if the rhythmic oscillation is held as a result of the synaptic modification before the application of the synchronous signal $u_1^{(2)}(t)$.

In Fig.4.9a and b is shown the result of further synaptic modification carried out under the application of the synchronous signal to inhibitory cell No.1 in Network 4. Here the peak value

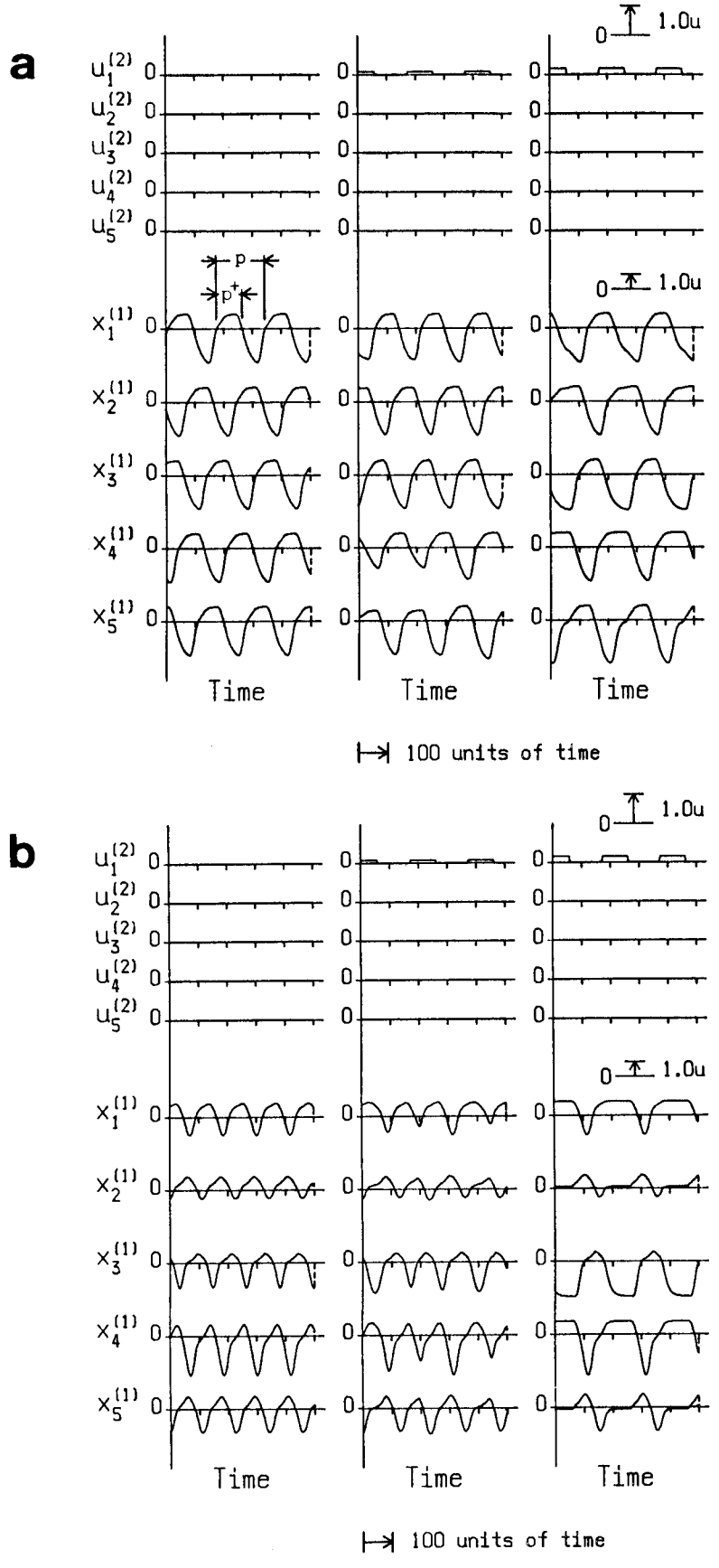

Fig.4.7a and b. The membrane potentials of excitatory cells when the oscillatory and excitatory signal is applied to inhibitory cell No.1. The peak values of the square input $u_1^{(2)}(t)$ are 0, 0.1u, and 0.2u in turn from the left, and its periods p and p^+ are 200 and 90, respectively. a Network 3. b Network 4.

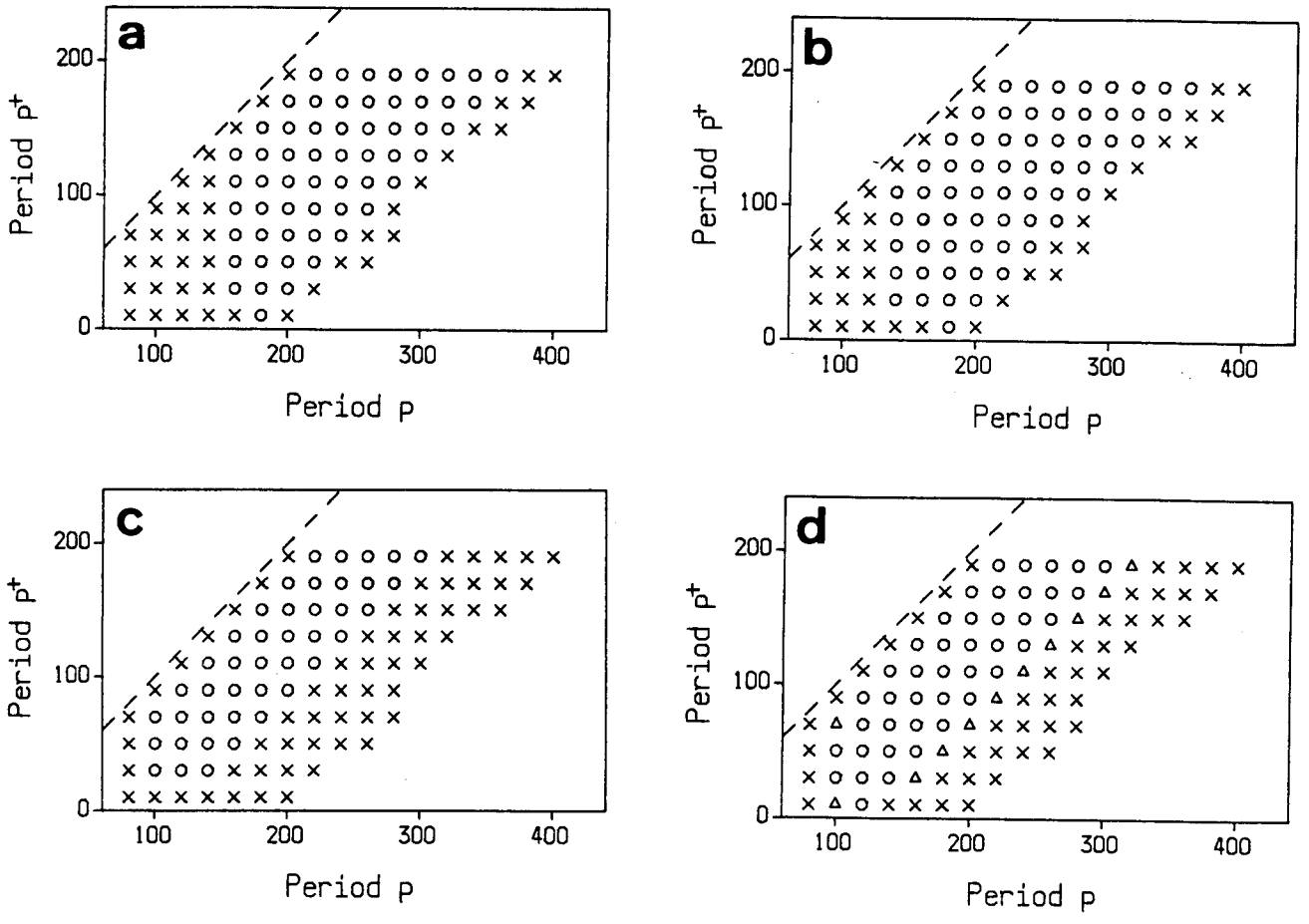

Fig.4.8a-d. The lockable pairs of the periods p and p^+ of the synchronous signal $u_1^{(2)}(t)$. Here the symbols ○, △, and × indicate lockable, almost lockable, and un-lockable pairs respectively.

a $\max_t u_1^{(2)}(t)$ = 0.2u in Network 3.

b $\max_t u_1^{(2)}(t)$ = 0.3u in Network 3.

c $\max_t u_1^{(2)}(t)$ = 0.2u in Network 4.

d $\max_t u_1^{(2)}(t)$ = 0.3u in Network 4.

of $u_1^{(2)}(t)$ is 0.2u. Figure 4.9a shows the changes in the AIDs of excitatory cells caused by the synaptic modification, and Fig.4.9b shows the membrane potentials $x_i^{(1)}(t)$ of excitatory cells at the sets of synaptic strengths after, in turn from the left, 0, 3000, and 6000 re-modification steps (see Appendix B-4). With the progress of the modification, the AIDs of excitatory cells alter gradually, and then change rapidly around 3000 re-

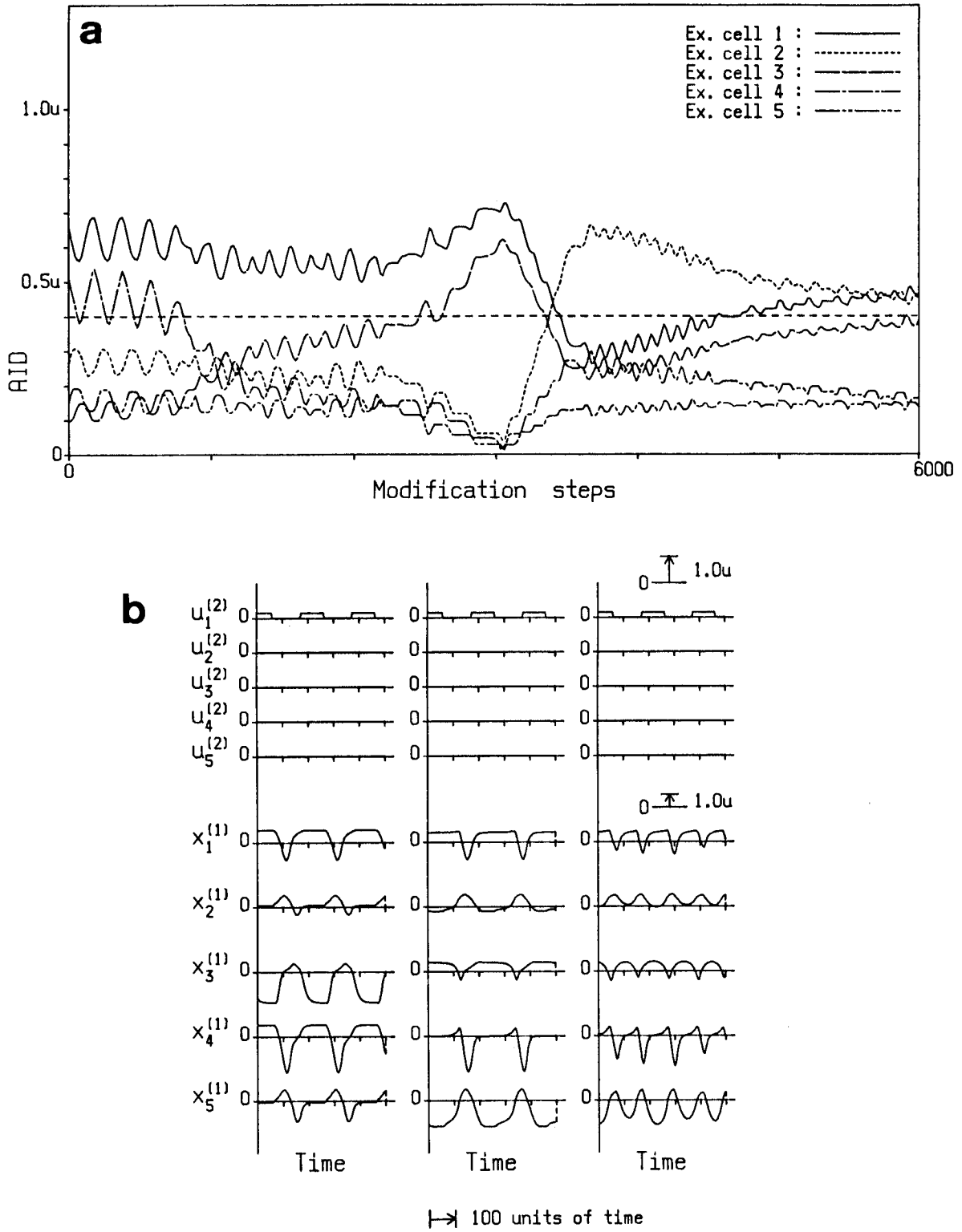

Fig.4.9a and b. Further synaptic modification under the application of the synchronous signal to inhibitory cell No.1 in Network 4. Here $\max_t u_1^{(2)}(t) = 0.2u$ and the constants in the algorithm are the same as those in Sect.4.3. **a** The changes in the AIDs of excitatory cells. **b** The membrane potentials of excitatory cells at the sets of synaptic strengths after 0, 3000, and 6000 re-modification steps (see Appendix B-4).

modification steps, as shown in the middle of Fig.4.9a. The synchronous signal locks the period p of the excitatory cells' output $\lceil x_i^{(1)}(t) \rceil^+$ at that point. However the modification after 3000 re-modification steps does not maintain the locking, and the period p of the network output begins to differ from that of the synchronous signal.

The algorithm has the effect of equalizing the AID of each cell, as can be seen from the results in Sect.4.3. Therefore the oscillatory and excitatory input to an inhibitory cell cannot act as a synchronous signal under synaptic modification, since the inputs $u_i^{(1)}(t)$ and $u_j^{(2)}(t)$ are integrated without distinction inside the cells. In other words, for the oscillatory and excitatory input to an inhibitory cell to work as a synchronous one, the application of the input must not restart the algorithm.

The two-mode selection mechanism described in Chap.3 offers a solution to the problem of re-modification. When $u_j^{(2)}(t)$ is oscillatory and excitatory, Eq.(3.2) holds and therefore Eq.(4.1) becomes

$$\tau_1 \tau_2 \frac{d^2}{dt^2} x_i^{(1)}(t) + (\tau_1 + \tau_2) \frac{d}{dt} x_i^{(1)}(t) + x_i^{(1)}(t)$$

$$= u - \sum_{j=1}^{N_2} d_{ij}\, u_j^{(2)}(t) - \sum_{i'=1}^{N_1} \Big(\sum_{j=1}^{N_2} d_{ij}\, c_{ji'} \Big) \lceil x_{i'}^{(1)}(t) \rceil^+ , \qquad (4.7)$$

Therefore when the excitatory input $^{\dagger}u$ to excitatory cells and

the oscillatory and excitatory input ${}^{\dagger}u_j^{(2)}(t)$ to an inhibitory cell are altered at the same rate, namely,

$$ {}^{\dagger}u = \kappa u \quad \text{and} \quad {}^{\dagger}u_j^{(2)}(t) = \kappa u_j^{(2)}(t) \tag{4.8} $$

the following locked output ${}^{\dagger}x_i^{(1)}(t)$ with a proportional level can be obtained:

$$ {}^{\dagger}x_i^{(1)}(t) = \kappa x_i^{(1)}(t) \ . \tag{4.9} $$

The lockable range of $u_j^{(2)}(t)$ is wide for a certain u as shown in Fig.4.8a-d. Therefore even if the inputs are set up as

$$ {}^{\dagger}u = \kappa u \quad \text{and} \quad u_j^{(2)}(t) = \gamma u_j^{(2)}(t) \quad (\gamma \neq \kappa) \tag{4.10} $$

instead of Eq.(4.8), the locked output may also be derived by choosing an adequate range of γ. For example, we will consider the following two cases with the same levels of synchronous signal whose periods p and p^+ are 180 and 90 respectively:

$$ \text{Input 1:} \quad u = 1.000 \quad \text{and} \quad \max_t u_1^{(2)}(t) = 0.200 \tag{4.11} $$

$$ \text{Input 2:} \quad u = 0.667 \quad \text{and} \quad \max_t u_1^{(2)}(t) = 0.200 \tag{4.12} $$

Input 1 corresponds to $\max_t u_1^{(2)}(t) = 0.2u$, and Input 2 corresponds to $\max_t u_1^{(2)}(t) = 0.3u$. In both cases the locked output can be obtained. In Input 1, the maximal AIDs of excitatory cells and inhibitory cells are calculated as follows:

$$\max_i \text{AID of ex. cells} = \begin{cases} 0.422 & \text{(in Network 3)} \\ 0.593 & \text{(in Network 4)} \end{cases}$$

$$\max_j \text{AID of in. cells} = \begin{cases} 0.471 & \text{(in Network 3)} \\ 0.498 & \text{(in Network 4)} \end{cases} . \quad (4.13)$$

In Input 2, they are calculated as follows:

$$\max_i \text{AID of ex. cells} = \begin{cases} 0.288 & \text{(in Network 3)} \\ 0.396 & \text{(in Network 4)} \end{cases}$$

$$\max_j \text{AID of in. cells} = \begin{cases} 0.353 & \text{(in Network 3)} \\ 0.324 & \text{(in Network 4)} \end{cases} . \quad (4.14)$$

In Input 2, where only the excitatory input to excitatory cells is reduced, the max AID of excitatory cells and the max AID of inhibitory cells are actually suppressed below 0.4 in both Network 3 and Network 4. Hence the algorithm cannot function if the constants in the algorithm are fixed as shown in Appendix B-5 (they are equal to those in Appendix B-2 if u=1.0). Thus if, in the recalling mode, the excitatory input u to excitatory cells is set low enough to avoid restarting the synaptic modification, the locked output can be obtained, even if the value of the AID disperses a little, by applying the synchronous signal to an inhibitory cell.

Above, we have discussed only a single excitatory synchronous input. For further reference, Fig.4.10a and b shows a case in which the oscillatory and excitatory input was applied to two adjacent inhibitory cells. The locked output was obtained

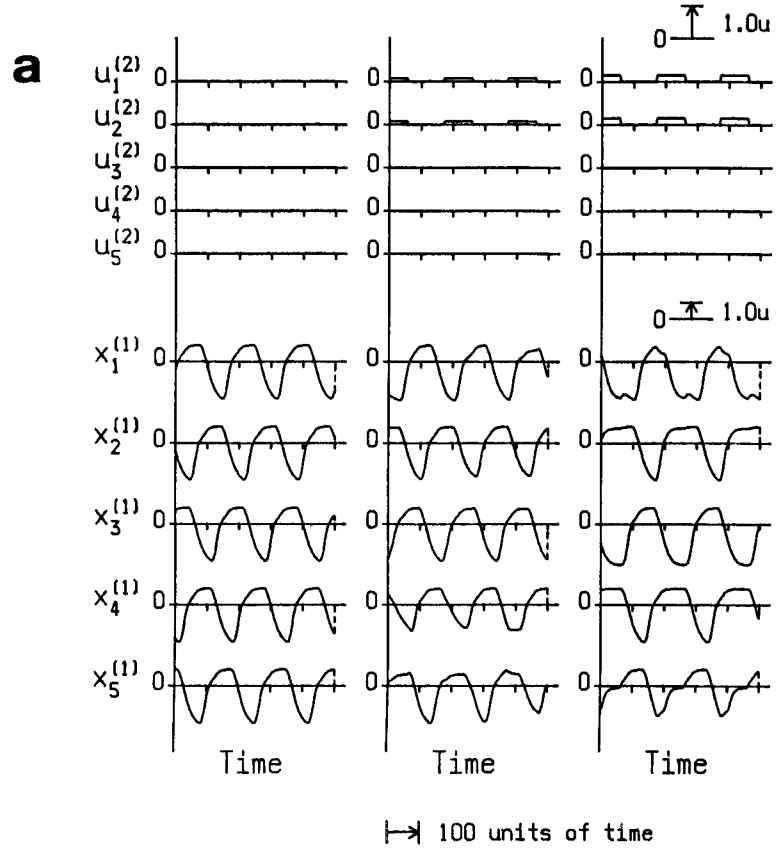

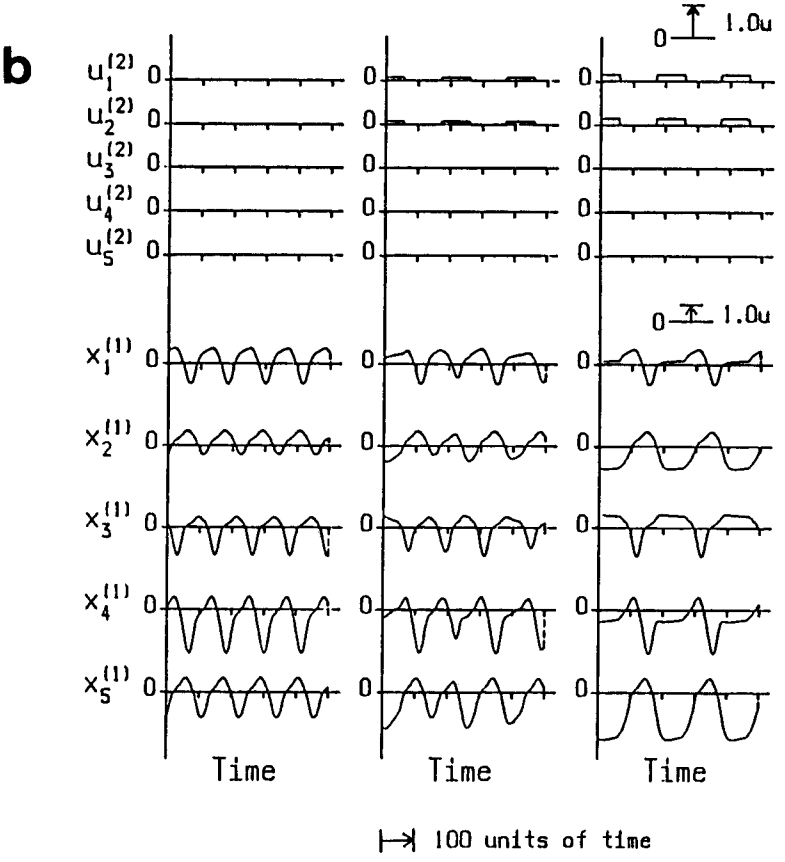

Fig.4.10a and b. The membrane potentials of excitatory cells when the oscillatory and excitatory signal is applied to two adjacent inhibitory cells. The shapes of the square inputs are the same as those in Fig.4.7a and b. a Network 3. b Network 4.

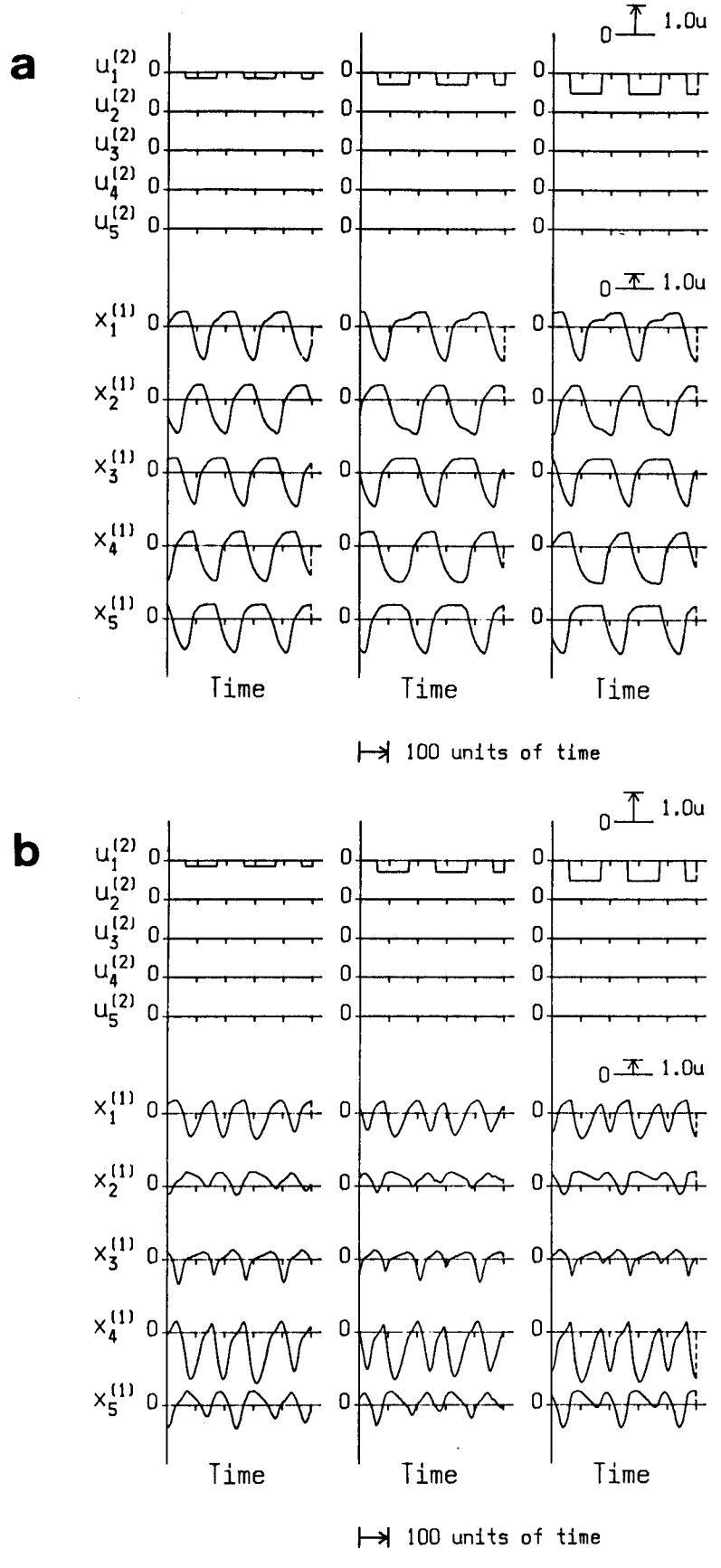

Fig.4.11a and b. The membrane potentials of excitatory cells when the oscillatory and inhibitory signal is applied to inhibitory cell No.1. The peak values of the square input $u_1^{(2)}(t)$ are -0.2u, -0.4u, and -0.7u in turn from the left, and its periods p and p^+ are 200 and 90, respectively. a Network 3. b Network 4.

in a similar way. Figure 4.11a and b shows a case in which the oscillatory and inhibitory input was applied to an inhibitory cell. The locked output was obtained in Network 3 but not in Network 4. It is clear that the excitatory synchronous input is effective for controlling the period.

4.7 Discussion

We have discussed the ring neural network qua a generator of rhythmic oscillation. In Fig.4.12, the way in which the ring neural network may function effectively to generate, maintain and control the period of rhythmic oscillation is summarized. Procedure 1 gives the process for generating rhythmic oscillation. It should be noted that the action of the algorithm to decrease the difference between the AIDs of cells is antagonistic to the period locking process. The algorithm of Eqs.(2.6) and (2.7) absorbs the change in the AID and obstructs the synchronous signal. Procedure 2 is necessary to prevent this obstruction. The period p of the output can be changed by applying the non-oscillatory input uniformly to inhibitory cells as described in Sect.4.5, but it is difficult in this way to obtain the desired period. Procedure 3 is better for controlling the period p.

One fundamental problem remaining to be solved is how or where the synchronous signal with the desired period p to inhibitory cells is created. The best course for solving this problem will be to collate the ring neural network described here

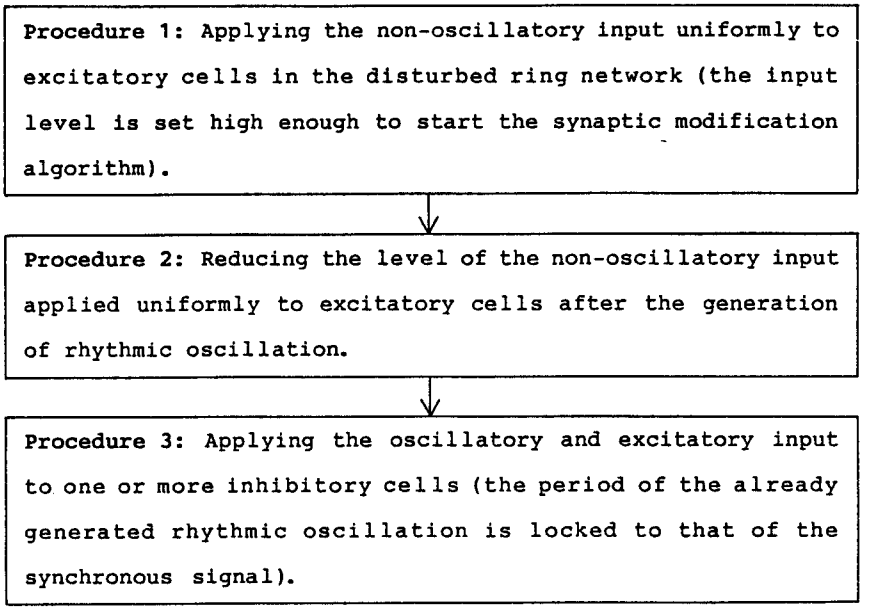

Fig.4.12. The summarization of the procedures for the ring neural network to function as a generator of rhythmic oscillation.

with the granule-Golgi network in the cerebellum, as shown in Fig.4.13. Such a comparison suggests the possibility that the granule-Golgi network in the cerebellum functions as a generator of rhythmic oscillation. In the many models for the cerebellum, the climbing fibers are thought to deliver learning instructions to the Purkinje cells and they are believed to hold the key to the solution of the learning mechanism (Albus, 1971; Melkonian et al., 1982). The climbing fibers are also connected to the Golgi cells (Szentagothai, 1968). If we assume that the signal on the climbing fibers controls the period of rhythmic oscillation in the granule-Golgi network, then this signal must be in the form of bursts of nerve impulses.

The basket-stellate-Purkinje network is connected backward to the granule-Golgi network through the parallel fibers in the

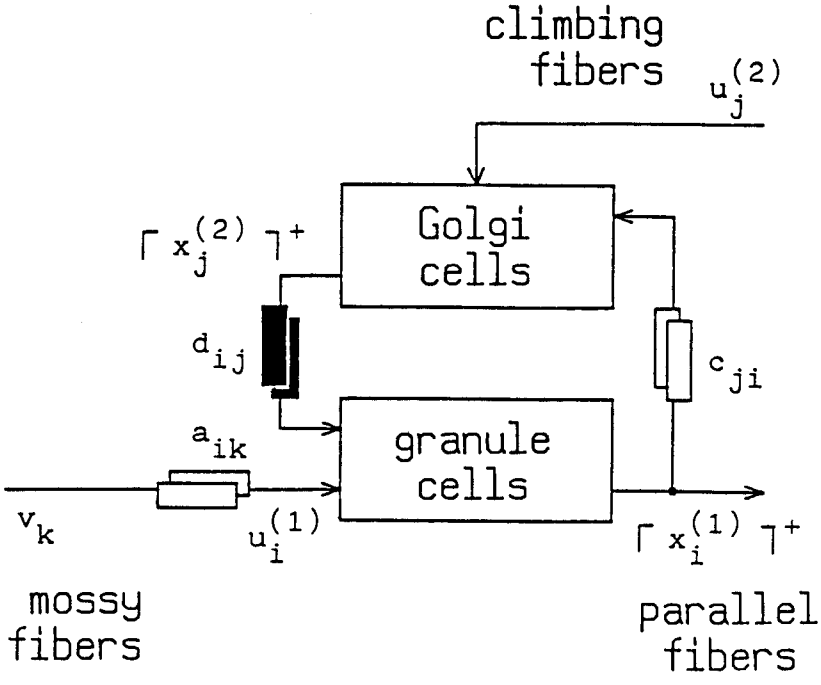

Fig.4.13. The block diagram of the granule-Golgi network in the cerebellum. The network has two input channels from the mossy fibers and the climbing fibers.

cerebellum. If the signal on the climbing fibers is assumed to be in the form of bursts of nerve impulses, it may be necessary to construct a new learning model of the cerebellum in which this type of signal is the final output. Therefore it will be important to clarify how the basket-stellate-Purkinje network can deal with rhythmic oscillation with the dispersed AIDs as mentioned in Sect.4.5. Any future research to prove the correctness of this collation of the ring neural network and the granule-Golgi network must also investigate the role of rhythmic oscillation in the nervous system.

Chapter 5

Synthesizer Learning Model of the Cerebellum

A new learning model of the cerebellum is proposed based on the theories described in Chaps.2, 3, and 4. The algorithm is applied to all the modifiable synapses in the model, by which process the granule-Golgi network works as a generator of a set of oscillations with different phases and the basket-stellate-Purkinje network acts as a wave synthesizer. This model can learn the signals from the climbing fibers to the Purkinje cells and the signals with their inverse phase are drawn out as the final output.

5.1 Introduction

The cerebellum has a homogeneous arrangement of cells and it has in recent years attracted the attention of neural modelers. The Perceptron was compared in detail with the cerebellar cortex (Marr, 1969; Eccles, 1973), and this collation is still often quoted. A template matching model functioning under a certain improved synaptic modification algorithm has been proposed and it is also collated with the cerebellum (Hirai, 1980a,b). Even though many models to explain the cerebellum's mechanism of information processing have been constructed, the principal discussions by modelers have concentrated on spacial pattern

processing. Since, however, the cerebellum is involved in the control of the actuator both spacially and temporally, its mechanism should be explained using a model which illustrates both the spacial and temporal surfaces of control simultaneously.

Recently the temporal control surface has come under investigation and the time delay of the signals travelling on the parallel fibers has been researched. A hypothesis has been proposed that the Purkinje cells work as a phase lead/lag compensator (Hassul, 1977; Fujita, 1982a,b). The impulse sequence for controlling the muscles is not of a constant interval but is in the form of bursts of nerve impulses and therefore the model of the cerebellum must learn this type of signal and draw it out as a final output.

In this chapter, developing the interpretation of the granule-Golgi network described in Chap.4, a new learning model of the cerebellum is advanced. In Sect.5.2, the five kinds of cells in the cerebellum are modeled and classified. Then the two stages, that is, the granule-Golgi network and the basket-stellate-Purkinje network, and the functions of each stage are described separately in Sects.5.3 and 5.4. In Sect.5.5, the two stages are connected and the total model of the cerebellum is detailed. Simulation shows that the output from the Purkinje cells after learning has the inverse phase of the signals from the climbing fibers. In Sect.5.6, the results are summarized and the course of future research is discussed.

5.2 Neural Cells in the Cerebellum

In the cerebellar cortex, there are five kinds of neural cells. In this chapter, the ordinary analog neuron models with integral time constants shown in Fig.5.1 (Type A cell) are employed as the excitatory granule, inhibitory Golgi, inhibitory basket, and inhibitory stellate cells. In the modifiable synapses connected to the Type A cell, the synaptic modification is carried out according to the algorithm described by Eqs.(2.6) and (2.7).

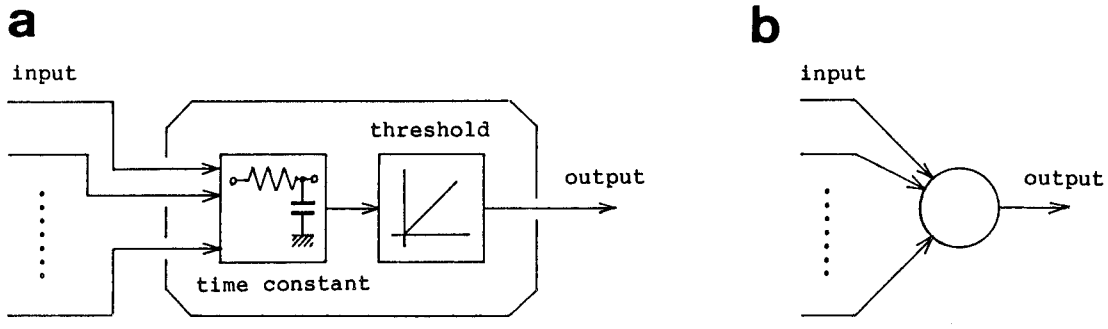

Fig.5.1a and b. A model of a neural cell with integral time constant and analog threshold (Type A cell). Here this model is employed as the granule, Golgi, basket, or stellate cell. **a** Schematic diagram. **b** Symbolic expression.

The inhibitory Purkinje cells receive synaptic connections from the basket and stellate cells and the climbing fibers. The synapses from the basket cells and the climbing fibers exist on the cell bodies, while those from the stellate cells connect to the dendritic trees (Szentagothai, 1969). Founded on this structural difference, we assume here that every part of the well-grown dendrite has a threshold effect. Hence the Purkinje cells are modeled as shown in Fig.5.2 (Type B cell), which can be

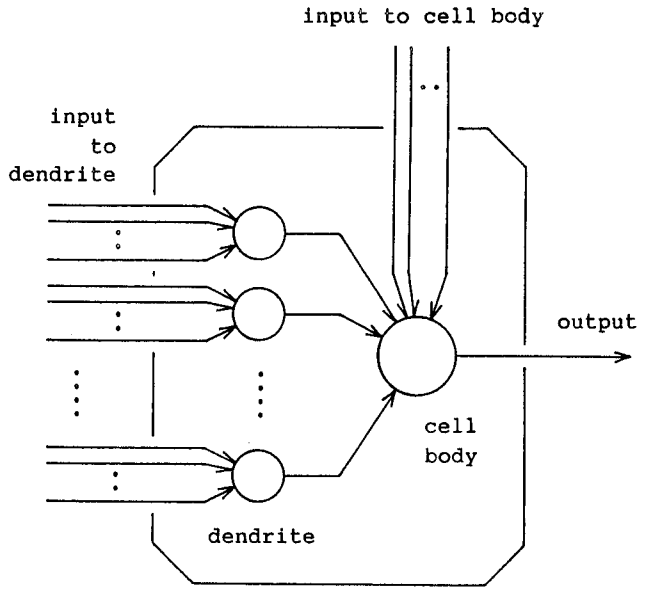

Fig.5.2. A model of a neural cell with a well-grown dendrite (Type B cell). Here this model is employed as the Purkinje cell. A Type B cell can be equivalently represented using Type A cells.

represented equivalently using Type A cells. In the modifiable synapses connected to the Type B cell, the synaptic modification progresses in a similar way to that of the Type A cell, except that the post-synaptic AMP is not that of any particular part of the dendrite but is that of the cell body.

5.3 Granule-Golgi Network

5.3.1 Learning Process

The granule-Golgi network forms feedback inhibition composed of the granule and Golgi cells. The network has two input channels from the outside: the granule cells receive the input from the mossy fibers and the Golgi cells do so from the climbing

fibers. Ignoring for the moment the input channel from the climbing fibers to the Golgi cells, the network behavior is examined here. The equations for the network employing Type A cells can be represented as follows:

$$\tau_g \frac{d}{dt} x_i^{(g)}(t) + x_i^{(g)}(t) = u_i^{(g)}(t) - \sum_{j=1}^{N_G} d_{ij}^* \lceil x_j^{(G)}(t) \rceil^+$$

$$(i=1,2,---,N_g)$$

$$\tau_G \frac{d}{dt} x_j^{(G)}(t) + x_j^{(G)}(t) = \sum_{i=1}^{N_g} c_{ji}^* \lceil x_i^{(g)}(t) \rceil^+ .$$

$$(j=1,2,---,N_G) \quad (5.1)$$

Here $x_i^{(g)}(t)$ and $x_j^{(G)}(t)$ are the membrane potentials of the granule and Golgi cells, and τ_g and τ_G are their integral time constants. c_{ji}^* and d_{ij}^* indicate the modifiable synaptic strengths between the granule and Golgi cells.

The algorithm is applied to the network as illustrated in Fig.5.3a (the network constants etc. are listed in Appendix C-1). Figure 5.3b-d shows the output of the granule cells in impulse density before modification (Network 5), after 2760 modification steps, and after 6000 modification steps (Network 6), respectively. Each granule cell initially outputs a non-oscillatory signal, and with the progress of the synaptic modification, rhythmic oscillation appears as happened in the networks used in Chaps.2, 3, and 4. The period of the rhythmic oscillation has a tendency to converge rapidly on a certain

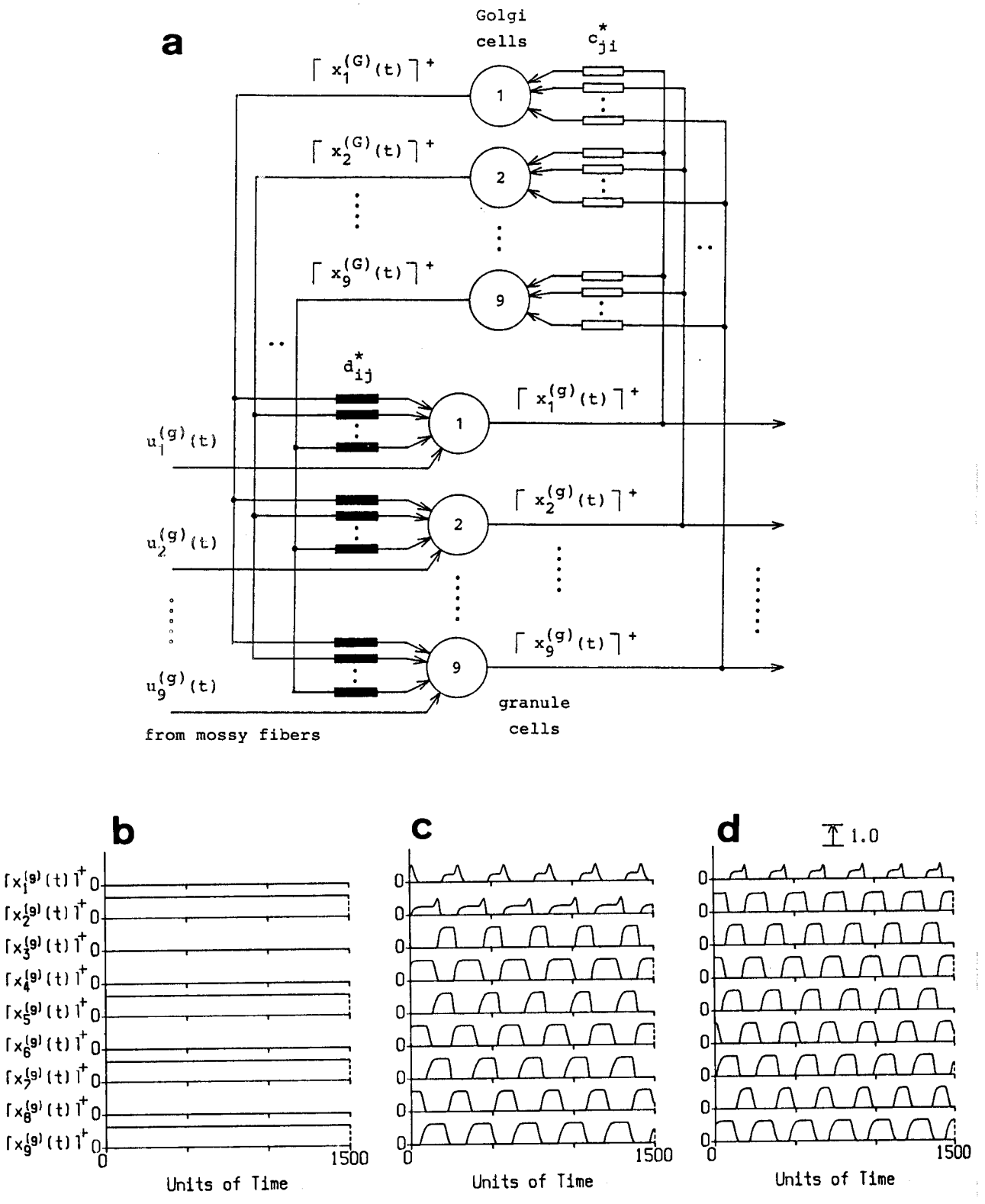

Fig.5.3a-d. Learning process as a result of the synaptic modification of c^*_{ji} and d^*_{ij} in the granule-Golgi network. **a** The schematic diagram of the simulated network (see Appendix C-1). **b** The output $\lceil x_i^{(g)}(t) \rceil^+$ of the granule cells before modification (Network 5). **c** After 2760 modification steps. **d** After 6000 modification steps (Network 6).

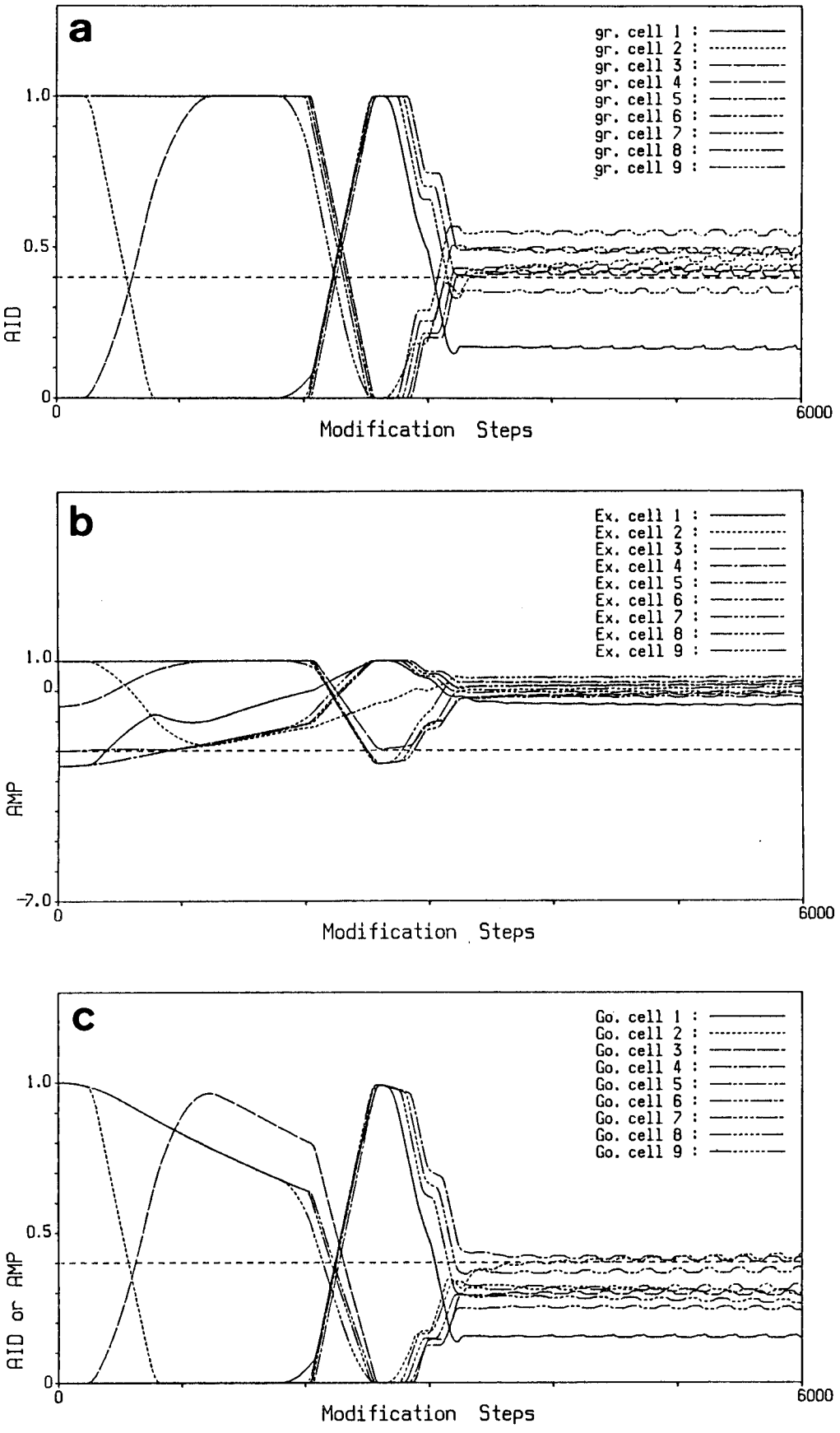

Fig.5.4a-c. The changes in the AIDs and the AMPs during the synaptic modification. **a** AID of the granule cells. **b** AMP of the granule cells. **c** AID of the Golgi cells.

value.

Figure 5.4a-c shows the changes in, respectively, the AIDs of the granule cells, the AMPs of the granule cells and the AIDs of the Golgi cells during the synaptic modification. The parameters all vary greatly until the oscillation appears at around 2700 modification steps and then the AIDs of both the granule and Golgi cells gather around the threshold $\theta^{(g)}$ or $\theta^{(G)}$. Since the progress of the synaptic modification depends on the difference of the AID and θ as is evident from Eqs.(2.6) and (2.7), the modification speed drops to an extremely low level once the rhythmic oscillation is brought back. The granule-Golgi network should be considered to have the function of generating rhythmic oscillation.

5.3.2 Period Locking Process

Taking into account the input channel from the climbing fibers, the behavior of the granule-Golgi network is analyzed. The equations of the network can be represented as follows:

$$\tau_g \frac{d}{dt} x_i^{(g)}(t) + x_i^{(g)}(t) = u_i^{(g)}(t) - \sum_{j=1}^{N_G} d_{ij} \lceil x_j^{(G)}(t) \rceil^+$$

$$(i=1,2,---,N_g)$$

$$\tau_G \frac{d}{dt} x_j^{(G)}(t) + x_j^{(G)}(t) = u_j^{(G)}(t) + \sum_{i=1}^{N_g} c_{ji} \lceil x_i^{(g)}(t) \rceil^+ .$$

$$(j=1,2,---,N_G) \quad (5.2)$$

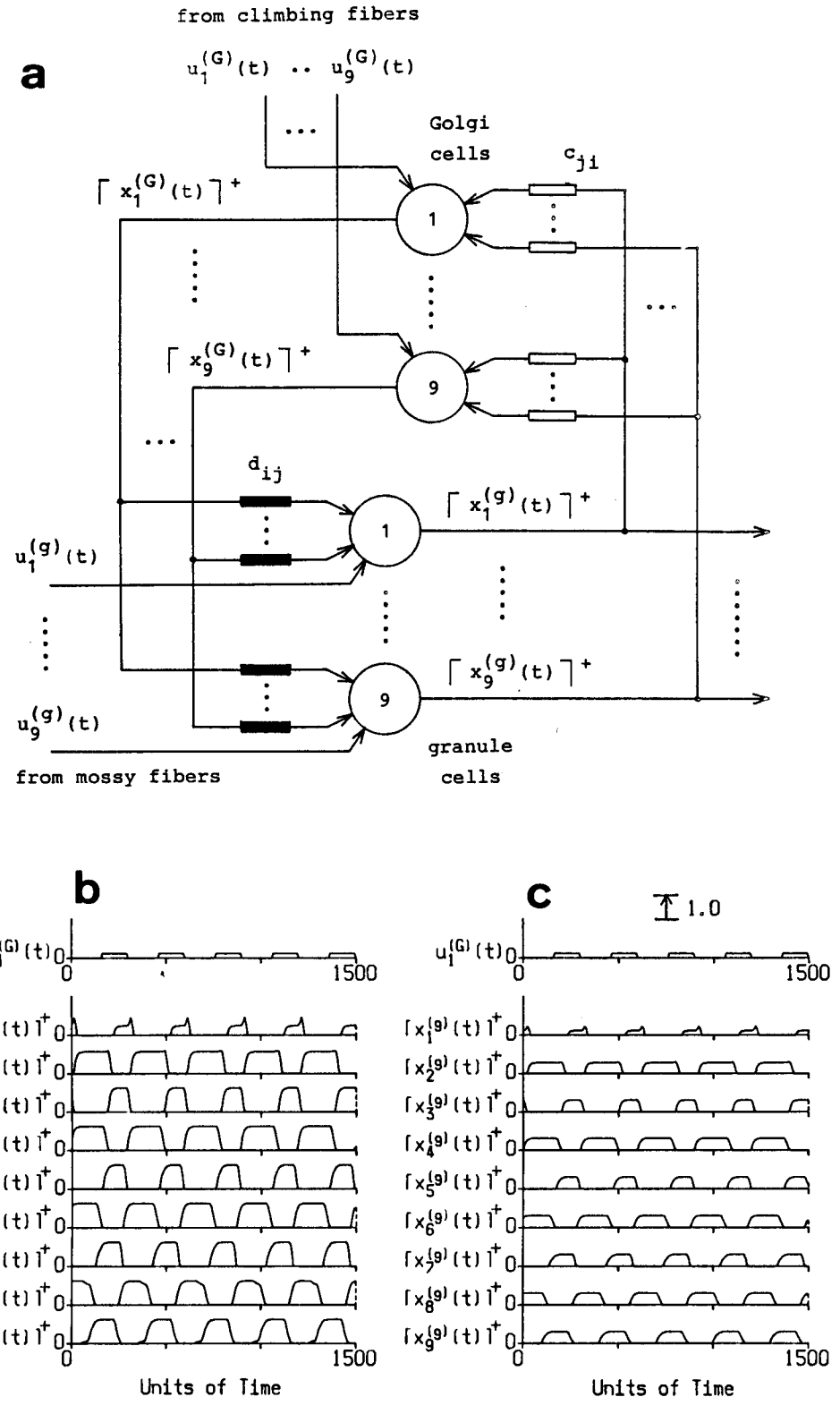

Fig.5.5a-c. Period locking process due to the square input $u_1^{(G)}(t)$ from the climbing fiber to the Golgi cell in the granule-Golgi network. Here the peak value of $u_1^{(G)}(t)$ is 0.2 and the set of synaptic strengths is fixed as in Network 6. **a** The schematic diagram of the simulated network. **b** The output $\lceil x_i^{(g)}(t) \rceil^+$ of the granule cells when $u_i^{(g)}(t)=1.0$. **c** When $u_i^{(g)}(t)=0.5$.

where c_{ji} and d_{ij} are taken to be fixed.

Figure 5.5a illustrates the schematic diagram of the simulated network with the same set of synaptic strengths as Network 6 and Fig.5.5b and c shows the results when the oscillatory and excitatory signal $u_1^{(G)}(t)$ is applied from the climbing fiber. The period of the oscillatory signal $u_1^{(G)}(t)$ is set differently from that of the already generated rhythmic oscillation. If the level of $u_1^{(G)}(t)$ with an adequate period is high enough, the period of the output $\lceil x_i^{(g)}(t) \rceil^+$ of the granule cells coincides with that of $u_1^{(G)}(t)$ (see Fig.5.5b). If c_{ji} and d_{ij} are modifiable, the dispersion of the AIDs caused by the application of $u_1^{(G)}(t)$ often restarts the synaptic modification and obstructs the period locking. As detailed in Chap.4, the two-mode selection mechanism solves this obstruction: even if the level of $u_i^{(g)}(t)$ is reduced to half, a locked output can be obtained (see Fig.5.5c). Hence the input channel from the climbing fibers to the Golgi cells should be considered to control the period of the rhythmic oscillation in the granule-Golgi network.

5.4 Basket-Stellate-Purkinje Network

5.4.1 Suppression of Large Input

The basket-stellate-Purkinje network located behind the granule-Golgi network forms feedforward inhibition. In this subsection, firstly the effect of the basket cells on the

Purkinje cells is studied. The equations of the network employing Type A cells as basket cells and Type B cells as Purkinje cells are represented as follows:

$$\tau_p \frac{d}{dt} x_l^{(P)}(t) + x_l^{(P)}(t) = \sum_{q=1}^{N_d} \lceil x_{lq}^{(d)}(t) \rceil^+ - \sum_{n=1}^{N_b} o_{ln} \lceil x_n^{(b)}(t) \rceil^+$$

$$(l=1,2,---,N_p)$$

$$\tau_d \frac{d}{dt} x_{lq}^{(d)}(t) + x_{lq}^{(d)}(t) = \sum_{p=1}^{N_F} e_{lqp} v_p^{(F)}(t)$$

$$(q=1,2,---,N_d)$$

$$\tau_b \frac{d}{dt} x_n^{(b)}(t) + x_n^{(b)}(t) = u_n^{(b)}(t) + \sum_{p=1}^{N_F} h_{np} v_p^{(F)}(t) \quad .$$

$$(n=1,2,---,N_b) \quad (5.3)$$

Here $x_l^{(P)}(t)$ and $x_n^{(b)}(t)$ represent the membrane potentials of the Purkinje cell bodies and the basket cells, and $x_{lq}^{(d)}(t)$ represent the local membrane potentials of the Purkinje dendrites. τ_p, τ_d, and τ_b are the corresponding integral time constants and e_{lqp}, h_{np}, and o_{ln} are the synaptic strengths between cells or from fibers to cells, and they are fixed in this case. The input $u_n^{(b)}(t)$ from the outside to the basket cells is taken into account in order to control the thresholds equivalently.

The simulation is carried out in the network illustrated in Fig.5.6a (the network constants etc. are listed in Appendix C-2), and the result is shown in Fig.5.6b and c. When rhythmic

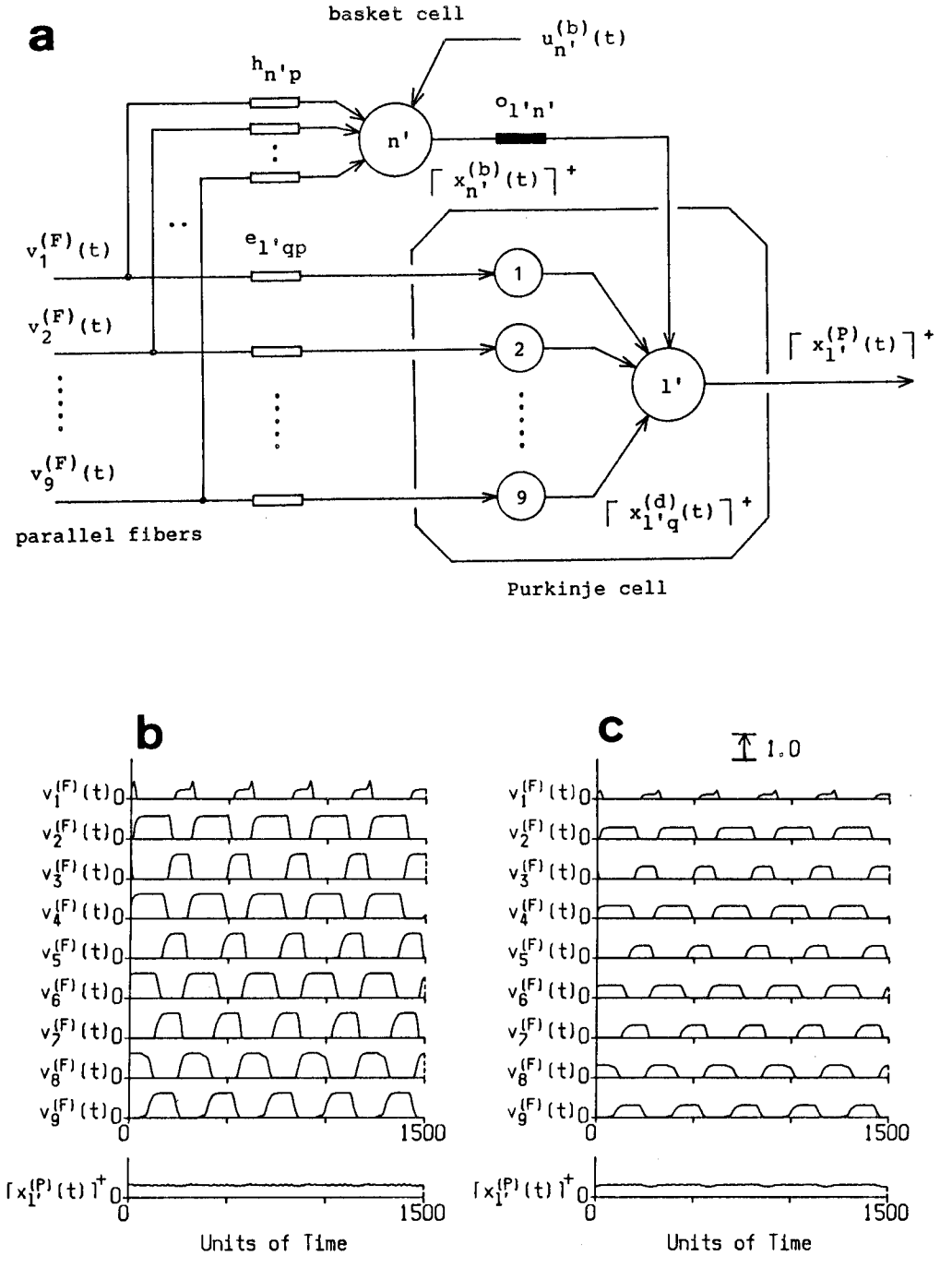

Fig.5.6a-c. Suppression of the large input in the basket-Purkinje cells. **a** The schematic diagram of the simulated network (see Appendix C-2). **b** The output $\lceil x_{1'}^{(P)}(t) \rceil^+$ of the Purkinje cell when the peak value of the input $v_p^{(F)}(t)$ is equal to 1.0. **c** When the peak value of $v_p^{(F)}(t)$ is equal to 0.5.

oscillation is applied from the parallel fibers, the oscillation is combined in the basket cell via homogeneous $h_{n'p}$ and non-oscillatory inhibition is provided to the Purkinje cell body. Since $u_{n'}^{(b)}(t)$ is set negative, the threshold of the basket cell increases correspondingly. Therefore the inhibition starts to work only when the amount of the input from the parallel fibers exceeds $u_{n'}^{(b)}(t)$. In the case of the application of a large input, the membrane potential $x_{1'}^{(P)}(t)$ of the Purkinje cell body is suppressed within a certain value (see Fig5.6b). In other words, even if the peak level of rhythmic oscillation is reduced in order to obtain a locked output without synaptic modification in the granule-Golgi network, the membrane potential of the Purkinje cell body can be kept almost constant (see Fig.5.6c). Choosing the level of $u_{n'}^{(b)}(t)$ and $h_{n'p}$ adequately, also realized is a case in which the positive membrane potential of the Purkinje cell body can be obtained only when the peak level of rhythmic oscillation is reduced.

Although various sets of synaptic strengths are conceivable, those used in this section enable the basket cells to work most effectively as a suppessor of a large input to the Purkinje cells. It is evident that this effect can be obtained in a similar way when a Type A cell instead of a Type B cell is employed as a Purkinje cell.

5.4.2 Filtering of Rhythmic Oscillation

Since the synapses from the stellate cells are connected to

the Purkinje dendrites, the inhibitory effect of the stellate cells must differ from that of the basket cells.

The equations of the stellate-Purkinje network can be represented as follows:

$$\tau_p \frac{d}{dt} x_l^{(P)}(t) + x_l^{(P)}(t) = \sum_{q=1}^{N_d} \lceil x_{lq}^{(d)}(t) \rceil^+$$

$$(l=1,2,---,N_p)$$

$$\tau_d \frac{d}{dt} x_{lq}^{(d)}(t) + x_{lq}^{(d)}(t) = \sum_{p=1}^{N_F} e_{lqp} v_p^{(F)}(t) - \sum_{m=1}^{N_s} g_{lqm} \lceil x_m^{(s)}(t) \rceil^+$$

$$(q=1,2,---,N_d)$$

$$\tau_s \frac{d}{dt} x_m^{(s)}(t) + x_m^{(s)}(t) = \sum_{p=1}^{N_F} f_{mp} v_p^{(F)}(t)$$

$$(m=1,2,---,N_s) \quad (5.4)$$

Here $x_m^{(s)}(t)$ represent the membrane potentials of the stellate cells. f_{mp} and g_{lqm} indicate, respectively, the synaptic strengths from the parallel fibers to the stellate cells and from the stellate cells to the Purkinje dendrites.

The simulated network is illustrated in Fig.5.7a (the network constants etc. are listed in Appendix C-3) and the result is shown in Fig.5.7b and c. When the non-oscillatory signals generated in Network 5 are applied to the network, the membrane potential $x_{l'}^{(P)}(t)$ of the Purkinje cell body is inhibited below zero shortly after the time delay (see Fig.5.7b). When, on the

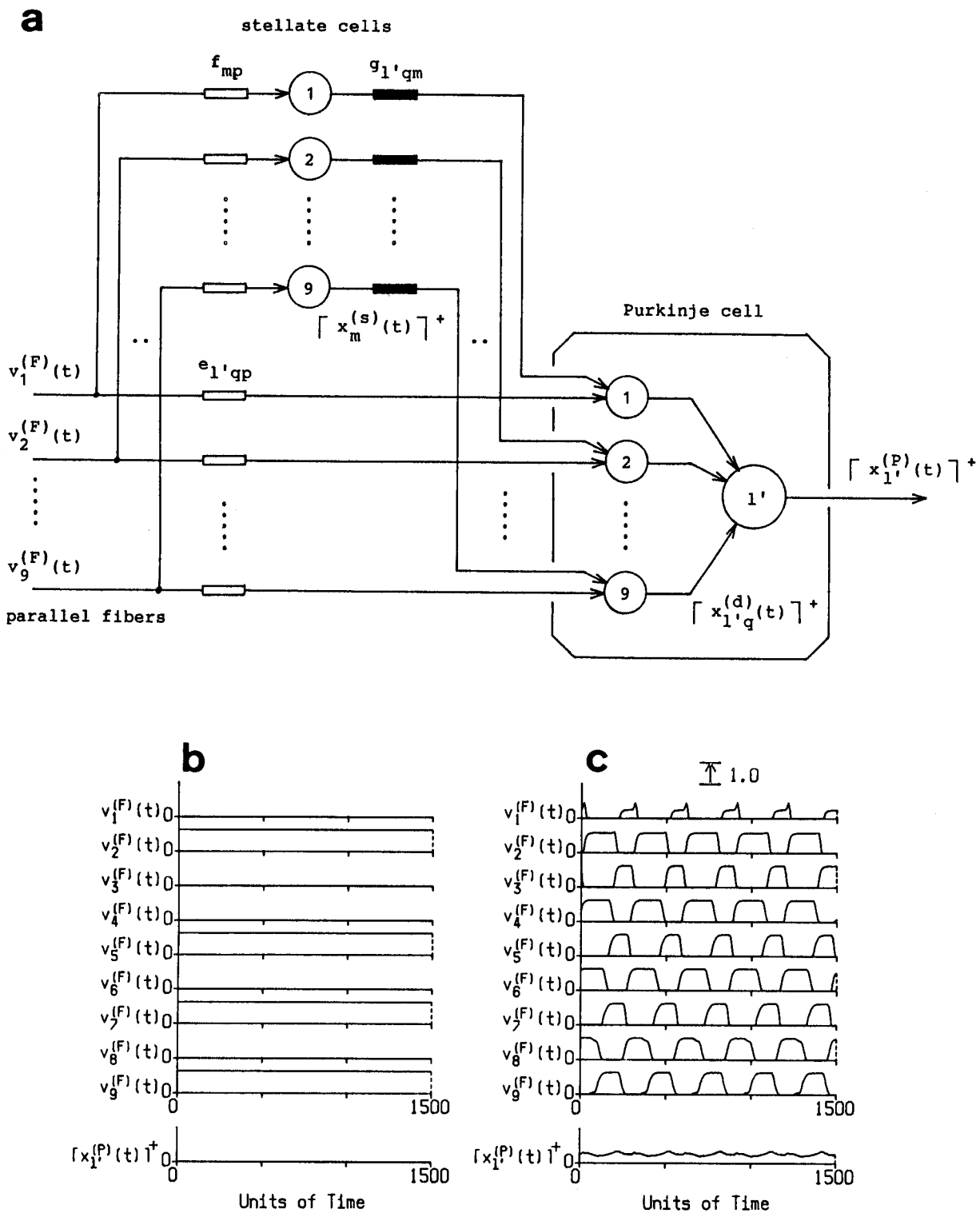

Fig.5.7a-c. Filtering of rhythmic oscillation in the stellate-Purkinje network. **a** The schematic diagram of the simulated network (see Appendix C-3). **b** The output $\lceil x_{1'}^{(P)}(t) \rceil^+$ of the Purkinje cell when the input $v_p^{(F)}(t)$ is non-oscillatory (the output of Network 5). **c** When the input $v_p^{(F)}(t)$ is oscillatory (the output of Network 6).

other hand, the oscillatory signals generated in Network 6 are applied, the phases of the direct signals and the inhibition via the stellate cells are shifted in the Purkinje dendrite. In this case, the negative membrane potentials caused by the inhibition of the stellate cells do not interfere with each other, because of the threshold effect in every part of the Purkinje dendrite. Therefore rhythmic oscillation passes through the Purkinje dendrite and reaches the cell body, where the non-oscillatory membrane potential is created by combining the signals (see Fig.5.7c).

As mentioned above, the stellate-Purkinje network employing a Type B cell as a Purkinje cell may function as a filter through which only rhythmic oscillation can pass. Although we have considered only the case in which $g_{l'qm}$ are diagonal, it is clear that the same effect can be obtained even if $g_{l'qm}$ are fairly disturbed.

5.4.3 Learning Mechanism on Purkinje Cell

In this subsection, the algorithm is applied to the synapses from the parallel fibers to the Purkinje cells and the latter stage of the learning mechanism is examined. The action on the Purkinje cells of the algorithm which effectively generates rhythmic oscillation in the granule-Golgi network is very interesting. The network including the parallel and climbing fibers and the Purkinje cells can be represented as follows:

$$\tau_P \frac{d}{dt} x_l^{(P)}(t) + x_l^{(P)}(t) = \sum_{q=1}^{N_d} \lceil x_{lq}^{(d)}(t) \rceil^+ + u_l^{(M)}(t)$$

$$(l=1,2,---,N_P)$$

$$\tau_d \frac{d}{dt} x_{lq}^{(d)}(t) + x_{lq}^{(d)}(t) = \sum_{p=1}^{N_F} e_{lqp}^* v_p^{(F)}(t) \quad .$$

$$(q=1,2,---,N_d) \quad (5.5)$$

Here $u_l^{(M)}(t)$ indicate the input from the climbing fibers.

Figure 5.8a shows the simulated network (the network constants etc. are listed in Appendix C-4) and Fig.5.8b-f shows the result. In this case, σ in the window function is set up at 20 units of time, while σ was equal to 500 units of time in the former stage. This means that the changes in the synaptic strengths $e_{l',qp}^*$ are assumed to have the less hysteresis than those in c_{ji}^* and d_{ij}^*.

Applying rhythmic oscillation from the parallel fibers (see Fig.5.8b), the non-oscillatory membrane potential appears in the Purkinje cell body by way of homogeneous $e_{l',qp}^*$ (see Fig.5.8c). Synaptic modification does not start yet since the threshold $\eta^{(P)}$ in the algorithm is set up at 0.4.

At this point, the square input $u_{l'}^{(M)}(t)$ with the same period as that of the rhythmic oscillation from the parallel fibers is applied via the climbing fiber to the Purkinje cell. The two inputs, from the parallel fibers and the climbing fiber, are combined in the Purkinje cell body. As a result, $x_{l'}^{(P)}(t)$ exceeds

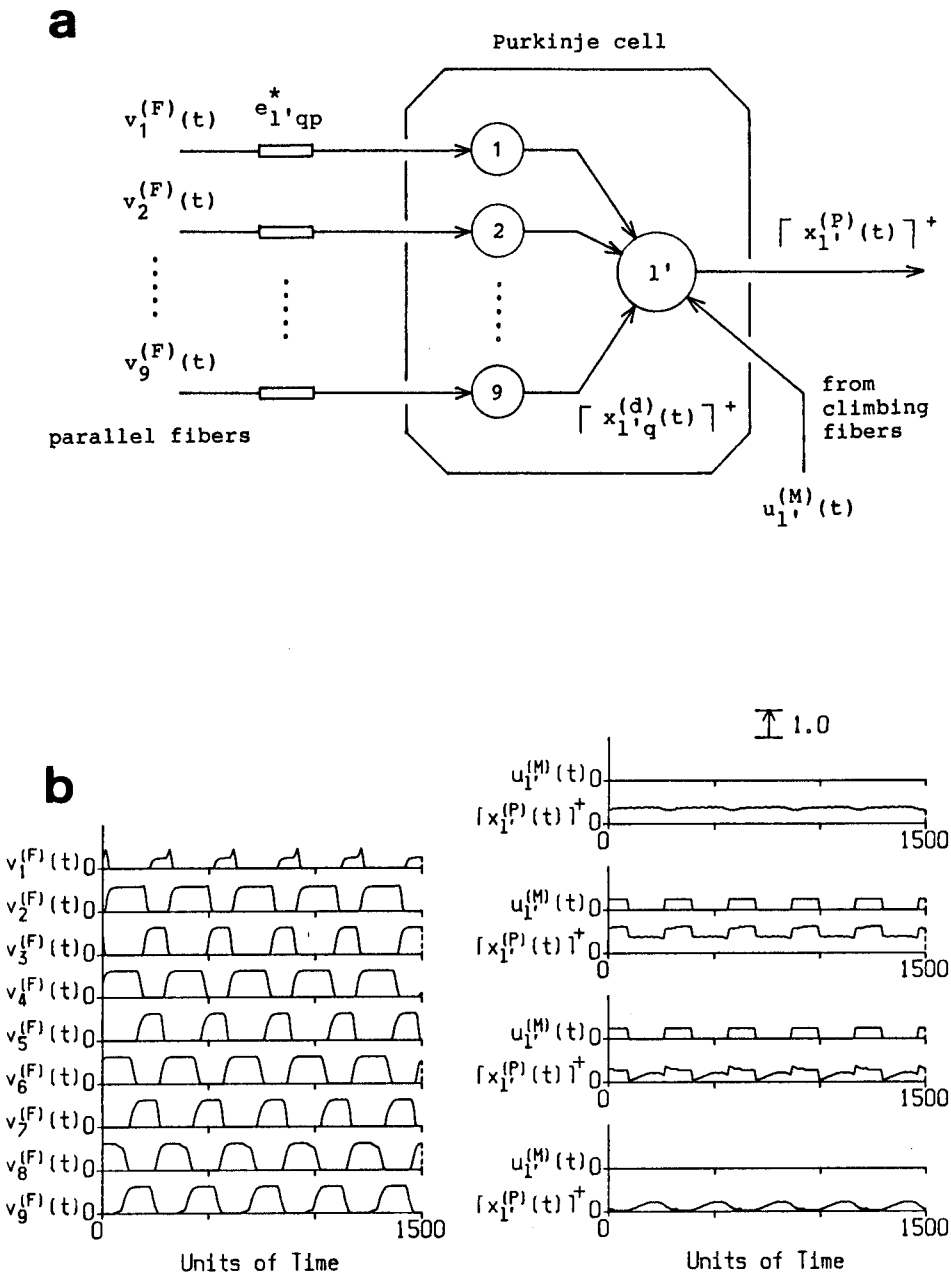

Fig.5.8a-f. Learning mechanism on the Purkinje cell as a result of the synaptic modification of e^*_{1qp}. **a** The schematic diagram of the simulated network (see Appendix C-4). **b** The input $v_p^{(F)}(t)$ from the parallel fibers. **c** The output $\lceil x_{1'}^{(P)}(t) \rceil^+$ of the Purkinje cell without the input $u_{1'}^{(M)}(t)$ from the climbing fiber. **d** $\lceil x_{1'}^{(P)}(t) \rceil^+$ immediately after the application of $u_{1'}^{(M)}(t)$. **e** $\lceil x_{1'}^{(P)}(t) \rceil^+$ after 6000 modification steps. **f** $\lceil x_{1'}^{(P)}(t) \rceil^+$ without $u_{1'}^{(M)}(t)$.

$\eta^{(P)}$ in the interval during which $u_{1'}^{(M)}(t)$ is positive (see Fig.5.8d).

Although the projection of $\lceil x_{1'}^{(P)}(t) \rceil^{+}$ shown in Fig.5.8d is caused by $u_{1'}^{(M)}(t)$, the algorithm with a small σ attenuates $e_{1',qp}^{*}$ so as to reduce the projection. That is, when both $v_{p}^{(F)}(t) - \theta^{(F)}$ and $x_{1'}^{(P)}(t) - \eta^{(P)}$ are positive at the same time, the corresponding $e_{1',qp}^{*}$ are reduced. The periods of $u_{1'}^{(M)}(t)$ and $v_{p}^{(F)}(t)$ are equal and therefore the $e_{1',qp}^{*}$ to be modified are always the same. Within a short time, the membrane potential $x_{1'}^{(P)}(t)$ of the Purkinje cell body drops below the threshold $\eta^{(P)}$ in spite of the application of $u_{1'}^{(M)}(t)$ (see Fig.5.8e). Then the synaptic modification stops.

When the application of $u_{1'}^{(M)}(t)$ is ceased, a signal with the inverse phase of $u_{1'}^{(M)}(t)$ appears in the membrane potential of the Purkinje cell body (see Fig.5.8f).

As a consequence of the above-mentioned mechanism, the network can synthesize the output which has the inverse phase of the signal from the climbing fiber. The learning is accomplished by copying the signal with precise timing so as to be able to control the actuator directly, which differs from the error-correction learning such as is employed in the Perceptron. In this sense, the signal from the climbing fiber should be known as 'master' rather than 'teacher'.

5.5 Synthesizer Learning Model of the Cerebellum

A new learning model of the cerebellum is now put forward,

incorporating all the preceding functions of the cells and the fibers. Putting

$$\lceil x_i^{(g)}(t) \rceil^+ = v_p^{(F)}(t) \qquad (i=p,\ N_g=N_F)$$

$$u_i^{(g)}(t) = \sum_{k=1}^{N_B} a_{ik}\, v_k^{(B)}(t)$$

$$u_j^{(G)}(t) = \sum_{l=1}^{N_P} s_{jl}\, v_l^{(M)}(t)$$

$$u_l^{(M)}(t) = r_l\, v_l^{(M)}(t) \tag{5.6}$$

in order to connect Eqs.(5.1), (5.2), (5.3), (5.4), and (5.5), the equations of the learning model of the cerebellum can be represented as follows:

$$\tau_g \frac{d}{dt} x_i^{(g)}(t) + x_i^{(g)}(t) = \sum_{k=1}^{N_B} a_{ik}\, v_k^{(B)}(t) - \sum_{j=1}^{N_G} d_{ij}^{*} \lceil x_j^{(G)}(t) \rceil^+$$

$$(i=1,2,---,N_g)$$

$$\tau_G \frac{d}{dt} x_j^{(G)}(t) + x_j^{(G)}(t) = \sum_{l=1}^{N_P} s_{jl}\, v_l^{(M)}(t) + \sum_{i=1}^{N_g} c_{ji}^{*} \lceil x_i^{(g)}(t) \rceil^+$$

$$(j=1,2,---,N_G)$$

$$\tau_P \frac{d}{dt} x_l^{(P)}(t) + x_l^{(P)}(t) = \sum_{q=1}^{N_d} \lceil x_{lq}^{(d)}(t) \rceil^+$$

$$+ r_l\, v_l^{(M)}(t) - \sum_{n=1}^{N_b} o_{ln} \lceil x_n^{(b)}(t) \rceil^+ \qquad (l=1,2,---,N_P)$$

$$\tau_d \frac{d}{dt} x_{lq}^{(d)}(t) + x_{lq}^{(d)}(t) = \sum_{i=1}^{N_g} e_{lqi}^{*} \lceil x_i^{(g)}(t) \rceil^{+} - \sum_{m=1}^{N_s} g_{lqm} \lceil x_m^{(s)}(t) \rceil^{+}$$

$$(q=1,2,---,N_d)$$

$$\tau_b \frac{d}{dt} x_n^{(b)}(t) + x_n^{(b)}(t) = u_n^{(b)}(t) + \sum_{i=1}^{N_g} h_{ni} \lceil x_i^{(g)}(t) \rceil^{+}$$

$$(n=1,2,---,N_b)$$

$$\tau_s \frac{d}{dt} x_m^{(s)}(t) + x_m^{(s)}(t) = \sum_{i=1}^{N_g} f_{mi} \lceil x_i^{(g)}(t) \rceil^{+} .$$

$$(m=1,2,---,N_s)$$

(5.7)

Figure 5.9 illustrates the block diagram of the model with parameters corresponding to those in Eq.(5.7). Figure 5.10a-e shows a typical operation of the model, where the synaptic strengths (the initial values in the case of c_{ji}^{*}, d_{ij}^{*}, and e_{lqi}^{*}) and the constants in the algorithm, etc. are listed in Appendix C-5. The sequences of its behavior are:

Sequence 1: rhythmic oscillation is applied as the input $v_k^{(B)}(t)$ from the mossy fibers. The master signals $v_l^{(M)}$ are not applied. This is equivalent to applying the non-oscillatory input uniformly to the granule cells, because of the homogeneous a_{ik}. In the granule-Golgi network with a disturbed ring structure, the

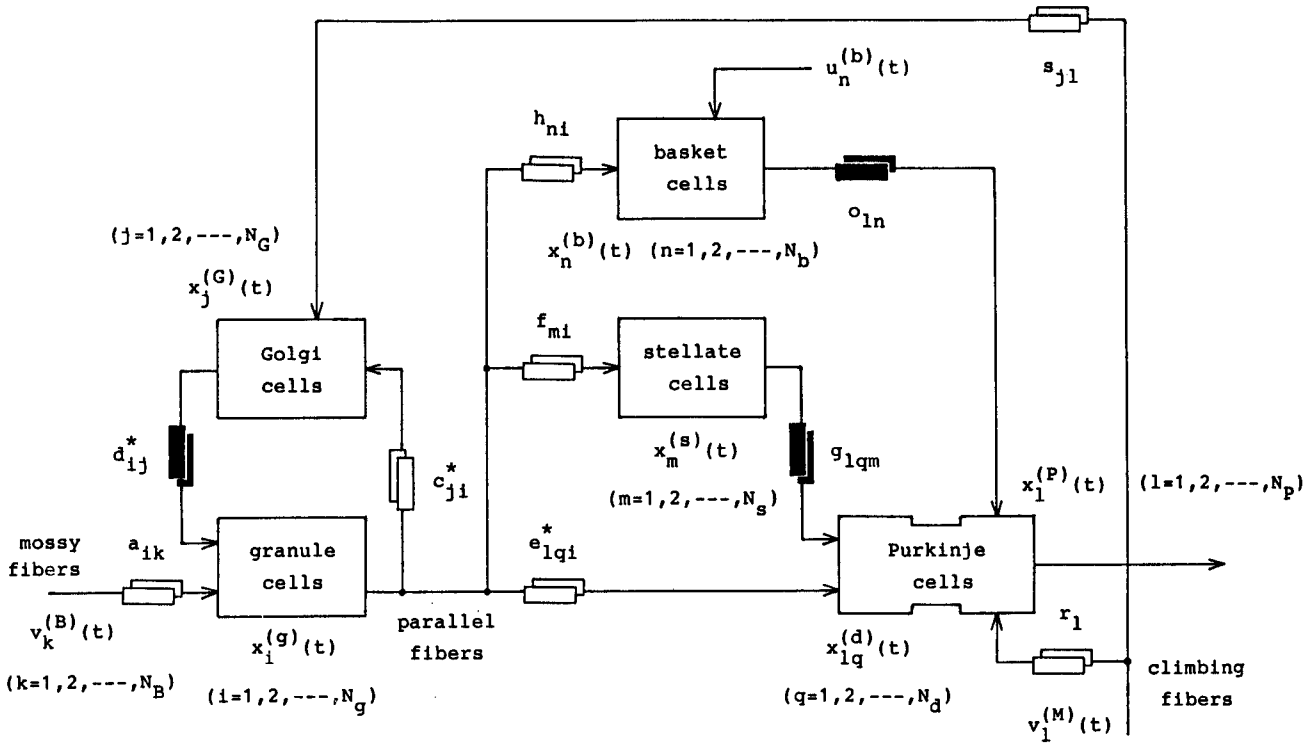

Fig.5.9. The block diagram of the synthesizer learning model of the cerebellum (see Appendix C-5).

imbalance of the inhibition produces the non-oscillatory outputs $\lceil x_i^{(g)}(t) \rceil^+$ and $\lceil x_j^{(G)}(t) \rceil^+$ from the granule and Golgi cells. If the level of $v_k^{(B)}(t)$ is high enough, some values of $\lceil x_i^{(g)}(t) \rceil^+$ or $\lceil x_j^{(G)}(t) \rceil^+$ exceed the threshold $\theta^{(g)}$ or $\theta^{(G)}$ and the synaptic modification of c_{ji}^* and d_{ij}^* starts. At this point, the membrane potentials of the Purkinje cell bodies are inhibited below zero by the stellate cells (see Sect.5.4.2). Therefore the e_{lqi}^* are not modified (see Fig.5.10a).

Sequence 2: with the progress of the synaptic modification of c_{ji}^* and d_{ij}^*, rhythmic oscillation appears in the granule-Golgi network. Once it appears, the AIDs of the granule or Golgi cells

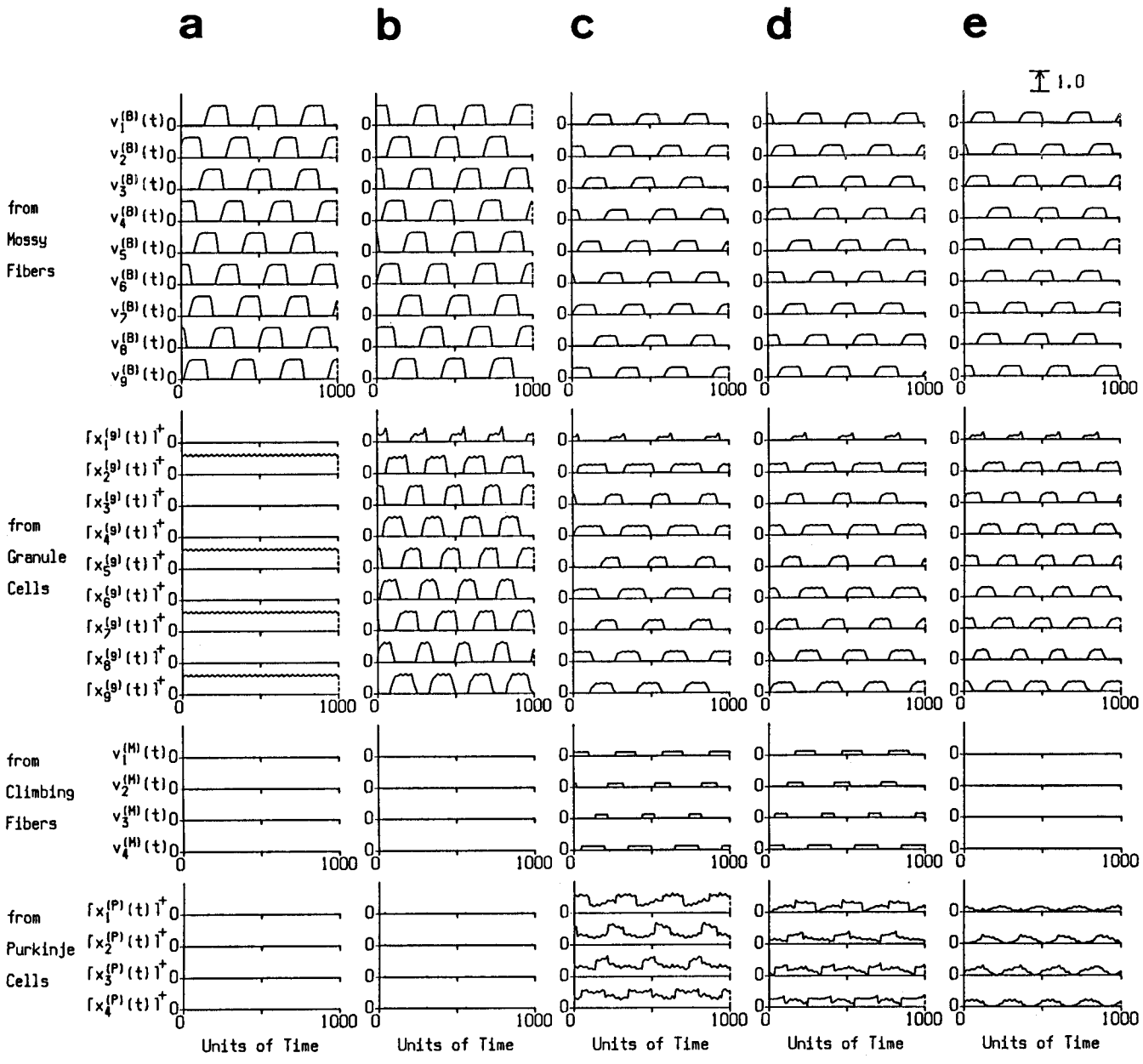

Fig.5.10a-e. A typical operation of the model. **a** Sequence 1: the application of $v_k^{(B)}(t)$. **b** Sequence 2: the synaptic modification in the granule-Golgi network (after 6000 modification steps). **c** Sequence 3: the reduction of the level of $v_k^{(B)}(t)$ and the application of $v_1^{(M)}(t)$. **d** Sequence 4: the synaptic modification in the basket-stellate-Purkinje network (after a further 6000 modification steps). **e** Sequence 5: The stoppage of $v_1^{(M)}(t)$.

gather around $\theta^{(g)}$ or $\theta^{(G)}$, after which the speed of the modification becomes very low and the rhythmic oscillation is caught and held (see Sect.5.3.1). The filtering effect of the stellate cells produces the non-oscillatory membrane potentials

of the Purkinje cells, while the inhibition by the basket cells suppresses the potential below zero (see Sect.5.4.1). Therefore the e_{lqi} are not yet modified (see Fig.5.10b).

Sequence 3: after 6000 modification steps, the level of $v_k^{(B)}(t)$ is reduced while a certain level of the oscillatory master signals $v_l^{(M)}(t)$ is applied simultaneously. This procedure helps the period of rhythmic oscillation in the granule-Golgi network coincide with that of the master signals, as well as avoiding the restarting of the synaptic modification of c_{ji}^* and d_{ij}^* (see Sect.5.3.2). As a result, the Purkinje cells output signals with square projection caused by the application of the master signals. Since the inhibition by the basket cells is still in effect, the non-oscillatory bias components of the membrane potentials $x_l^{(P)}(t)$ of the Purkinje cell bodies due to $v_k^{(B)}(t)$ are held below $\eta^{(P)}$ (see Fig.5.10c).

Sequence 4: the projection of $\lceil x_l^{(P)}(t) \rceil^+$ exceeds $\eta^{(P)}$ and therefore the synaptic modification of e_{lqi}^* starts. Since the periods of $\lceil x_i^{(g)}(t) \rceil^+$ and $v_l^{(M)}(t)$ are equal, the algorithm selectively attenuates the e_{lqi}^* which contribute to the projection of $x_l^{(P)}(t)$. After a short time, this modification suppresses $x_l^{(P)}(t)$ below $\eta^{(P)}$ again in spite of the application of $v_l^{(M)}(t)$, after which the e_{lqi}^* are no longer modified (see Fig.5.10d).

Sequence 5: ceasing the application of the master signals $v_l^{(M)}(t)$ after a further 6000 modification steps, the Purkinje cells

output signals which has the inverse phase of $v_1^{(M)}(t)$. When this occurs, the period of the rhythmic oscillation in the granule-Golgi network returns to its original length and therefore the period of the output $\lceil x_1^{(P)}(t) \rceil^+$ of the Purkinje cells also changes. However this model can learn the relative timing of the master signals (see Fig.5.10e).

Thus, the model of the cerebellum has finished learning. This state is maintained without any synaptic modification, since $\lceil x_i^{(g)}(t) \rceil^+$, $\lceil x_j^{(G)}(t) \rceil^+$, or $x_1^{(P)}(t)$ are less than $\theta^{(g)}$, $\theta^{(G)}$, or $\eta^{(P)}$ respectively.

5.6 Discussion

In this chapter, a new learning model of the cerebellum has been put forward, in which the algorithm proposed in Chap.2 was applied to all of the modifiable synapses. The algorithm is effective for the generation of rhythmic oscillation in the granule-Golgi network, while working to synthesize the output in the basket-stellate-Purkinje network. It is interesting that one algorithm can perform the two different functions.

In the model, both the output of the Purkinje cells after learning and the master signals from the climbing fibers are in the form of bursts of nerve impulses, and the former has the inverse phase of the latter. This result supports one of the two possible interpretations of the interaction of the cerebellar cortex and the cerebellar neuclei: the cerebellar afferent has a major influence on the cerebellar cortex and on the Purkinje

response, the nuclear action being subsidiary (Ito, 1970; Eccles, 1973).

It is important to consider some synaptic channels which, for the sake of simplicity, this model does not include. Also not analyzed here is how the period of the final output of the Purkinje cells after learning can be controlled. It will be necessary to clarify this mechanism.

Chapter 6

Conclusion

It has been discussed how the neural network acts as an information processing system through the medium of rhythmic oscillation, using the proposed synaptic modification algorithm.

In Chap.2, we put forward a new synaptic modification algorithm in consideration of the generation of rhythmic oscillation. Our preliminary investigations into the rhythmic oscillation in the regular ring network led to the selection of the average membrane potential (AMP) and the average impulse density (AID) in the synaptic modification algorithm, where the decrease of synaptic strength is taken to be essential. This synaptic modification algorithm using AMP and AID enables both the rhythmic oscillation and the non-oscillatory state to be dealt with in the algorithm without distinction. Simulation has demonstrated cases in which the algorithm catches and holds the rhythmic oscillation in disturbed ring networks where the rhythmic oscillation was previously extinguished.

In Chap.3, we considered the relationship between the mechanism of memory and bursts of nerve impulses, and presented a new memory model based on the algorithm. When the constants in the algorithm are fixed, two modes, namely the storing mode and the recalling mode, can be selected according to the excitatory input level to excitatory cells alone. This indicates that the ring neural network to which the synaptic modification algorithm

is applied may function as a memory which stores and recalls information in the form of bursts of nerve impulses. The possibility that multiple pieces of information can be selectively stored in the overlapped ring network was also discussed.

For the ring neural network to function as a generator of rhythmic oscillation, mechanisms are required by which rhythmic oscillation is generated and maintained and then its period controlled. In Chap.4, it was demonstrated by simulation that those mechanisms can be actualized by employing this synaptic modification algorithm and by applying inputs from the outside to excitatory and inhibitory cells. It was also confirmed that the two-mode selection mechanism described in Chap.3 solves the problem of the re-modification caused by the dispersion of AIDs with the application of the excitatory synchronous input to inhibitory cells.

In Chap.5, we proposed a new learning model of the cerebellum based on the theories described in Chaps.2, 3, and 4. In the model, the synaptic modification algorithm proposed in Chap.2 is applied to all of the modifiable synapses, as a result of which the granule-Golgi network works as a generator of rhythmic oscillation and the basket-stellate-Purkinje network acts as a wave synthesizer. Simulation shows that the final output of this model after learning has the inverse phase of the signals from the climbing fibers.

As for the neural network with feedback inhibition, the process for generating rhythmic oscillation depends on the set of synaptic strengths or the constants in the algorithm. In some

cases, rhythmic oscillation cannot be generated in the network in spite of the application of this algorithm. If no rhythmic oscillation appears after sufficient modification steps, the subsequent synaptic modification can seldom bring back the rhythmic oscillation because of the absolute lack of inhibition. This fact suggests the following points. First, that the impossibility of the generation of rhythmic oscillation is an essential fact for which the distribution of the memory compensates. Second, that the algorithm given by Eqs.(2.6) and (2.7) is not yet perfect especially in the matter of deciding the constants. As for the synthesizer learning mechanism in the neural network with feedforward inhibition, the amount of the master signals able to be learned depends on the number of oscillations with different phases. It is significant to quantitatively compare this with the signals in the real nervous system.

The fact that the mechanism of memory, the rhythm generator, and the function of the cerebellum can be explained using the proposed synaptic modification algorithm supports not only the propriety of the algorithm but also the possibility that the neural network works as an information processing system through the medium of rhythmic oscillation. It is expected that these ideas will establish a foundation for explaining the relationship between the rhythmical phenomena and the higher intelligence mechanism.

As described in Chap.5, the cerebellum, which controls locomotion, is a part of the central nervous system. Knowledge of the mechanism of the cerebellum is important to the technological

application of its complex functions. In snakes etc., the comparatively simple neural network effectively controls locomotion with many degrees of freedom (Pearson, 1979). In recent robotics research, the control of systems with such freedom, including cooperative or associative control has become one of the most difficult problems. Although one possible course would be to try to solve such problems using software technology, the solution may not necessarily exist along this line of investigation. It would be more useful, then, to investigate the methodology of the human brain: the information processing mechanism of the neural network involves many possible leads to the solution. Research into the neural network would appear to be a very attractive approach, not only as a scientific inquiry, but also from a technological point of view in order to create new and better information processing systems.

Appendix A-1

In the neural network considered here, all inputs to inhibitory cells are excitatory. Therefore,

$$\lceil x_j^{(2)}(t) \rceil^+ = x_j^{(2)}(t) . \tag{A.1}$$

Supposing that $u_i^{(1)}(t)=u$ (u:non-oscillatory), the following equations are obtained from Eqs.(2.1) and (A.1).

$$\tau_1 \frac{d}{dt} x_i^{(1)}(t) + x_i^{(1)}(t) = u - \sum_{j=1}^{N_2} d_{ij} x_j^{(2)}(t) \tag{A.2}$$

$$\tau_1 \tau_2 \frac{d^2}{dt^2} x_i^{(1)}(t) + \tau_2 \frac{d}{dt} x_i^{(1)}(t) = - \sum_{j=1}^{N_2} d_{ij} \tau_2 \frac{d}{dt} x_j^{(2)}(t) \tag{A.3}$$

By adding Eq.(A.3) to Eq.(A.2), we finally get

$$\tau_1 \tau_2 \frac{d^2}{dt^2} x_i^{(1)}(t) + (\tau_1 + \tau_2) \frac{d}{dt} x_i^{(1)}(t) + x_i^{(1)}(t) = u - \sum_{i'=1}^{N_1} (\sum_{j=1}^{N_2} d_{ij} c_{ji'}) \lceil x_{i'}^{(1)}(t) \rceil^+ . \tag{A.4}$$

Thus, it is concluded that the influence of τ_1 and τ_2 on the parameters is equal.

Appendix A-2

(1) c_{ji} and d_{ij} before modification

$$c_{ji} = \begin{bmatrix} 1.0 & 0. & 0. & 0. & 0. \\ 0. & 1.0 & 0. & 0. & 0. \\ 0. & 0. & 1.0 & 0. & 0. \\ 0. & 0. & 0. & 1.0 & 0. \\ 0. & 0. & 0. & 0. & 1.0 \end{bmatrix}$$

$$d_{ij} = \begin{bmatrix} 0. & 3.0 & 0.75 & 0. & 0.5 \\ 0.5 & 0. & 3.0 & 0. & 0. \\ 0. & 0.5 & 0. & 3.0 & 0. \\ 0. & 0. & 0.5 & 0. & 3.0 \\ 3.0 & 0. & 0. & 0.5 & 0. \end{bmatrix}$$

(2) c_{ji} and d_{ij} after 180 modification steps

$$c_{ji} = \begin{bmatrix} 1.0 & 0. & 0. & 0. & 0. \\ 0. & 1.0 & 0. & 0. & 0. \\ 0. & 0. & 0.97098 & 0. & 0. \\ 0. & 0. & 0. & 1.0 & 0. \\ 0. & 0. & 0. & 0. & 0.97098 \end{bmatrix}$$

$$d_{ij} = \begin{bmatrix} 0. & 3.0 & 0.59686 & 0. & 0.34686 \\ 0.5 & 0. & 2.99982 & 0. & 0. \\ 0. & 0.5 & 0. & 3.0 & 0. \\ 0. & 0. & 0.5 & 0. & 3.0 \\ 3.0 & 0. & 0. & 0.5 & 0. \end{bmatrix}$$

(3) c_{ji} and d_{ij} after 3000 modification steps

$$c_{ji} = \begin{bmatrix} 1.0 & 0. & 0. & 0. & 0. \\ 0. & 0.99529 & 0. & 0. & 0. \\ 0. & 0. & 0.91610 & 0. & 0. \\ 0. & 0. & 0. & 0.99921 & 0. \\ 0. & 0. & 0. & 0. & 0.92678 \end{bmatrix}$$

$$d_{ij} = \begin{bmatrix} 0. & 2.94689 & 0.23899 & 0. & 0.04381 \\ 0.5 & 0. & 2.91846 & 0. & 0. \\ 0. & 0.44871 & 0. & 2.99224 & 0. \\ 0. & 0. & 0.43449 & 0. & 2.95306 \\ 3.0 & 0. & 0. & 0.49122 & 0. \end{bmatrix}$$

Appendix A-3

(1) c_{ji} and d_{ij} before modification

$$c_{ji} = \begin{bmatrix} 1.0 & 0. & 0.3 & 1.0 & 0. \\ 0. & 1.0 & 0. & 0. & 0. \\ 0. & 0. & 1.0 & 0. & 0. \\ 0.4 & 0.7 & 0. & 1.0 & 0. \\ 0. & 1.0 & 0. & 0. & 1.0 \end{bmatrix}$$

$$d_{ij} = \begin{bmatrix} 0. & 3.0 & 1.5 & 0. & 0.5 \\ 0.5 & 0. & 3.0 & 0. & 0. \\ 0. & 0.5 & 0. & 3.0 & 0.5 \\ 0. & 3.0 & 0.5 & 0. & 3.0 \\ 3.0 & 1.2 & 0.7 & 0.5 & 0. \end{bmatrix}$$

(2) c_{ji} and d_{ij} after 3000 modification steps

$$c_{ji} = \begin{bmatrix} 1.0 & 0. & 0.3 & 0. & 0. \\ 0. & 0.47086 & 0. & 0. & 0. \\ 0. & 0. & 1.0 & 0. & 0. \\ 0.4 & 0.32785 & 0. & 1.0 & 0. \\ 0. & 0.16798 & 0. & 0. & 0.44577 \end{bmatrix}$$

$$d_{ij} = \begin{bmatrix} 0. & 2.76300 & 1.5 & 0. & 0. \\ 0.5 & 0. & 3.0 & 0. & 0. \\ 0. & 0. & 0. & 2.88330 & 0. \\ 0. & 3.0 & 0.5 & 0. & 2.99891 \\ 3.0 & 0. & 0.7 & 0. & 0. \end{bmatrix}$$

(3) c_{ji} and d_{ij} after 6000 modification steps

$$c_{ji} = \begin{bmatrix} 0.99995 & 0. & 0.3 & 1.0 & 0. \\ 0. & 0.45615 & 0. & 0. & 0. \\ 0. & 0. & 1.0 & 0. & 0. \\ 0.39996 & 0.30213 & 0. & 1.0 & 0. \\ 0. & 0.15286 & 0. & 0. & 0.44089 \end{bmatrix}$$

$$d_{ij} = \begin{bmatrix} 0. & 2.76300 & 1.5 & 0. & 0. \\ 0.06521 & 0. & 3.0 & 0. & 0. \\ 0. & 0. & 0. & 2.71687 & 0. \\ 0. & 3.0 & 0.5 & 0. & 2.99565 \\ 2.81887 & 0. & 0.7 & 0. & 0. \end{bmatrix}$$

Appendix B-1

$$c_{ji} = \begin{bmatrix} 1.0 & 0. & 0. & 0. & 0. \\ 0. & 1.0 & 0. & 0. & 0. \\ 0. & 0. & 1.0 & 0. & 0. \\ 0. & 0. & 0. & 1.0 & 0. \\ 0. & 0. & 0. & 0. & 1.0 \end{bmatrix}$$

$$d_{ij} = \begin{bmatrix} 0. & 3.0 & 0. & 0. & 0.5 \\ 0.5 & 0. & 3.0 & 0. & 0. \\ 0. & 0.5 & 0. & 3.0 & 0. \\ 0. & 0. & 0.5 & 0. & 3.0 \\ 3.0 & 0. & 0. & 0.5 & 0. \end{bmatrix}$$

Appendix B-2

(1) The constants in the synaptic modification algorithm described by Eqs.(2.6) and (2.7):

$$\delta^{(1)} = 0.001/u^2, \quad \theta^{(1)} = 0.4u, \quad \eta^{(1)} = -2.0u,$$

$$\delta^{(2)} = 0.003/u^2, \quad \theta^{(2)} = 0.4u, \text{ and } \quad \eta^{(2)} = 0.0u.$$

(2) The window function $\psi(t', \sigma)$:

$$\psi(t', \sigma) = \begin{cases} 1/\sigma & t-\sigma \leq t' \leq t \\ 0 & \text{otherwise} \end{cases}$$

where t means the present time and σ is set up at 500 units of time.

Appendix B-3

(1) c_{ji} and d_{ij} before modification

$$c_{ji} = \begin{bmatrix} 0.5 & 0. & 1.0 & 0. & 0. \\ 0. & 0.7 & 0. & 0. & 0.6 \\ 0. & 0. & 1.2 & 0. & 0. \\ 0.7 & 0.5 & 0. & 0.9 & 0. \\ 0. & 0. & 0.4 & 0. & 1.5 \end{bmatrix}$$

$$d_{ij} = \begin{bmatrix} 0. & 2.5 & 1.3 & 0. & 1.5 \\ 2.0 & 0. & 1.6 & 0. & 0.5 \\ 0. & 0.7 & 0. & 4.0 & 0. \\ 0.7 & 1.4 & 1.0 & 0. & 3.2 \\ 2.1 & 0. & 3.0 & 1.2 & 0. \end{bmatrix}$$

(2) c_{ji} and d_{ij} after 3000 modification steps

$$c_{ji} = \begin{bmatrix} 0.36728 & 0. & 0.73856 & 0. & 0. \\ 0. & 0.14474 & 0. & 0. & 0.40514 \\ 0. & 0. & 0.89528 & 0. & 0. \\ 0.34807 & 0.22330 & 0. & 0.65766 & 0. \\ 0. & 0. & 0.28443 & 0. & 1.26492 \end{bmatrix}$$

$$d_{ij} = \begin{bmatrix} 0. & 2.48723 & 0. & 0. & 1.33139 \\ 1.63139 & 0. & 1.43510 & 0. & 0. \\ 0. & 0. & 0. & 3.89114 & 0. \\ 0.14584 & 1.4 & 0.78897 & 0. & 3.2 \\ 2.05961 & 0. & 2.99143 & 0. & 0. \end{bmatrix}$$

(3) c_{ji} and d_{ij} after 6000 modification steps

$$c_{ji} = \begin{bmatrix} 0.34498 & 0. & 0.73856 & 0. & 0. \\ 0. & 0.14304 & 0. & 0. & 0.40514 \\ 0. & 0. & 0.89528 & 0. & 0. \\ 0.30091 & 0.21601 & 0. & 0.63456 & 0. \\ 0. & 0. & 0.28443 & 0. & 1.26492 \end{bmatrix}$$

$$d_{ij} = \begin{bmatrix} 0. & 2.48723 & 0. & 0. & 1.27460 \\ 1.63139 & 0. & 1.43510 & 0. & 0. \\ 0. & 0. & 0. & 3.83900 & 0. \\ 0.14584 & 1.4 & 0.78897 & 0. & 3.16484 \\ 2.05961 & 0. & 2.99143 & 0. & 0. \end{bmatrix}$$

Appendix B-4

(1) c_{ji} and d_{ij} before modification

$$c_{ji} = \begin{bmatrix} 0.34498 & 0. & 0.73856 & 0. & 0. \\ 0. & 0.14304 & 0. & 0. & 0.40514 \\ 0. & 0. & 0.89528 & 0. & 0. \\ 0.30091 & 0.21601 & 0. & 0.63456 & 0. \\ 0. & 0. & 0.28443 & 0. & 1.26492 \end{bmatrix}$$

$$d_{ij} = \begin{bmatrix} 0. & 2.48723 & 0. & 0. & 1.27460 \\ 1.63139 & 0. & 1.43510 & 0. & 0. \\ 0. & 0. & 0. & 3.83900 & 0. \\ 0.14584 & 1.4 & 0.78897 & 0. & 3.16484 \\ 2.05961 & 0. & 2.99143 & 0. & 0. \end{bmatrix}$$

(2) c_{ji} and d_{ij} after 3000 modification steps

$$c_{ji} = \begin{bmatrix} 0.08373 & 0. & 0.71170 & 0. & 0. \\ 0. & 0.14304 & 0. & 0. & 0.40514 \\ 0. & 0. & 0.87312 & 0. & 0. \\ 0.11549 & 0.21601 & 0. & 0.61408 & 0. \\ 0. & 0. & 0.27481 & 0. & 1.26492 \end{bmatrix}$$

$$d_{ij} = \begin{bmatrix} 0. & 2.48723 & 0. & 0. & 1.27460 \\ 0.73673 & 0. & 1.31824 & 0. & 0. \\ 0. & 0. & 0. & 3.56577 & 0. \\ 0. & 1.4 & 0.65543 & 0. & 3.16484 \\ 1.57789 & 0. & 2.95388 & 0. & 0. \end{bmatrix}$$

(3) c_{ji} and d_{ij} after 6000 modification steps

$$c_{ji} = \begin{bmatrix} 0.01732 & 0. & 0.68555 & 0. & 0. \\ 0. & 0.08747 & 0. & 0. & 0.40514 \\ 0. & 0. & 0.85023 & 0. & 0. \\ 0.09287 & 0.13727 & 0. & 0.61408 & 0. \\ 0. & 0. & 0.26436 & 0. & 1.26492 \end{bmatrix}$$

$$d_{ij} = \begin{bmatrix} 0. & 2.48723 & 0. & 0. & 1.26307 \\ 0.46867 & 0. & 1.17731 & 0. & 0. \\ 0. & 0. & 0. & 3.56577 & 0. \\ 0. & 1.4 & 0.50598 & 0. & 3.15723 \\ 1.49177 & 0. & 2.91330 & 0. & 0. \end{bmatrix}$$

Appendix B-5

The constants in the synaptic modification algorithm described by Eqs.(2.6) and (2.7):

$\delta^{(1)} = 0.001$, $\theta^{(1)} = 0.4$, $\eta^{(1)} = -2.0$,

$\delta^{(2)} = 0.003$, $\theta^{(2)} = 0.4$, and $\eta^{(2)} = 0.0$.

Appendix C-1

(1) The network constants etc.

$\tau_g = 2.0$, $\tau_G = 10.0$, $N_g = 9$, and $N_G = 9$.

$\delta^{(g)} = 0.0004$, $\theta^{(g)} = 0.4$, $\eta^{(g)} = -2.0$,

$\delta^{(G)} = 0.0012$, $\theta^{(G)} = 0.4$, and $\eta^{(G)} = 0.0$.

σ = 500 units of time

(2) c^*_{ji} and d^*_{ij} before modification (Network 5)

$$c^*_{ji} = \begin{bmatrix} 1.0 & 0. & 0. & 0. & 0. & 0. & 0. & 0. & 0. \\ 0. & 1.0 & 0. & 0. & 0. & 0. & 0. & 0. & 0. \\ 0. & 0. & 1.0 & 0. & 0. & 0. & 0. & 0. & 0. \\ 0. & 0. & 0. & 1.0 & 0. & 0. & 0. & 0. & 0. \\ 0. & 0. & 0. & 0. & 1.0 & 0. & 0. & 0. & 0. \\ 0. & 0. & 0. & 0. & 0. & 1.0 & 0. & 0. & 0. \\ 0. & 0. & 0. & 0. & 0. & 0. & 1.0 & 0. & 0. \\ 0. & 0. & 0. & 0. & 0. & 0. & 0. & 1.0 & 0. \\ 0. & 0. & 0. & 0. & 0. & 0. & 0. & 0. & 1.0 \end{bmatrix}$$

$$d^*_{ij} = \begin{bmatrix} 0. & 3.0 & 2.0 & 0. & 0. & 0. & 0. & 0. & 0.5 \\ 0.5 & 0. & 3.0 & 1.0 & 0. & 0. & 0. & 0. & 0. \\ 0. & 0.5 & 0. & 3.0 & 0. & 0. & 1.0 & 0. & 0. \\ 0. & 0. & 0.5 & 0. & 3.0 & 0. & 0. & 0. & 0. \\ 0. & 0. & 0. & 0.5 & 0. & 3.0 & 0. & 0. & 0. \\ 0. & 0. & 0. & 0. & 0.5 & 0. & 3.0 & 0. & 0. \\ 0. & 0. & 0. & 0. & 0. & 0.5 & 0. & 3.0 & 0. \\ 0. & 0. & 0. & 0. & 0. & 0. & 0.5 & 0. & 3.0 \\ 3.0 & 0. & 0. & 0. & 0. & 0. & 0. & 0.5 & 0. \end{bmatrix}$$

(3) c^*_{ji} and d^*_{ij} after 2760 modification steps

$$c^*_{ji} = \begin{bmatrix} 0.924 & 0. & 0. & 0. & 0. & 0. & 0. & 0. & 0. \\ 0. & 0.908 & 0. & 0. & 0. & 0. & 0. & 0. & 0. \\ 0. & 0. & 0.719 & 0. & 0. & 0. & 0. & 0. & 0. \\ 0. & 0. & 0. & 0.926 & 0. & 0. & 0. & 0. & 0. \\ 0. & 0. & 0. & 0. & 0.575 & 0. & 0. & 0. & 0. \\ 0. & 0. & 0. & 0. & 0. & 0.921 & 0. & 0. & 0. \\ 0. & 0. & 0. & 0. & 0. & 0. & 0.579 & 0. & 0. \\ 0. & 0. & 0. & 0. & 0. & 0. & 0. & 0.918 & 0. \\ 0. & 0. & 0. & 0. & 0. & 0. & 0. & 0. & 0.592 \end{bmatrix}$$

$$d^*_{ij} = \begin{bmatrix} 0. & 2.989 & 0.851 & 0. & 0. & 0. & 0. & 0. & 0. \\ 0.119 & 0. & 2.586 & 0.630 & 0. & 0. & 0. & 0. & 0. \\ 0. & 0.003 & 0. & 2.923 & 0. & 0. & 0. & 0. & 0. \\ 0. & 0. & 0.135 & 0. & 2.769 & 0. & 0. & 0. & 0. \\ 0. & 0. & 0. & 0.472 & 0. & 2.964 & 0. & 0. & 0. \\ 0. & 0. & 0. & 0. & 0.271 & 0. & 2.779 & 0. & 0. \\ 0. & 0. & 0. & 0. & 0. & 0.470 & 0. & 2.964 & 0. \\ 0. & 0. & 0. & 0. & 0. & 0. & 0.267 & 0. & 2.798 \\ 2.963 & 0. & 0. & 0. & 0. & 0. & 0. & 0.462 & 0. \end{bmatrix}$$

(4) c^*_{ji} and d^*_{ij} after 6000 modification steps (Network 6)

$$c^*_{ji} = \begin{bmatrix} 0.906 & 0. & 0. & 0. & 0. & 0. & 0. & 0. & 0. \\ 0. & 0.886 & 0. & 0. & 0. & 0. & 0. & 0. & 0. \\ 0. & 0. & 0.714 & 0. & 0. & 0. & 0. & 0. & 0. \\ 0. & 0. & 0. & 0.824 & 0. & 0. & 0. & 0. & 0. \\ 0. & 0. & 0. & 0. & 0.565 & 0. & 0. & 0. & 0. \\ 0. & 0. & 0. & 0. & 0. & 0.863 & 0. & 0. & 0. \\ 0. & 0. & 0. & 0. & 0. & 0. & 0.549 & 0. & 0. \\ 0. & 0. & 0. & 0. & 0. & 0. & 0. & 0.883 & 0. \\ 0. & 0. & 0. & 0. & 0. & 0. & 0. & 0. & 0.537 \end{bmatrix}$$

$$d^*_{ij} = \begin{bmatrix} 0. & 2.946 & 0.851 & 0. & 0. & 0. & 0. & 0. & 0. \\ 0. & 0. & 2.586 & 0.103 & 0. & 0. & 0. & 0. & 0. \\ 0. & 0. & 0. & 2.704 & 0. & 0. & 0. & 0. & 0. \\ 0. & 0. & 0.135 & 0. & 2.769 & 0. & 0. & 0. & 0. \\ 0. & 0. & 0. & 0.288 & 0. & 2.908 & 0. & 0. & 0. \\ 0. & 0. & 0. & 0. & 0.271 & 0. & 2.779 & 0. & 0. \\ 0. & 0. & 0. & 0. & 0. & 0.388 & 0. & 2.912 & 0. \\ 0. & 0. & 0. & 0. & 0. & 0. & 0.267 & 0. & 2.798 \\ 2.924 & 0. & 0. & 0. & 0. & 0. & 0. & 0.364 & 0. \end{bmatrix}$$

Appendix C-2

$\tau_p = 2.0$, $\tau_d = 2.0$, $\tau_b = 10.0$,

$N_p = 1$, $N_d = 9$, $N_b = 1$, and $N_F = 9$.

$$e_{l'qp} = \begin{cases} 0.25 & \text{if } p=q \\ 0. & \text{otherwise} \end{cases}, \quad h_{n'p} = 0.25, \text{ and } o_{l'n'} = 1.0.$$

$u_{n'}^{(b)}(t) = -0.5$

Appendix C-3

$\tau_p = 2.0$, $\tau_d = 2.0$, $\tau_s = 200.0$,

$N_p = 1$, $N_d = 9$, $N_s = 9$, and $N_F = 9$.

$$e_{l'qp} = \begin{cases} 0.25 & \text{if } p=q \\ 0. & \text{otherwise} \end{cases}, \quad f_{mp} = \begin{cases} 0.25 & \text{if } p=m \\ 0. & \text{otherwise} \end{cases},$$

and $$g_{l'qm} = \begin{cases} 1.00 & \text{if } m=p \\ 0. & \text{otherwise} \end{cases}.$$

Appendix C-4

$\tau_p = 2.0$, $\tau_d = 2.0$, $N_p = 1$, $N_d = 9$, and $N_F = 9$.

$$e^*_{l'qp} = \begin{cases} 0.15 & \text{if } p=q \\ 0. & \text{otherwise} \end{cases}$$

$\delta^{(F)} = 0.0012$, $\theta^{(F)} = 0.4$, and $\eta^{(P)} = 0.4$.

$\sigma = 20$ units of time

Appendix C-5

(1) The granule-Golgi network

$\tau_g = 2.0$ and $\tau_G = 10.0$.

$N_g = 9$ and $N_G = 9$.

$\delta^{(g)} = 0.0004$, $\theta^{(g)} = 0.4$, $\eta^{(g)} = -2.0$,

$\delta^{(G)} = 0.0012$, $\theta^{(G)} = 0.4$, and $\eta^{(G)} = 0.0$.

σ = 500 units of time

$a_{ik} = 0.25$

$$c^*_{ji} = \begin{bmatrix} 1.0 & 0. & 0. & 0. & 0. & 0. & 0. & 0. & 0. \\ 0. & 1.0 & 0. & 0. & 0. & 0. & 0. & 0. & 0. \\ 0. & 0. & 1.0 & 0. & 0. & 0. & 0. & 0. & 0. \\ 0. & 0. & 0. & 1.0 & 0. & 0. & 0. & 0. & 0. \\ 0. & 0. & 0. & 0. & 1.0 & 0. & 0. & 0. & 0. \\ 0. & 0. & 0. & 0. & 0. & 1.0 & 0. & 0. & 0. \\ 0. & 0. & 0. & 0. & 0. & 0. & 1.0 & 0. & 0. \\ 0. & 0. & 0. & 0. & 0. & 0. & 0. & 1.0 & 0. \\ 0. & 0. & 0. & 0. & 0. & 0. & 0. & 0. & 1.0 \end{bmatrix}$$

$$d^*_{ij} = \begin{bmatrix} 0. & 3.0 & 2.0 & 0. & 0. & 0. & 0. & 0. & 0.5 \\ 0.5 & 0. & 3.0 & 1.0 & 0. & 0. & 0. & 0. & 0. \\ 0. & 0.5 & 0. & 3.0 & 0. & 0. & 1.0 & 0. & 0. \\ 0. & 0. & 0.5 & 0. & 3.0 & 0. & 0. & 0. & 0. \\ 0. & 0. & 0. & 0.5 & 0. & 3.0 & 0. & 0. & 0. \\ 0. & 0. & 0. & 0. & 0.5 & 0. & 3.0 & 0. & 0. \\ 0. & 0. & 0. & 0. & 0. & 0.5 & 0. & 3.0 & 0. \\ 0. & 0. & 0. & 0. & 0. & 0. & 0.5 & 0. & 3.0 \\ 3.0 & 0. & 0. & 0. & 0. & 0. & 0. & 0.5 & 0. \end{bmatrix}$$

$$s_{j1} = \begin{cases} 1.00 & \text{if } 1=j=1 \\ 0. & \text{otherwise} \end{cases}$$

(2) The basket-stellate-Purkinje network

$\tau_p = 2.0$, $\tau_d = 2.0$, $\tau_s = 200.0$, and $\tau_b = 10.0$.

$N_p = 4$, $N_d = 9$, $N_s = 9$, and $N_b = 4$.

$$e^*_{1qi} = e^*_{2qi} = e^*_{3qi} = e^*_{4qi} = \begin{cases} 0.60 & \text{if } i=q \\ 0. & \text{otherwise} \end{cases}$$

$$f_{mi} = \begin{cases} 0.60 & \text{if } i=m \\ 0. & \text{otherwise} \end{cases}$$

$$g_{1qm} = g_{2qm} = g_{3qm} = g_{4qm} = \begin{cases} 1.00 & \text{if } m=q \\ 0. & \text{otherwise} \end{cases}$$

$h_{ni} = 0.25$

$$o_{1n} = \begin{cases} 5.00 & \text{if } n=1 \\ 0. & \text{otherwise} \end{cases}$$

$r_1 = 2.00$

$u_n^{(b)}(t) = -0.5$

$\delta^{(g)} = 0.003$, $\theta^{(g)} = 0.2$, and $\eta^{(P)} = 0.4$.

σ = 20 units of time

References

(1) Albus,J.S.: A theory of cerebellar function. Math. Biosci. **10**, 25-61(1971)

(2) Barto,A.G., Sutton,R.S., Brouwer,P.S.: Associative search network: a reinforcement learning associative memory. Biol. Cybern. **40**, 201-211(1981)

(3) Barto,A.G., Sutton,R.S.: Landmark learning: an illustration of associative search. Biol. Cybern. **42**, 1-8(1981)

(4) Barto,A.G., Anderson,C.W., Sutton,R.S.: Synthesis of nonlinear control surfaces by a layered associative search network. Biol. Cybern. **43**, 175-185(1982)

(5) Block,H.D.: The perceptron: a model for brain functioning.I. Revs. Mod. Phys. **34**, 123-135(1962)

(6) Block,H.D., Knight,Jr.,W.B., Rosenblatt,F.: Analysis of a four-layer series-coupled perceptron.II. Revs. Mod. Phys. **34**, 135-142(1962)

(7) Calvert,T.W., Meno,F.: Neural systems modeling applied to the cerebellum. IEEE Trans. on SMC 2, 363-374(1972)

(8) Clarac,F., Cruse,H.: Comparison of forces developed by the leg of the rock lobster when walking free or on a treadmill. Biol. Cybern. **43**, 109-114(1982)

(9) Deutsch,S.: A simplified version of Kunihiko Fukushima's neocognitron. Biol. Cybern. **42**, 17-21(1981)

(10) Eccles,J.C.: The cerebellum as a computer: patterns in space and time. J. Physiol. **229**, 1-32(1973)

(11) Ellias,S.A., Grossberg,S.: Pattern formation, contrast control, and oscillations in the short term memory of shunting on-center off-surround networks. Biol. Cybern. **20**, 69-98(1975)

(12) Fujita,M.: Adaptive filter model of the cerebellum. Biol. Cybern. **45**, 195-206(1982)

(13) Fujita,M.: Simulation of adaptive modification of the vestibulo-ocular reflex with an adaptive filter model of the cerebellum. Biol. Cybern. **45**, 207-214(1982)

(14) Fukushima,K.: A model of associative memory in the brain. Kybernetik **12**, 58-63(1973)

(15) Fukushima,K.: Cognitron: a self-organizing multilayered neural network. Biol. Cybern. **20**, 121-136(1975)

(16) Fukushima,K.: Neocognitron: a self-organizing neural network model for a mechanism of pattern recognition unaffected by shift in pattern. Biol. Cybern. **36**, 193-202(1980)

(17) Friesen,W.O., Stent,G.S.: Generation of a locomotory rhythm by a neural network with recurrent cyclic inhibition. Biol. Cybern. **28**, 27-40(1977)

(18) Hassul,M., Daniels,P.D.: Cerebellar Dynamics: the mossy fiber input. IEEE Trans. on BME **24**, 449-456(1977)

(19) Heetderks,W.J., Batruni,R.: Multivariate statistical analysis of the response of the cockroach giant interneuron system to wind puffs. Biol. Cybern. **43**, 1-11(1982)

(20) Hirai,Y., Fukushima,K.: A model of neural network extracting binocular parallax. Biol. Cybern. **18**, 19-29(1975)

(21) Hirai,Y., Fukushima,K.: An inference upon the neural network finding binocular correspondence. Biol. Cybern. **31**, 209-217(1978)

(22) Hirai,Y.: A new hypothesis for synaptic modification: an interactive process between postsynaptic competition and presynaptic regulation. Biol. Cybern. **36**, 41-50(1980)

(23) Hirai,Y.: A template matching model for pattern recognition: self-organization of templates and template matching by a disinhibitory neural network. Biol. Cybern. **38**, 91-101(1980)

(24) Holden,A.V., Ramadan,S.M.: The response of a molluscan neurone to a cyclic input: entrainment and phase-locking. Biol. Cybern. **41**, 157-163(1981)

(25) Holden,A.V., Ramadan,S.M.: Repetitive activity of a molluscan neurone driven by maintained currents: a supercritical bifurcation. Biol. Cybern. **42**, 79-85(1981)

(26) Holden,A.V., Winlow,W., Haydon,P.G.: The induction of periodic and chaotic activity in a molluscan neurone. Biol. Cybern. **43**, 169-173(1982)

(27) Ito,M.: Neurophysiological aspects of the cerebellar motor control system. Internat. J. Neurol. **7**, 162-176(1970)

(28) Kawahara,K., Mori,S.: A two compartment model of the stepping generator: analysis of the roles of a stage-setter and a rhythm generator. Biol. Cybern. **43**, 225-230(1982)

(29) Kuijpers,K., Smith,J.: A computer simulation of a neuron net model as a self-organizing system. Kybernetik **12**, 216-222(1973)

(30) Maginu,K.: Stability of periodic travelling wave solutions of a nerve conduction equation. J. Math. Biol. **6**, 49-57(1978)

(31) Malsburg,Chr.von der: Self-organization of orientation sensitive cells in the striate cortex. Kybernetik **14**, 85-100(1973)

(32) Malsburg,Chr.von der: Development of ocularity domains and growth behaviour of axon terminals. Biol. Cybern. **32**, 49-62(1979)

(33) Marr,D.: A theory of cerebellar cortex. J. Physiol. **202**, 437-470(1969)

(34) Melkonian,D.S., Mkrtchian,H.H., Fanardjian,V.V.: Simulation of learning processes in neural networks of the cerebellum. Biol. Cybern. **45**, 79-88(1982)

(35) Mitchell,C.E., Friesen,W.O.: A neuromime system for neural circuit analysis. Biol. Cybern. **40**, 127-137(1981)

(36) Minsky,M., Papert,S.: Perceptrons: an introduction of computational geometry. The Science Press, Inc., (1969)

(37) Morishita,I., Yajima,A.: Analysis and simulation of networks of mutually inhibiting neurons. Kybernetik **11**,154-165(1972)

(38) Nagano,T.: A model of visual development. Biol. Cybern. **26**, 45-52(1977)

(39) Nagano,T., Fujiwara,M.: A neural network model for the development of direction selectivity in the visual cortex. Biol. Cybern. **32**, 1-8(1979)

(40) Nagano,T., Kurata,K.: A model of the complex cell based on recent neurophysiological findings. Biol. Cybern. **38**, 103-105(1980)

(41) Nagano,T., Kurata,K.: A self-organizing neural network model for the development of complex cells. Biol. Cybern. **40**, 195-200(1981)

(42) Nakano,K.: Associatron: a model of associative memory. IEEE Trans. on SMC **2**, 380-388(1972)

(43) Neumann,J. von: First draft of a report on the EDVAC. Moore School of Electrical Engineering, Univ. of Pennsylvania, (1945)

(44) Pearson,K.: The control of walking. In: Vertebrates: Adaptation. Wessels,N.K, ed. San Francisco: Freeman, (1979)

(45) Scott,A.C.: The electrophysics of a nerve fiber. Revs. Mod. Phys. **47**, 487-533(1975)

(46) Stanley,J.C.: Simulation studies of a temporal sequence memory model. Biol. Cybern. **24**, 121-137(1976)

(47) Stein,R.B., Leung,K.V., Mangeron,D., Oğŭztöreli,M.N.: Improved neuronal models for studying neural networks. Kybernetik **15**, 1-9(1974)

(48) Stein,R.B., Leung,K.V., Oğŭztöreli,M.N., Williams,D.W.: Properties of small neural networks. Kybernetik **14**, 223-230(1974)

(49) Szentagothai,J.: Structuro-functional considerations of the cerebellar neuron network. Proc. IEEE **56**, 960-968(1968)

(50) Thompson,R.S.: A model for basic pattern generating mechanisms in the lobster stomatogastric ganglion. Biol. Cybern. **43**, 71-78(1982)

(51) Toda,M.: Studies of a non-linear lattice. Physics Reports (Sect. C of Physics Letters) **18**, 1-124(1975)

(52) Tokura,T., Morishita,I.: Analysis and simulation of double-layer neural networks with mutually inhibiting interconnections. Biol. Cybern. **25**, 83-92(1977)

(53) Tsutsumi,K., Matsumoto,H.: A synaptic modification algorithm in consideration of the generation of rhythmic oscillation in a ring neural network. Biol. Cybern. **50**, 419-430(1984)

(54) Tsutsumi,K., Matsumoto,H.: A memory model: neural network storing and recalling information in the form of bursts of nerve impulses. Mem. Grad. School Sci. & Technol., Kobe Univ., (to appear)

(55) Tsutsumi,K., Matsumoto,H.: Ring neural network qua a generator of rhythmic oscillation with period control mechanism. Biol. Cybern. (to appear)

(56) Tsutsumi,K., Matsumoto,H.: Synthesizer learning model of the cerebellum. Biol. Cybern. (in review)

(57) Wigström,H.: A neuron model with learning capability and its relation to mechanisms of association. Kybernetik **12**, 204-215(1973)

(58) Wigström,H.: A model for a neural network with recurrent inhibition. Kybernetik **16**, 103-112(1974)

(59) Wigström,H.: Associative recall and formation of stable modes of activity in neural network models. J. Neurosci. Res. **1**, 287-313(1975)

(60) Willwacher,G.: Storage of a temporal pattern sequence in a network. Biol. Cybern. **43**, 115-126(1982)